

Strategic Design of Catalytic Lysine-Targeting Reversible Covalent BCR-ABL Inhibitors

David Quach, Guanghui Tang, Jothi Anantharajan, Nithya Baburajendran, Anders Poulsen, John Wee, Priya Retna, Rong Li, Boping Liu, Doris Tee, Perlyn Kwek, Joma Joy, Wan-Qi Yang, Chong-Jing Zhang, Klement Foo, Thomas Keller, **Shao Yao**

Submitted date: 04/02/2021 • Posted date: 04/02/2021

Licence: CC BY-NC-ND 4.0

Citation information: Quach, David; Tang, Guanghui; Anantharajan, Jothi; Baburajendran, Nithya; Poulsen, Anders; Wee, John; et al. (2021): Strategic Design of Catalytic Lysine-Targeting Reversible Covalent BCR-ABL Inhibitors. ChemRxiv. Preprint. <https://doi.org/10.26434/chemrxiv.13710097.v1>

Targeted covalent inhibitors have re-emerged as validated drugs to overcome acquired resistance in cancer treatment. Herein, by using a carbonyl boronic acid warhead, we report the structure-based design of BCR-ABL inhibitors via reversible covalent targeting of the catalytic lysine with improved single-digit nanomolar potency against both wild-type and mutant ABL kinases, especially ABL^{T315I} bearing the gatekeeper residue mutation. We show that, by using techniques including mass spectrometry, time-dependent biochemical assays and X-ray crystallography, the evolutionarily conserved lysine can be targeted selectively. Furthermore, we show that the selectivity depends largely on molecular recognition of the non-covalent pharmacophore in this class of inhibitors, probably due to the moderate reactivity of the warhead. We report the first co-crystal structures of covalent inhibitor-ABL kinase domain complexes, providing insights into the interaction of this warhead with the catalytic lysine. We also employed label-free mass spectrometry to evaluate potential off-targets of our compounds at proteome-wide level in different cancer cell lines.

File list (2)

David_YSQ Main Text ChemRxiv.pdf (1.37 MiB)

[view on ChemRxiv](#) • [download file](#)

David_YSQ SI_ChemRxiv.pdf (18.35 MiB)

[view on ChemRxiv](#) • [download file](#)

Strategic Design of Catalytic Lysine-Targeting Reversible Covalent BCR-ABL Inhibitors

David Quach,^{[a][b]} Guanghui Tang,^[c] Jothi Anantharajan,^[b] Nithya Baburajendran,^[b] Anders Poulsen,^[b] John L. K. Wee,^[b] Priya Retna,^[b] Rong Li,^[b] Boping Liu,^[b] Doris H. Y. Tee,^[b] Perlyn Z. Kwek,^[b] Joma K. Joy,^[b] Wan-Qi Yang,^[d] Chong-Jing Zhang,^[d] Klement Foo,^{*,[b]} Thomas H. Keller,^{*} Shao Q. Yao^{*,[a][c]}

- [a] Dr. D. Quach, Prof. Dr. S. Q. Yao
NUS Graduate School for Integrative Sciences and Engineering, 21 Lower Kent Ridge, University Hall, Tan China Tuan Wing, #04-02, Singapore 119077
E-mail: chmyaosq@nus.edu.sg
- [b] Dr. D. Quach, Dr. J. Anantharajan, Dr. N. Baburajendran, Dr. A. Poulsen, J. L. K. Wee, P. Retna, R. Li, B. Liu, D. H. Y. Tee, P. Z. Kwek, Dr. J. K. Joy, Dr. K. Foo, Dr. T. H. Keller
Experimental Drug Development Centre, 10 Biopolis Road, Chromos, #05-01, Singapore 138670
E-mail: thkeller@eddc.a-star.edu.sg, klementfoo@gmail.com
- [c] Dr. G. Tang, Prof. Dr. S. Q. Yao
Department of Chemistry, National University of Singapore, Singapore 117543
- [d] W.-Q. Yang, Dr. C.-J. Zhang
State Key Laboratory of Bioactive Substances and Functions of Natural Medicines and Beijing Key Laboratory of Active Substances Discovery and Druggability Evaluation, Institute of Materia Medica Peking Union Medical College and Chinese Academy of Medical Sciences, Beijing, China, 100050

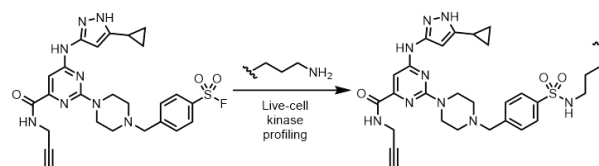
Supporting information for this article is given via a link at the end of the document.

Abstract: Targeted covalent inhibitors have re-emerged as validated drugs to overcome acquired resistance in cancer treatment. Herein, by using a carbonyl boronic acid warhead, we report the structure-based design of BCR-ABL inhibitors via reversible covalent targeting of the catalytic lysine with improved single-digit nanomolar potency against both wild-type and mutant ABL kinases, especially ABL^{T315I} bearing the gatekeeper residue mutation. We show that, by using techniques including mass spectrometry, time-dependent biochemical assays and X-ray crystallography, the evolutionarily conserved lysine can be targeted selectively. Furthermore, we show that the selectivity depends largely on molecular recognition of the non-covalent pharmacophore in this class of inhibitors, probably due to the moderate reactivity of the warhead. We report the first co-crystal structures of covalent inhibitor-ABL kinase domain complexes, providing insights into the interaction of this warhead with the catalytic lysine. We also employed label-free mass spectrometry to evaluate potential off-targets of our compounds at proteome-wide level in different cancer cell lines.

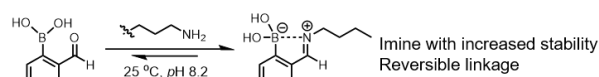
Introduction

Chronic myeloid leukemia (CML) arises from a genetic abnormality in human chromosome 22, which is unusually short and defective because of the reciprocal translocation of genetic material from chromosome 9.^[1] Gene expression leads to the formation of a constitutively active BCR-ABL1 kinase, which aberrantly activates multiple signaling pathways that bring about uncontrollable cell growth and differentiation.^[2] Despite the clinical success of ATP-competitive inhibitors,^[3] a significant number of patients

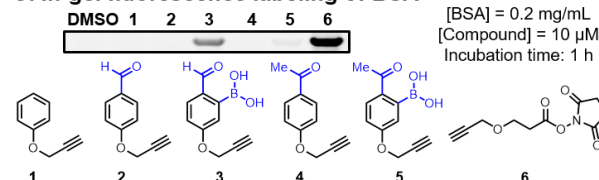
A. Reported lysine modification by Taunton^[22]



B. Iminoboronate mechanism^[30]



C. In-gel fluorescence labeling of BSA

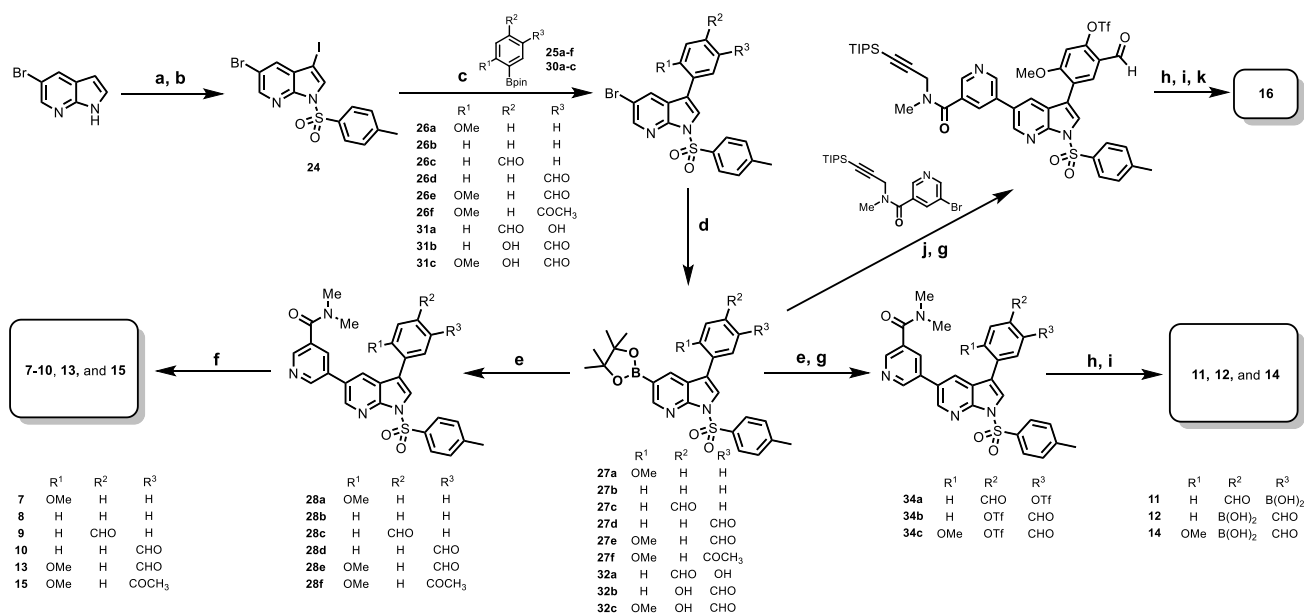


D. This work



Figure 1. (A) A previously reported sulfonyl fluoride probe for covalent lysine labeling of kinases in live cells.^[22] (B) Lysine modification based on the formation of a stable iminoboronate with 2-formylbenzene boronic acid.^[30] (C) Model study of various lysine-targeting probes by using bovine serum albumin (BSA). (D) Structure-based design of BCR-ABL inhibitors targeting the catalytic lysine K271, based on a previously reported inhibitor PPY-A (7).^[32]

have suffered from relapse due to drug resistance, which can arise from point mutations that severely reduce the effect of such inhibitors.^[4,5] An important mutant in CML is BCR-ABL^{T315I} which can only be inhibited by ponatinib (Iclusig).^[6] Targeted covalent



Scheme 1. Synthesis of key inhibitors used in this work. (a) NIS, acetone, rt, 1 h, 98%; (b) TsCl, NaH, THF, 0 °C, 3 h, 96%; (c) Pd(dppf)Cl₂, K₂CO₃, 1,4-dioxane/H₂O (9:1), 70 °C, 7 h, 60-80%; (d) B₂pin₂, Pd(dppf)Cl₂, KOAc, 1,4-dioxane, 100 °C, 7 h, 70-90%; (e) 5-bromo-*N,N*-dimethylnicotinamide, Pd(dppf)Cl₂, K₂CO₃, 1,4-dioxane/H₂O (9:1), 95 °C, 7 h, 70-80%; (f) LiOH, MeOH/dioxane/H₂O (2:2:1), rt, 1 h, up to 90%; (g) CF₃SO₂Cl, K₂CO₃, DMF, rt, 2-4 h, 80-90%; (h) B₂pin₂, Pd(dppf)Cl₂, KOAc, 1,4-dioxane, 100 °C, 7 h; (i) Cs₂CO₃, THF/MeOH (2:1), 40-50 °C, 1 h, 10-20% (2-step yields from (h) and (i)); (j) 5-bromo-*N*-methyl-*N*-(3-(triisopropylsilyl)prop-2-yn-1-yl)nicotinamide, Pd(dppf)Cl₂, K₂CO₃, 1,4-dioxane/H₂O (9:1), 95 °C, 7 h, 80-90%; (k) TBAF, THF/H₂O, rt, 2.5% (3-step yield from (h), (i) and (k)).

inhibitors offer advantages such as greater potency and prolonged duration of action over non-covalent inhibitors, and they have reemerged in recent years as demonstrated by the clinical success of, for example, osimertinib.^[7-11] The standard strategy to design irreversible kinase inhibitors uses Michael acceptors to target poorly conserved cysteine residues near the active site of kinases.^[12] This was thought to provide a measure of selectivity; however, Cravatt and coworkers have demonstrated that even carefully designed cysteine-targeting covalent inhibitors have off-target effects.^[13] Furthermore, resistance mechanisms including cysteine point mutations (EGFR^{C797S} and BTK^{C481S}) often render cysteine-targeting covalent drugs ineffective.^[11] To our knowledge, no covalent drugs against any of the known BCR-ABL mutants have been reported up to date due to a lack of targetable cysteine residues.^[14]

Since the catalytic lysine residue is essential for the enzymatic activity of all protein kinases and therefore, considered less prone to mutation,^[15,16] we have been interested to study this evolutionarily conserved residue in the ATP pocket with the aim to produce covalent kinase inhibitors as an alternative strategy in drug design. Many non-selective lysine-modifying probes, including the use of sulfonyl fluorides and activated esters, have been reported.^[17-23] Taunton and coworkers were the first who reported sulfonyl fluoride probes for lysine-targeting in kinases (Figure 1A).^[22] Campos et al later identified lysine-targeting kinase inhibitors that used an activated ester.^[23] Since cellular toxicity is a major concern for both tool compounds and

drug candidates, many research groups aspire to tune the reactivity of covalent warheads.^[24-28] For example, Taunton and co-workers used electron-deficient Michael acceptors for the design of cysteine-targeting reversible covalent kinase inhibitors.^[29] Iminoboronates have recently been shown to reversibly but covalently modify amino groups in proteins;^[30] however, this chemistry, to the best of our knowledge, has not been used to develop covalent kinase inhibitors (Figure 1B).^[31] Our aim was therefore to design reversible, covalent inhibitors targeting the catalytic lysine residue in kinases as a general approach to combat drug resistance. We report herein the first successful examples of lysine-targeting reversible covalent kinase inhibitors based on iminoboronate chemistry (Figure 1C/D); our results showed that such compounds possessed potent and long-lasting inhibition against BCR-ABL wild type and mutants.

Results and Discussion

At the outset, a mechanistic study was carried out to compare the relative reactivity of model probes **3** and **5** with an NHS probe (**6**) and other controls by using BSA as reference (Figure 1C); removal of either carbonyl or boronic acid (or both; e.g. **1**, **2** and **4**) caused complete abolishment in fluorescent labeling of BSA in **3** and **5**. Between **3** and **5**, the former consistently labeled BSA more strongly, indicating the aldehyde was more reactive than the ketone. As expected, both **3** and **5** produced much weaker fluorescence labeling of BSA compared to **6**, suggesting iminoboronates have attenuated lysine reactivity compared to the highly

reactive NHS-based irreversible lysine modifier.^[18] We next designed suitable iminoboronate-containing BCR-ABL kinase inhibitors (Figure 1D). Molecular modeling studies were first carried out by incorporating a carbonyl boronic acid warhead into a previously reported ABL1 inhibitor PPY-A (**7**) (PDB ID: 2QOH; Figure S1);^[32] results showed that introducing the required functionality would not disrupt the binding to the protein, and with the distance between the proposed carbonyl boronic acid and the highly flexible catalytic lysine K271 being ~3.5 Å, formation of an iminoboronate in the kinase/inhibitor complex was indeed possible.

A library of analogs was synthesized in order to establish structure-activity relationship (Figures 1D and S2, Scheme 1). The synthesis of a common intermediate **24** was done in two steps via iodination and tosylation of 5-bromoazaindole. **7-10** were obtained in four steps via Suzuki-Miyaura coupling reactions involving **24** to generate **26a-d**, which underwent Miyaura borylation that led to **27a-d**. The Suzuki-Miyaura cross coupling reaction was performed at a lower temperature of 60 °C in order to chemoselectively differentiate Br and I. **27a-d** then underwent a second

Suzuki-Miyaura coupling reaction with 5-bromo-*N,N*-dimethylnicotinamide followed by subsequent removal of tosyl group with LiOH, leading to the formation of the desired inhibitors. The synthesis of carbonyl boronic acid inhibitors **11** and **12** occurred via a different route in which an additional step involving the conversion of OH to OTf, led to intermediates **34a** and **34b**; CF₃SO₂Cl and K₂CO₃ were shown to be the optimal choice. Other electrophiles such as PhNTf₂ and (CF₃SO₂)₂O in the presence of bases such as triethylamine, NaH and pyridine did not work well, however, despite heating. **34a** and **34b** underwent borylation and subsequent deprotection of the tosyl group by using Cs₂CO₃ was carried out to generate covalent inhibitors **11** and **12** (Supporting Information).

By using a mobility shift assay based on Caliper's microfluidics capillary electrophoresis, the IC₅₀ value of PPY-A (**7**) against wildtype ABL was determined to be 2 nM (Figure S2). Removal of the *o*-methoxy group reduced the potency by 20 folds (compound **8**). Introduction of *m*-aldehyde (compound **10**), however, improved the IC₅₀ to 8 nM. Shifting the aldehyde functional group to the *para* position was not tolerated

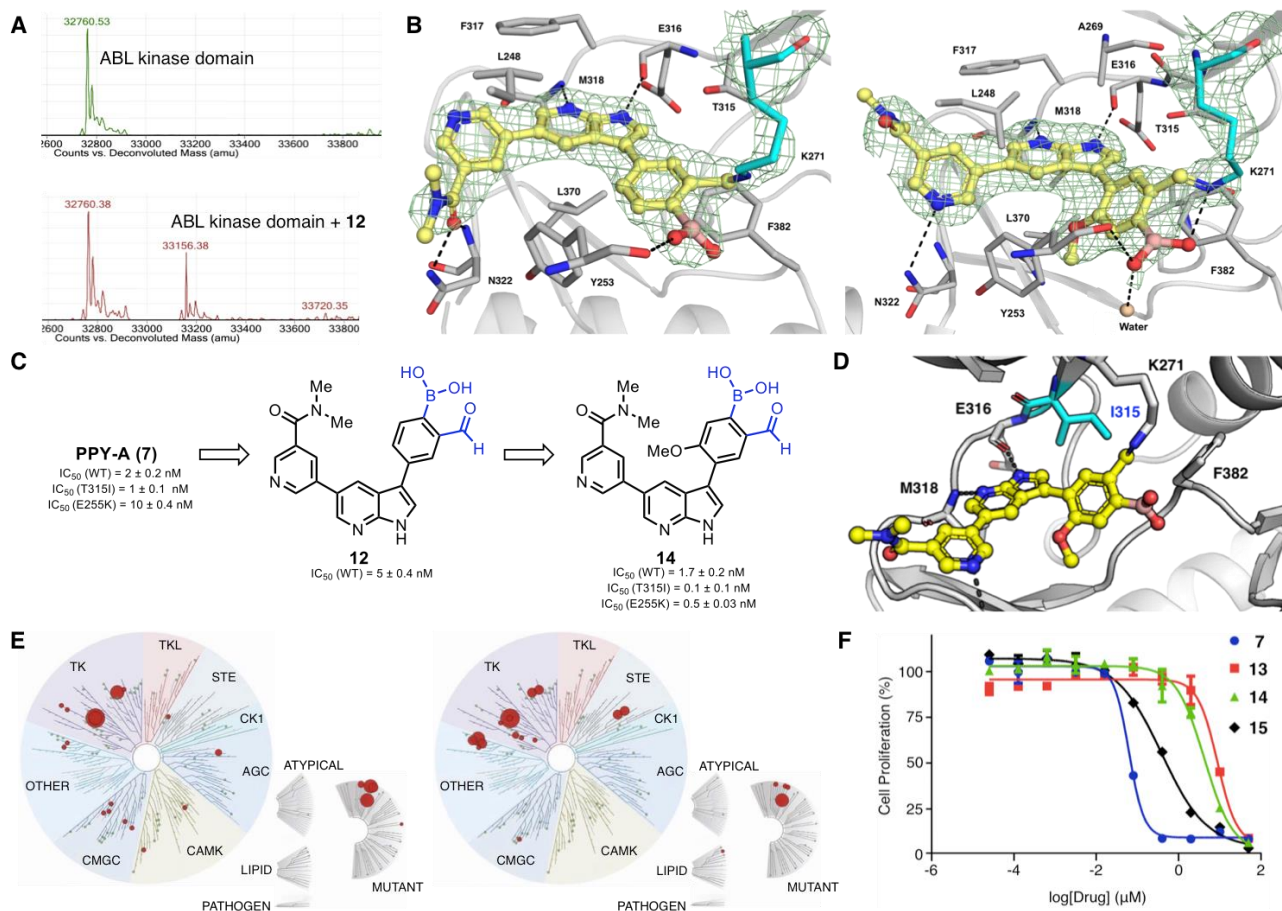


Figure 2. (A) Mass spectrometric analysis of the ABL kinase domain-12 complex. (B) Cocrystal structures of the ABL kinase domain with **12** (left) and **14** (right) showing the composite omit map (2F_o-F_c) contoured to 1σ in green mesh. The front loop was removed for better visibility. (C) Comparison of ABL inhibition (WT and mutants) of PPY-A (**7**), **12** and **14** after 6 or 12 h. (D) Modeled structure of ABL^{T315I} kinase domain-**14** complex based on the obtained cocrystal structure of ABL^{WT} kinase domain-**14** complex. (E) Dendrograms showing Kinome Scan™ of **7** (left) and **14** (right) at 1000 nM against 90 different kinases. (F) Anti-proliferative activity of **7**, **13**, **14** and **15** against K562 cells determined by CellTiter-Glo® viability assay.

(compound **9**). Introduction of a boronic acid functionality led to inhibitors **11** and **12**. As expected of covalent inhibitors, the enzyme inhibition of compound **12** improved from 83 nM ($T = 0$ h) to 5 nM ($T = 12$ h) as the incubation time was increased (Figure S3A). Compound **10** did not show time-dependence of the IC_{50} , suggesting that the presence of the boronic acid in **12** may have led to the formation of an iminoboronate.^[33]

To determine whether **12** was selective towards the catalytic lysine in ABL, mass spectrometric analysis was performed. MALDI-TOF analysis suggested that a single lysine-modified covalent adduct was formed with an observed m/z of 33156.38 Da (Figure 2A; compared to calculated mass of 33156.59 Da). The reaction did not reach completion regardless of the concentration (up to 1 mM) and incubation time (up to 24 h) of **12**, indicating that an equilibrium was established.^[30,31] Since the OMe group in **7** was important for ABL inhibition, the same functionality was added to **12**, providing compound **14** which was synthesized via a similar route (Scheme 1, Figure S6C). As expected, **14** showed time-dependent IC_{50} values against ABL from 13 nM at 0 h to 1.7 nM after 12 h (Figure 2C); further testing of **7** and **14** against two ABL mutants indicated that **14** was about ten-fold more potent against both ABL^{T315I} and ABL^{E255K} than **7**, and at the same time also showed time-dependent inhibition against both mutants (Figures S3C and S3D). In particular, **14** demonstrated an improved potency from 25 nM ($T = 0$ h) to 0.1 nM ($T = 6$ h) against ABL^{T315I} (250-fold improvement) and from 43 nM ($T = 0$ h) to 0.5 nM ($T = 12$ h) against ABL^{E255K} (100-fold improvement). The effect of point mutation on restricting access to the binding pocket or stabilizing certain protein conformations has been shown to adversely affect drug binding which tends to favor only a very specific target conformation;^[10] however, our examples showed that targeting the catalytic lysine residues gave an advantage in this context.

The X-ray cocrystal structures of **12** and **14** with the ABL kinase domain (229-510) were solved up to 2.7 Å and 2.3 Å resolution, respectively, giving more insights into how this particular warhead interacts with the catalytic lysine residue (Figure 2B; PDB IDs: 7CC2 and 7DT2); the continuous electron density from K271 in the ABL kinase domain to **12** and **14** suggests that the imine product was formed. We did not however observe the formation of the expected dative bond between the imine nitrogen and the boron atom. In fact, the lone pair of the imine appeared to be orientated away from the boron atom in both crystal structures. One of the reasons could be due to the vast structural difference between the macromolecule-inhibitor complex and small molecules given the tight binding pocket of a protein target (our data ¹¹B NMR showed that an iminoboronate could be captured for small molecules, Figure S14). Since the biochemical assays and the MALDI-TOF analysis suggested that the boronic acid plays an important role in the formation of the adduct,

we propose that the obtained cocrystal structures had successfully captured the key intermediate during the formation of the iminoboronates. Given the fact that **14** was able to potently inhibit ABL^{T315I} while imatinib and second-generation kinase inhibitors such as nilotinib, dasatinib failed to do so,^[32] we next rationalized this observation by using the newly obtained structural data (Figure 2D); by building a modeled structural complex of **14** and ABL kinase domain in which the T315 residue was artificially changed to I315, we observed no steric clash upon inhibitor binding. Imatinib, nilotinib and dasatinib possess crucial elongated structures that are extended to the back cleft of the ATP binding pocket in ABL, and T315I point mutation was expected to restrict access to the hydrophobic region at the rear of this pocket.^[32] This is not the case for **14** which does not have any substituent that occupies this pocket. Finally, **14** demonstrated better biochemical activity than that of **7** due to apparent covalent modification,^[34] and the incorporation of both boronic acid and aldehyde did not appear to cause any steric clash with the I315 residue.

The kinetic parameters of inactivation were next determined to better understand the non-bonded interaction of **12** and **14** with the kinase (Figures S4);^[34] both compounds showed similar k_{inact} values. while **14** had a smaller K_i compared to that of **12**, thus confirming that the critical role of OMe in **14** for increased affinity between the inhibitor and the ABL kinase domain.

One of the potential concerns for covalent inhibitors like **14**, which target a key amino acid in the active site of kinases, is the selectivity. We therefore carried out Kinome ScanTM with a panel of ~100 protein kinases (Figure 2E); results showed highly similar interaction maps for compounds **7** (left) and **14** (right), suggesting that the degree of compound selectivity largely depended on the initial step of molecular recognition presumably due to the moderately reactive 2-carbonyl boronic acid warhead in **14**. The conclusion was further strengthened by the selectivity scores (Table S4). To evaluate the anti-proliferative activity of this class of inhibitors, compounds **7** and **14**, as well as reference compounds **13** and **15** (boronic acid-free versions of **14**; see Figure 1D), were tested in K562 cells. As shown in Figure 2F, compound **7** showed GI_{50} of 0.114 μ M whereas compounds **13**, **14** and **15** were less active with GI_{50} values of 3.85 μ M, 1.19 μ M and 0.384 μ M, respectively. In an attempt to understand the loss of activity, the cell permeability of three compounds were tested (Tables S5 and S6); Compound **13** showed poor recovery rates which could be due to metabolism of the aldehyde functional group.^[35] The 10-fold improvement in the anti-proliferative activity of its ketone counterpart (e.g. **15**; $GI_{50} = 0.384 \mu$ M) suggests that the aldehyde might not be the optimal choice for this scaffold in the cellular systems.

Finally, to evaluate the proteome-wide reactivity and potential off-targets of **14** in live mammalian cells, we synthesized its alkyne-containing analog (**16**; Scheme

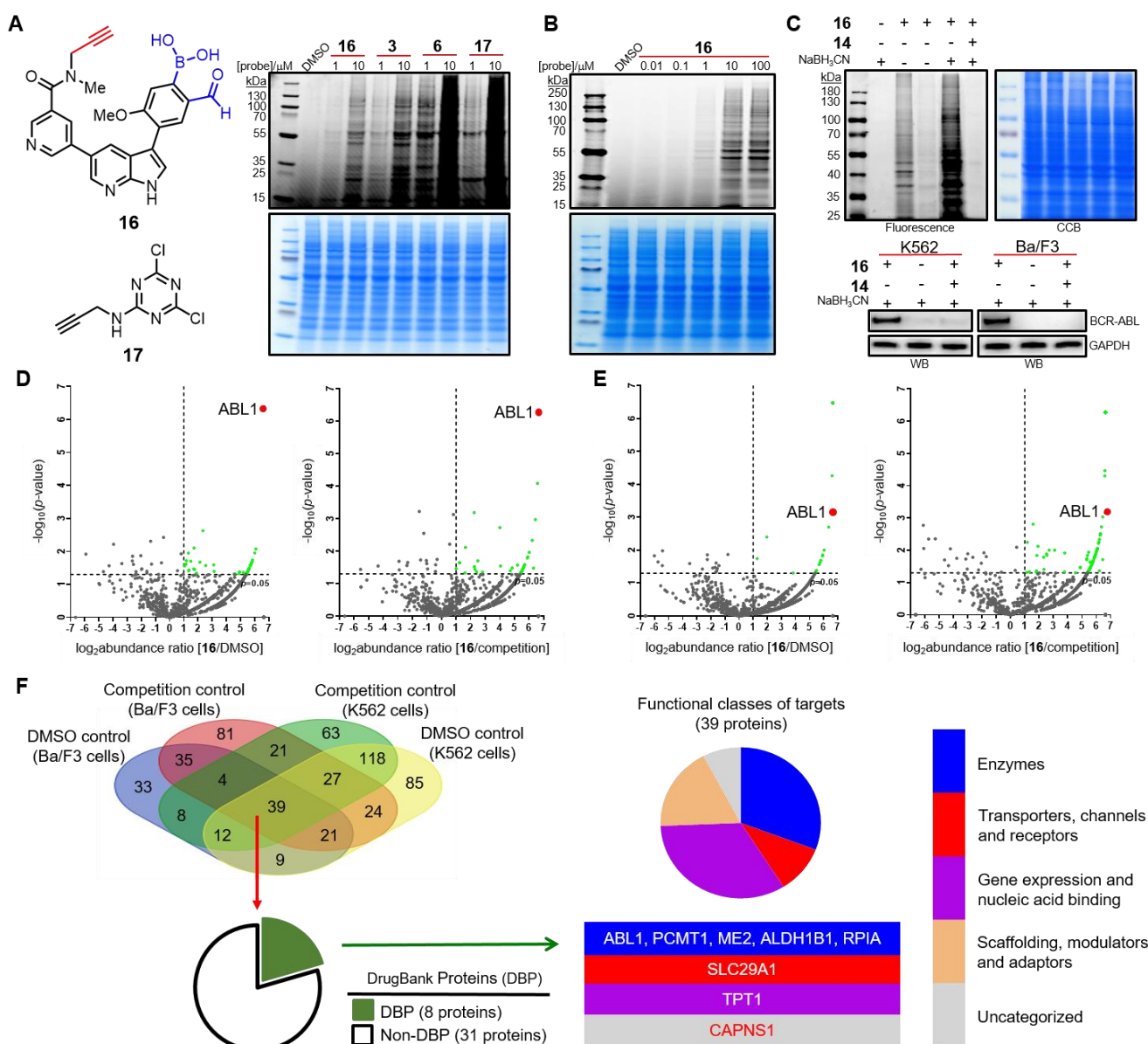


Figure 3. (A) Proteome reactivity profiles of compound **16** compared to **3**, **6** and **17** in K562 cell lysates (in PBS with 0.1% Triton, pH 7.5). (Top): in-gel fluorescence scanning; (Bottom): Coomassie staining (CBB). (B) Concentration-dependent proteomic reactivity profiles of **16** (0–100 μ M) in Ba/F3 cells overexpressing BCR-ABL^{WT}. (C) Effect of washing by cold acetone and cold methanol of probe-labeled K562 (see Figure S13 for corresponding Ba/F3 results) lysates in the absence and presence of excess NaBH₃CN (top); Western blotting (WB) detection of BCR-ABL^{WT} in lysates of both K562 and Ba/F3 cells following pull-down (PD) assays. GAPDH = loading control. (D/E) Volcano plots of potential cellular targets of **16** from probe-treated K562 and Ba/F3 cell lysates, respectively. (F) Data analysis of shared targets identified from chemoproteomic experiments in (D/E). See Figures S12, S13 and Table S7 for details.

1) and carried out large-scale chemoproteomic studies (Figure 3).^[36] We first compared the proteome reactivity of the aldehyde-boronic acid moiety to other well-known lysine-targeting functionalities by using lysates from K562 cells (Figure 3A);^[17,18] in-gel fluorescence scanning analysis of probe-labeled lysates, followed by CuAAC with rhodamine azide,^[37] showed that **3** demonstrated better selectivity at both 1 μ M and 10 μ M when compared to **6** and **17** which are known lysine-reactive electrophiles, but was predictably less selective compared to the kinase-targeting **16**, suggesting that molecular recognition was the dominant factor for similar compounds that contain low-reactivity

electrophiles such as iminoboronates.^[38,39] In **16**-treated samples, we observed a concentration-dependent labeling of proteomes, with saturated fluorescence signals at \sim 10 μ M of the probe (Figure 3B). We next repeated the labeling experiment in the presence of NaBH₃CN which helped trap the reversible covalent iminoboronates into more stable amine adducts (Figure 3C); a concomitant increase in the fluorescence intensity of the **16**-labeled proteome was observed. In contrast, in the absence of NaBH₃CN, washing the **16**-labeled proteome with cold acetone and methanol significantly reduced or abolished the labeling, thus confirming the reversibility of iminoboronate bond

(Figures S13 and S14). Upon further enrichment of the labeled proteomes by pull-down (PD) experiments followed by Western blotting (WB) analysis, we confirmed successful labeling of endogenous BCR-ABL from both K562 and Ba/F3 cell lysates (Figure 3C bottom). By using DMSO-treated and **14**-competed samples as controls, we carried out large-scale LC-MS analysis (Figures 3C-E, S11 and S12, Table S7).^[22,36,37] Consistent with strong labeling shown by in-gel fluorescence scanning (Figure 3C), **16** captured a number of off-targets in addition to the expected BCR-ABL (highlighted in red in Figure 3D/E). Upon combining analyses of enriched hits from **16**-labeled proteomes of both K562 and Ba/F3 cells, we identified a total of 39 potential cellular targets out of which 8 were DrugBank proteins including ABL1, PCMT1, ME2, ALDH1B1, RPIA, SLC29A1, TPT1 and CAPNS1 at a high confidence level (Figure 3F and Table S7). Unlike protein kinases which have a known catalytic lysine residue in their kinase active site, most of these shared targets possess solvent-exposed lysine residues, rendering them susceptible to probe labeling. Interestingly, ABL1 was the only kinase successfully identified from our experiments in both cell lines, indicating **16** was a selective ABL-targeting probe towards kinases.

Conclusion

In summary, we have successfully demonstrated, for the first time, that the catalytic lysine of ABL can be selectively targeted by inhibitors bearing the aldehyde boronic acid moiety, leading to a reversible covalent adduct. The incorporation of the two substituents required for covalent bond formation reduced the affinity to the ABL active site; however, the slow formation of the iminoboronate led to highly potent inhibitors of ABL kinase and its mutants. We also showed that the aldehyde boronic acid, which is a low-reactivity electrophile, can be used to design highly selective kinase inhibitors by maximizing molecular recognition. Such compounds might be attractive tools for chemical biology studies given recent interests in the development of reversible covalent inhibitors,^[29,31,40] but could also serve as potential drug candidates in cases where improved potency might be desirable once they are fully optimized.

Acknowledgements

Financial support was provided by the Synthetic Biology Research & Development Programme (SBP) of National Research Foundation (SBP-P4 and SBP-P8) for Shao Q. Yao, the National Medical Research Council (NMRC) via the Open Fund – Young Individual Research Grant for Klement Foo and by the Agency for Science, Technology and Research (A*STAR) via the A*STAR Graduate Scholarship (AGS) for David Quach. Financial support from CAMS Innovation Fund for Medical Sciences (CIFMS) (2017-I2M-4-005) of China

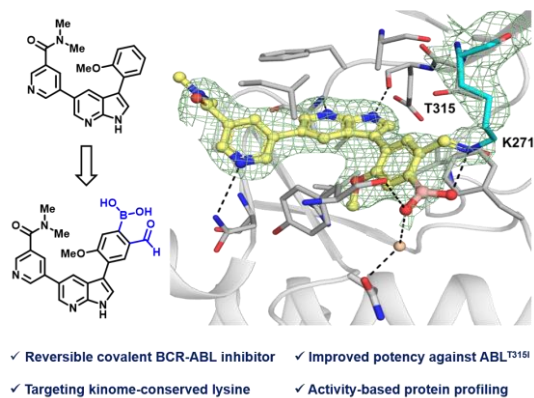
is also acknowledged. The ABL protein construct and glycerol stock were prepared by Yvonne Y. W. Tan and Dario B. Heymann.

Keywords: cancer • lysine • covalent • reversible • proteomics

- [1] R. Kurzrock, J. U. Gutterman, M. Talpaz, *N. Engl. J. Med.* **1988**, *319*, 990–998.
- [2] T. G. Lugo, A. M. Pendergast, A. J. Muller, O. N. Witte, *Science* **1990**, *247*, 1079–1082.
- [3] E. Jabbour, H. Kantarjian, *Am. J. Hematol.* **2016**, *91*, 252–265.
- [4] H. M. Kantarjian, M. Baccarani, E. Jabbour, G. Saglio, J. E. Cortes, *Clin. Cancer Res.* **2011**, *17*, 1674–1683.
- [5] Z. Iqbal, A. Aleem, M. Iqbal, M. I. Naqvi, A. Gill, A. S. Taj, A. Qayyum, N. ur-Rehman, A. M. Khalid, I. H. Shah, M. Khalid, R. Haq, M. Khan, S. M. Baig, A. Jamil, M. N. Abbas, M. Absar, A. Mahmood, M. Rasool, T. Akhtar, *PLoS One* **2013**, *8*, e55717.
- [6] T. Anagnostou, M. R. Litzow, *Blood Lymphat. Cancer* **2017**, *2018*, 1–9.
- [7] D. S. Johnson, E. Weerapana, B. F. Cravatt, *Future Med. Chem.* **2010**, *2*, 949–964.
- [8] A. Chaikuad, P. Koch, S. A. Laufer, S. Knapp, *Angew. Chem. Int. Ed.* **2018**, *57*, 4372–4385.
- [9] Z. Zhao, P. E. Bourne, *Drug Discov. Today* **2018**, *23*, 727–735.
- [10] J. Engel, J. Lategahn, D. Rauh, *ACS Med. Chem. Lett.* **2016**, *7*, 2–5.
- [11] S-H. I. Ou, *Crit. Rev. Oncol. Hematol.* **2012**, *83*, 407–421.
- [12] Q. S. Liu, Y. Sabnis, Z. Zhao, T. H. Zhang, S. J. Buhrlage, L. H. Jones, N. S. Gray, *Chem. Biol.* **2013**, *20*, 146–159.
- [13] S. Niessen, M. M. Dix, S. Barbas, Z. E. Potter, S. Lu, O. Brodsky, S. Planken, D. Behenna, C. Almaden, K. S. Gajiwala, K. Ryan, R. Ferre, M. R. Lazear, M. M. Hayward, J. C. Kath, B. F. Cravatt, *Cell Chem. Bio.* **2017**, *24*, 1388–1400.
- [14] F. Rossari, F. Minutolo, E. Orciuolo, *J. Hematol. Oncol.* **2018**, *11*, 1–14.
- [15] A. C. Carrera, K. Alexandrov, T. M. Roberts, *Proc. Natl. Acad. Sci. U. S. A.* **1993**, *90*, 442–446.
- [16] R. Liu, Z. Yue, C. C. Tsai, J. Shen, *J. Am. Chem. Soc.* **2019**, *141*, 6553–6560.
- [17] D. A. Shannon, R. Banerjee, E. R. Webster, D. W. Bak, C. Wang, E. Weerapana, *J. Am. Chem. Soc.* **2014**, *136*, 3330–3333.
- [18] C. C. Ward, J. L. Kleinman, D. K. Nomura, *ACS Chem. Biol.* **2017**, *12*, 1478–1483.
- [19] A. Cuesta, J. Taunton, *Annu. Rev. Biochem.* **2019**, *88*, 365–381.
- [20] M. Gehringer, S. A. Laufer, *J. Med. Chem.* **2019**, *62*, 5673–5724.
- [21] S. M. Hacker, K. M. Backus, M. R. Lazear, S. Forli, B. E. Correia, B. F. Cravatt, *Nat. Chem.* **2017**, *9*, 1181–1190.
- [22] Q. Zhao, X. Ouyang, X. Wan, K. S. Gajiwala, J. C. Kath, L. H. Jones, A. L. Burlingame, J. Taunton, *J. Am. Chem. Soc.* **2017**, *139*, 680–685.
- [23] S. E. Dalton, L. Dittus, D. A. Thomas, M. A. Convery, J. Nunes, J. T. Bush, J. P. Evans, T. Werner, M. Bantscheff, J. A. Murphy, S. Campos, *J. Chem. Am. Soc.* **2018**, *140*, 932–939.
- [24] U. P. Dahal, A. M. Gilbert, R. S. Obach, M. E. Flanagan, J. M. Chen, C. Garcia-Irizarry, J. T. Starr, B. Schuff, D. P. Uccello, J. A. Young, *Med. Chem. Commun.* **2016**, *7*, 864–872.
- [25] J. Pettinger, K. Jones, M. D. Cheeseman, *Angew. Chem. Int. Ed.* **2017**, *56*, 15200–15209.
- [26] P. Martín-Gago, C. A. Olsen, *Angew. Chem. Int. Ed.* **2019**, *58*, 957–966.
- [27] L. H. Jones, *Angew. Chem. Int. Ed.* **2018**, *57*, 9220–9223.
- [28] D. E. Mortenson, G. J. Brighty, L. Plate, G. Bare, W. Chen, S. Li, H. Wang, B. F. Cravatt, S. Forli, E. T. Powers, K. B. Sharpless, I. A. Wilson, J. W. Kelly, *J. Am. Chem. Soc.* **2018**, *140*, 200–210.
- [29] I. M. Serafimova, M. A. Pufall, S. Krishnan, K. Duda, M. S. Cohen, R. L. Maglathlin, J. M. McFarland, R. M. Miller, M. Frödin, J. Taunton, *Nat. Chem. Biol.* **2012**, *8*, 471–476.

-
- [30] S. Cambray, J. Gao, *Acc. Chem. Res.* **2018**, *51*, 2198-2206.
- [31] G. Akçay, M. A. Belmonte, B. Aquila, C. Chuaqui, A.W. Hird, M. L. Lamb, P. B. Rawlins, N. Su, S. Tentarelli, N. P. Grimster, Q. Su, *Nat. Chem. Biol.* **2016**, *12*, 931-936.
- [32] T. Zhou, L. Parillon, F. Li, Y. Wang, J. Keats, S. Lamore, Q. Xu, W. Shakespeare, D. Dalgarno, X. Zhu, *Chem. Biol. Drug Des.* **2007**, *70*, 171-181.
- [33] P. M. S. D. Cal, J. B. Vicente, E. Pires, A. V. Coelho, L. F. Veiros, C. Cordeiro, P. M. P. Gois, *J. Am. Chem. Soc.* **2012**, *134*, 10299-10305.
- [34] R. A. Bauer, *Drug Discov. Today* **2015**, *20*, 1061-1073.
- [35] L. A. Admed, H. Younus, *Drug Metab. Rev.* **2019**, *51*, 42-64.
- [36] B. R. Lanning, L. R. Whitby, M. M. Dix, J. Douhan, A. M. Gilbert, E. C. Hett, T. O. Johnson, C. Joslyn, J. C. Kath, S. Niessen, L. R. Roberts, M. E. Schnute, C. Wang, J. J. Hulce, B. Wei, L. O. Whiteley, M. M. Hayward, B. F. Cravatt, *Nat. Chem. Biol.* **2014**, *10*, 760-767.
- [37] H. Shi, C.-J. Zhang, G. Y. J. Chen, S. Q. Yao, *J. Am. Chem. Soc.* **2012**, *134*, 3001-3014.
- [38] K. M. Backus, B. E. Correia, K. M. Lum, S. Forli, B. D. Horning, G. E. González-Páez, S. Chatterjee, B. R. Lanning, J. R. Teijaro, A. J. Oison, D. W. Wolan, B. F. Cravatt, *Nature* **2016**, *534*, 570-574.
- [39] S. Pan, S. Y. Jang, S. S. Liew, J. Fu, D. Wang, J. S. Lee, S. Q. Yao, *Angew. Chem. Int. Ed.* **2018**, *57*, 579-583.
- [40] a) W.-H. Guo, X. Qi, X. Yu, Y. Liu, C.-I. Chung, F. Bai, X. Lin, D. Lu, L. Wang, J. Chen, L. H. Su, K. J. Nornie, F. Li, M. C. Wang, X. Shu, J. N. Onuchic, J. A. Woyach, M. L. Wang, J. Wang, *Nat. Commun.* **2020**, *11*, 4268; b) R. Gabizon, A. Shraga, P. Gehrtz, E. Livnah, Y. Shorer, N. Gurwicz, L. Avram, T. Unger, H. Aharoni, S. Albeck, A. Brandis, Z. Shulman, B.-Z. Katz, Y. Herishanu, N. London, *J. Am. Chem. Soc.* **2020**, *142*, 11734-11742.

Entry for the Table of Contents



Using the iminoboronate chemistry, we report the first successful examples of catalytic lysine-targeting reversible covalent BCR-ABL inhibitors which inhibited both ABL^{WT} and ABL^{T315I} at improved nanomolar potency. We also demonstrated for the first time how the study of off-targets for this class of compounds could be performed using activity-based protein profiling and proteomic mass spectrometry.

David_YSQ Main Text ChemRxiv.pdf (1.37 MiB)

[view on ChemRxiv](#) • [download file](#)

Strategic Design of Catalytic Lysine-Targeting Reversible Covalent BCR-ABL Inhibitors

David Quach, Guanghui Tang, Jothi Anantharajan, Nithya Baburajendran, Anders Poulsen, John L. K. Wee, Priya Retna, Rong Li, Boping Liu, Doris H. Y. Tee, Perlyn Z. Kwek, Joma K. Joy, Wan-Qi Yang, Chong-Jing Zhang, Klement Foo,^{*} Thomas H. Keller,^{*} Shao Q. Yao^{*}

SUPPLEMENTARY INFORMATION

Table of Contents

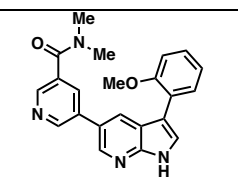
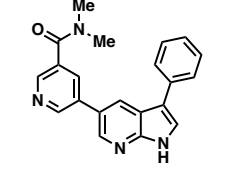
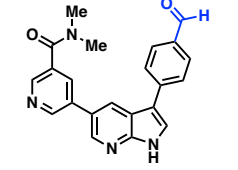
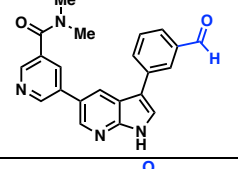
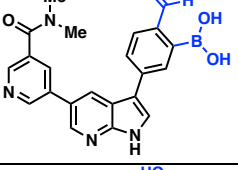
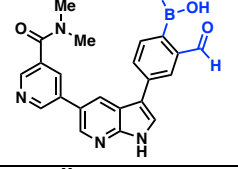
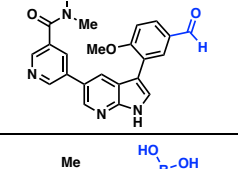
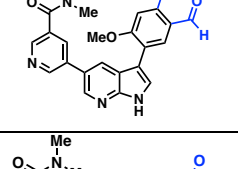
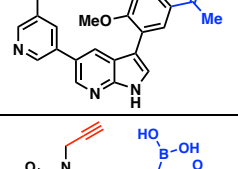
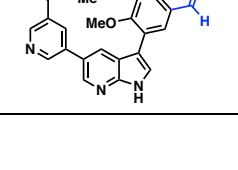
1. List of Abbreviations	2
2. Chemistry	5
2.1. General Information	5
2.2. Synthesis and Characterizations	5
Scheme S1 Synthesis of 1 , 2 and 4	5
Scheme S2 Synthesis of 3 and 5	6
Scheme S3 Synthesis of 7 , 8 , 9 , 10 , 13 and 15	8
Scheme S4 Synthesis of 11 , 12 and 14	18
Scheme S5 Synthesis of alkyne probe 16	25
3. Other Experimental Details	28
3.1. Modeling Methodology	28
3.2. Biochemical Assay	28
3.3. Kinetic Assay	29
3.4. Protein Mass Spectrometry	29
3.5. Protein Purification for ABL Kinase Domain	29
3.6. X-ray Crystallography	30
3.7. KINOMEscan	31
3.8. Cell Culture	31
3.9. Anti-Proliferation Assay	31
3.10. Caco-2 Test	31
3.11. In-Gel Fluorescence Scanning Analysis	32
3.12. Chemoproteomics and Off-Target Identification	33
4. Results and Discussion	36
Figures S1 and S2	36
Figure S3	37
Figure S4	38
Figure S5	39
Figure S6	40
Table S2	41
Figure S7	42
Figure S8	43
Figure S9	44
Table S3	45
Tables S4, S5 and S6	46
Figure S10	47
Figure S11	48
Figure S12	49
Table S7	50
Figure S13	51
Figures S14 and S15	52
5. References	53
6. NMR Spectra	54

1. List of Abbreviations

ABL	Abelson murine leukemia viral oncogene homolog 1
ABPP	Activity-based protein profiling
ACN	Acetonitrile
ATP	Adenosine triphosphate
BCA	Bicinchoninic acid
BCR	Breakpoint cluster region
B ₂ pin ₂	Bis(pinacolato)diboron
BSA	Bovine serum albumin
CR3	Coating reagent 3
CTG	CellTiter-Glo®
DCM	Dichloromethane
DIPEA	<i>N,N</i> -diisopropylethylamine
DMEM	Dulbecco's Modified Eagle's Medium
DMF	<i>N,N</i> -dimethylformamide
DMSO	Dimethylsulfoxide
DNA	Deoxyribonucleic acid
DTT	Dithiothreitol
EDTA	Ethylenediaminetetraacetic acid
EtOAc	Ethyl acetate
FBS	Fetal bovine serum
GADPH	Glyceraldehyde 3-phosphate dehydrogenase
HATU	Hexafluorophosphate azabenzotriazole tetramethyl uronium 1-[Bis(dimethylamino)methylene]-1 <i>H</i> -1,2,3-triazolo[4,5- <i>b</i>]pyridinium 3-oxid hexafluorophosphate
HBSS	Hank's Balanced Salt Solution
HEPES	(4-(2-Hydroxyethyl)-1-piperazineethanesulfonic acid
HRP	Horseradish peroxidase
IC ₅₀	Half maximal inhibitory concentration
IMAC	Immobilized metal ion affinity chromatography
IMDM	Iscove's Modified Dulbecco's Medium
IPTG	Isopropyl- β -D-thiogalactopyranoside
KD	Kinase domain
LC	Liquid chromatography
MES	2-(<i>N</i> -Morpholino)ethanesulfonic acid
MS	Mass spectrometry
NIS	<i>N</i> -Iodosuccinimide
NMR	Nuclear magnetic resonance
NTA	Nitrilotriacetic acid
OD	Optical density
PBD	Protein data bank
PBS	Phosphate-buffered saline
PCR	Polymerase chain reaction
PD	Pull-down
Pd(dppf)Cl ₂	[1,1'-Bis(diphenylphosphino)ferrocene]dichloropalladium(II)
PEG	Polyethylene glycol
PMSF	Phenylmethylsulfonyl fluoride
PVDF	Polyvinylidene fluoride
RMPI	Roswell Park Memorial Institute

RMS	Root-mean-square
SDS	Sodium dodecyl sulfate
TB	Terrific broth
TBAF	Tetra- <i>n</i> -butylammonium fluoride
TBS	Tris-buffered saline
TCEP	Tris(2-carboxyethyl)phosphine
TEA	Triethylamine
TEER	Transepithelial/transendothelial electrical resistance
TEV	Tobacco etch virus
THF	Tetrahydrofuran
THPTA	Tris(3-hydroxypropyltriazolymethyl)amine
TIPS	Triisopropylsilyl
TLC	Thin-layer chromatography
TOF	Time-of-flight
WB	Western blotting
XDS	X-ray detector software

Table S1. Summary of key compounds (7-16) used in this work

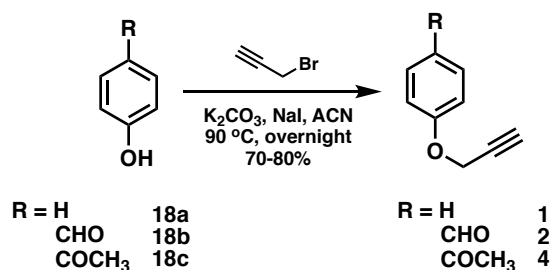
Compound	Chemical Structure	Study Goal	Results
PPY-A (7)		Synthetic starting point A reversible BCR-ABL inhibitor used as a reference compound in biochemical assay, KINOMEScan and anti-proliferation assay	Has been reported as an ABL kinase inhibitor ^[1] and showed an IC ₅₀ of 2 nM in our hands
8		To establish the structure-activity relationship	Removal of the <i>o</i> -methoxy group lead to a 20-fold reduction in activity (IC ₅₀ = 43 nM)
9		To establish the structure-activity relationship	The aldehyde group at the <i>para</i> position did not have a strong effect on IC ₅₀ compared to 8 (IC ₅₀ = 75 nM)
10		To establish the structure-activity relationship; Control in the biochemical assay and mass spectrometry	The aldehyde group at the <i>meta</i> position improved the IC ₅₀ of 8 compared 9 (IC ₅₀ = 8 nM)
11		To establish the structure-activity relationship	The introduction of the boronic acid lead to an increase in the IC ₅₀ compared to 8 (IC ₅₀ = 414 nM)
12		To establish the structure-activity relationship; Model compound for biochemical and kinetic assays, X-ray crystallography and mass spectrometry	Successfully showed time-dependent IC ₅₀ and covalently modified the catalytic lysine residue (IC ₅₀ = 5 nM after 12 h)
13		To establish the structure-activity relationship; Control in the biochemical assay and anti-proliferation assay	Showed the importance of OMe group (IC ₅₀ = 3 nM)
14		Optimized model compound used in biochemical and kinetic assays, KINOMEScan and anti-proliferation assay	More potent than the reference compound 7 against ABL ^{WT} , ABL ^{T315I} and ABL ^{E255K} ; showed time-dependent IC ₅₀ and importance of OMe
15		Improved model compound used in the anti-proliferation assay	10-fold improved cellular activity compared to 13 and 14
16		Model compound used in chemoproteomic experiments	Successfully labeled off-targets in general in-gel fluorescence experiments; labeled ABL kinase domain in competition assay and BCR-ABL in pull-down

2. Chemistry

2.1. General Information

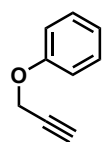
All chemicals and solvents were purchased commercially and used without further purification, unless indicated otherwise. All reactions that required anhydrous conditions were carried out under nitrogen or argon atmosphere using oven-dried glassware. Heating of reactions was accomplished with a silicon oil bath on top of a stirring hotplate equipped with an electronic contact thermometer to maintain the indicated temperature. Reactions were monitored by analytical thin layer chromatography (TLC) on pre-coated silica gel plates (Merck 60 F₂₅₄, 2.5 × 7.5 cm) and spots were visualized by UV (254/365 nm) or developed with KMnO₄ stain. Flash column chromatography was performed using a medium-pressure CombiFlash[®] R_f/R_{ft} instrument (Teledyne ISCO) with commercial pre-packed silica gel cartridges, unless otherwise stated. Reverse-phase chromatography was performed by using preparative HPLC system (Shimadzu) and Phenomenex Luna[®] 5 μM C₁₈₍₂₎ 100 Å 250 × 21.2 mm columns. The purity of all tested compounds were determined by HPLC (Shimadzu) and were found to be ≥ 95%, unless stated otherwise. Molecular weights (M_r) of intermediates and tested compounds were determined by a quadrupole LC/MS instrument (Agilent Technologies). ¹H NMR and ¹³C NMR were measured by using a Bruker Ultrashield[™] 400 Plus/R (400 MHz and 101 MHz) spectrometer, using Me₄Si as an internal standard. Chemical shifts (δ) were reported in parts per million with respect to appropriate internal standards or residual solvent peaks (CDCl₃ = 7.26 ppm and (CD₃)₂SO = 2.50 ppm for ¹H NMR; CDCl₃ = 77.0 ppm and (CD₃)₂SO = 39.5 ppm for ¹³C NMR). The following abbreviations were used for reporting ¹H NMR spectra: chemical shift (δ ppm), s = singlet, d = doublet, t = triplet, q = quartet, quin = quintuplet, sext = sextet, sep = septet, dd = doublet of doublets, ddd = doublets of doublets of doublets, td = triplets of doublets, dt = doublets of triplets, br. = broad, app. = apparent, obs. = obscured and m = multiplet. Coupling constants, *J*, are measured to the nearest 0.1 Hz. Chemical shifts are quoted to 0.01 ppm. All the measurements were performed at 25 °C.

2.2. Synthesis and Characterizations



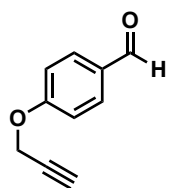
Scheme S1. Synthesis of alkynylated probes **1**, **2** and **4**.

(Prop-2-yn-1-yloxy)benzene (**1**)



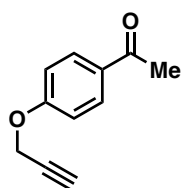
Phenol **18a** (188 mg, 2.0 mmol) was dissolved in 6 mL of ACN/DMF (2:1), followed by addition of a solution of propargyl bromide (0.335 mL, 3.0 mmol, $\rho = 1.335$ g/mL, 80 wt. % in toluene), K₂CO₃ (414 mg, 3.0 mmol) and NaI (150 mg, 1.0 mmol). The mixture was then heated overnight for 16 h at 100 °C. The reaction was monitored by LC-MS and TLC. The mixture was then cooled and the solvent was evaporated under reduced pressure. The crude product was partitioned between EtOAc and water and extracted using EtOAc (3 × 20 mL). The combined organic extract was washed with brine, dried over Na₂SO₄ and evaporated under reduced pressure. The product was purified by flash column chromatography (Hexane/EtOAc 0% → 20%) to afford the pure product **1** as a yellow oil (185 mg, 70%). ¹H NMR (400 MHz, CDCl₃) δ 7.32 (m, *J* = 4.0 Hz, 2 H), 7.00 (m, *J* = 4.2 Hz, 3 H), 4.70 (d, *J* = 2.4 Hz, 2 H), 2.52 (t, *J* = 2.4 Hz, 1 H). ¹³C NMR (101 MHz, CDCl₃) δ 157.54, 129.46, 121.57, 114.89, 78.62, 75.41, 55.73.

4-(Prop-2-yn-1-yloxy)benzaldehyde (**2**)

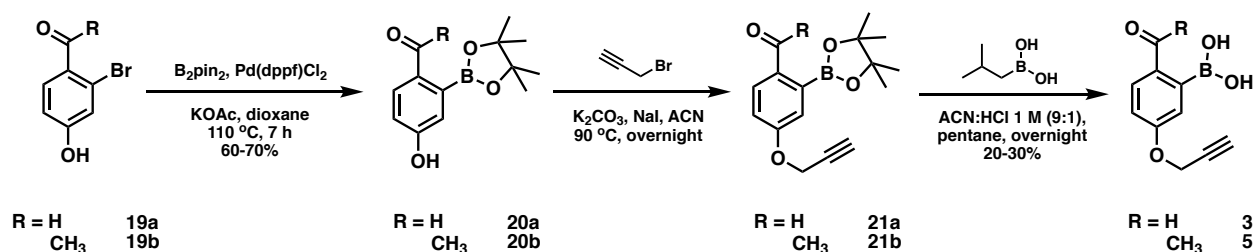


4-Hydroxybenzaldehyde **18b** (244 mg, 2.0 mmol) was dissolved in 6 mL of ACN/DMF (2:1), followed by addition of a solution of propargyl bromide (0.335 mL, 3.0 mmol, $\rho = 1.335$ g/mL, 80 wt. % in toluene), K_2CO_3 (414 mg, 3.0 mmol) and NaI (450 mg, 3.0 mmol). The mixture was then heated overnight for 16 h at 100 °C. The reaction was monitored by LC-MS. The mixture was then cooled and the solvent was evaporated under reduced pressure. The crude product was partitioned between EtOAc and water, and extracted using EtOAc (3 \times 20 mL). The combined organic extract was washed with brine, dried over Na_2SO_4 and evaporated under reduced pressure. The product was purified by flash column chromatography (Hexane/EtOAc 0% \rightarrow 20%) to afford the pure product **2** as a white powder (250 mg, 78%). LC-MS: m/z 161 $[M+H]^+$. 1H NMR (400 MHz, $CDCl_3$) δ 9.90 (s, 1 H), 7.86 (d, $J = 8.8$ Hz, 2 H), 7.09 (d, $J = 8.8$ Hz, 2 H), 4.78 (d, $J = 2.4$ Hz, 2 H), 2.57 (t, $J = 2.4$ Hz, 1 H). ^{13}C NMR (101 MHz, $CDCl_3$) δ 190.72, 162.36, 131.86, 130.61, 115.17, 77.52, 76.33, 55.94.

1-(4-(Prop-2-yn-1-yloxy)phenyl)ethan-1-one (**4**)

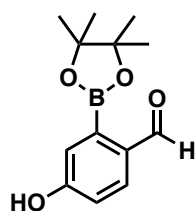


4-Hydroxyacetophenone **18c** (272 mg, 2.0 mmol) was dissolved in 6 mL of ACN/DMF (2:1), followed by addition of a solution of propargyl bromide (0.335 mL, 3.0 mmol, $\rho = 1.335$ g/mL, 80 wt. % in toluene), K_2CO_3 (414 mg, 3.0 mmol) and NaI (450 mg, 3.0 mmol). The mixture was then heated overnight for 16 h at 100 °C. The reaction was monitored by LC-MS. The mixture was then cooled and the solvent was evaporated under reduced pressure. The crude product was partitioned between EtOAc and water, and extracted using EtOAc (3 \times 20 mL). The combined organic extract was washed with brine, dried over Na_2SO_4 and evaporated under reduced pressure. The product was purified by flash column chromatography (Hexane/EtOAc 0% \rightarrow 20%) to afford the pure product **4** as a white powder (261 mg, 75%). LC-MS: m/z 175 $[M+H]^+$. 1H NMR (400 MHz, $CDCl_3$) δ 7.95 (d, $J = 8.8$ Hz, 2 H), 7.02 (d, $J = 8.8$ Hz, 2 H), 4.76 (d, $J = 2.4$ Hz, 2 H), 2.56 (s, 3 H), 2.55 (t, $J = 2.4$ Hz, 1 H). ^{13}C NMR (101 MHz, $CDCl_3$) δ 196.67, 161.26, 131.06, 130.49, 114.56, 77.74, 76.11, 55.83, 26.34.



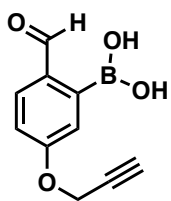
Scheme S2. Synthesis of alkynylated carbonyl boronic acid probes **3** and **5**.

4-Hydroxy-2-(4,4,5,5-tetramethyl-1,3,2-dioxaborolan-2-yl)benzaldehyde (**20a**)



The intermediate was synthesized following the reported procedure.^[2] A mixture of 2-bromo-4-hydroxybenzaldehyde **19a** (500 mg, 2.49 mmol), B_2pin_2 (822 mg, 3.24 mmol), $Pd(dppf)Cl_2 \cdot CH_2Cl_2$ (203 mg, 0.249 mmol) and KOAc (733 mg, 7.47 mmol) was dissolved in 8 mL of dioxane and then stirred at 100 °C in a sealed tube for 7 h. The product formation was confirmed by TLC and LC-MS and the solvent was evaporated under reduced pressure. The crude product was partitioned between EtOAc and water and extracted using EtOAc (3 \times 20 mL). The combined organic extract was washed with brine, dried over Na_2SO_4 and evaporated under reduced pressure. The crude product was purified by flash chromatography ($\lambda_{max} = 285$ nm, hexane/EtOAc = 9:1) to give a bright orange solid **20a** (438 mg, 71%). LC-MS: m/z 249.2 $[M+H]^+$, m/z 247.1 $[M-H]^-$.

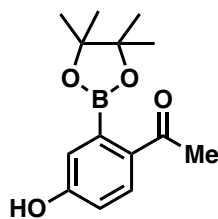
(2-Formyl-5-(prop-2-yn-1-yloxy)phenyl)boronic acid (**3**)



4-Hydroxy-2-(4,4,5,5-tetramethyl-1,3,2-dioxaborolan-2-yl)benzaldehyde **20a** (203 mg, 0.82 mmol) was dissolved in 6 mL of ACN/DMF (2:1), followed by addition of a solution of propargyl bromide (0.143 mL, 1.28 mmol, $\rho = 1.335$ g/mL, 80 wt. % in toluene), K_2CO_3 (177 mg, 1.28 mmol) and NaI (192 mg, 1.28 mmol). The mixture was then heated overnight for 16 h at 100 °C. The reaction was monitored by LC-MS and both boronic acid and boronic ester products were observed. The mixture was then cooled and the solvent was

evaporated under reduced pressure. The crude product **21a** was partitioned between EtOAc and water and extracted using EtOAc (3 \times 20 mL). The combined organic extract was washed with brine, dried over Na_2SO_4 and evaporated under reduced pressure. (2-Methylpropyl)boronic acid (418 mg, 4.1 mmol) dissolved in 5 mL of ACN/1 M HCl (9:1) was added to the crude product. The deprotection was monitored by LC-MS for 24 h. The product was purified by reverse-phase chromatography using 5% to 95% acetonitrile in H_2O with 0.1% formic acid ($\lambda_{max} = 290$ nm, eluted at 30% acetonitrile in water) to afford the pure product as a white powder **3** (33 mg, 20%). LC-MS: m/z 249.1 $[M-H+2Na]^+$. 1H NMR (400 MHz, $(CD_3)_2SO$) δ 9.97 (s, 1 H), 8.26 (s, 2 H), 7.87 (d, $J = 4.4$ Hz, 1 H), 7.12 (d, $J = 7.8$ Hz, 2 H), 4.92 (d, $J = 2.4$ Hz, 2 H), 3.62 (t, $J = 2.3$ Hz, 1 H). ^{13}C NMR (101 MHz, $(CD_3)_2SO$) δ 192.37, 160.83, 132.92, 132.26, 119.08, 114.51, 78.73, 78.68, 55.62.

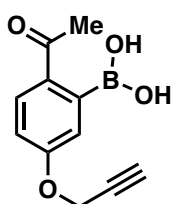
1-(4-Hydroxy-2-(4,4,5,5-tetramethyl-1,3,2-dioxaborolan-2-yl)phenyl)ethan-1-one (**20b**)



A mixture of 1-(2-bromo-4-hydroxyphenyl)ethanone **19b** (430 mg, 2.0 mmol), B_2pin_2 (660 mg, 2.6 mmol), $Pd(dppf)Cl_2 \cdot CH_2Cl_2$ (163 mg, 0.2 mmol) and KOAc (589 mg, 6.0 mmol) was dissolved in 8 mL of dioxane and then stirred at 100 °C in a sealed tube for 7 h. The product formation was confirmed by TLC and LC-MS and the solvent was evaporated under reduced pressure. The crude product was partitioned between EtOAc and water, and extracted using EtOAc (3 \times 20 mL). The combined organic extract was

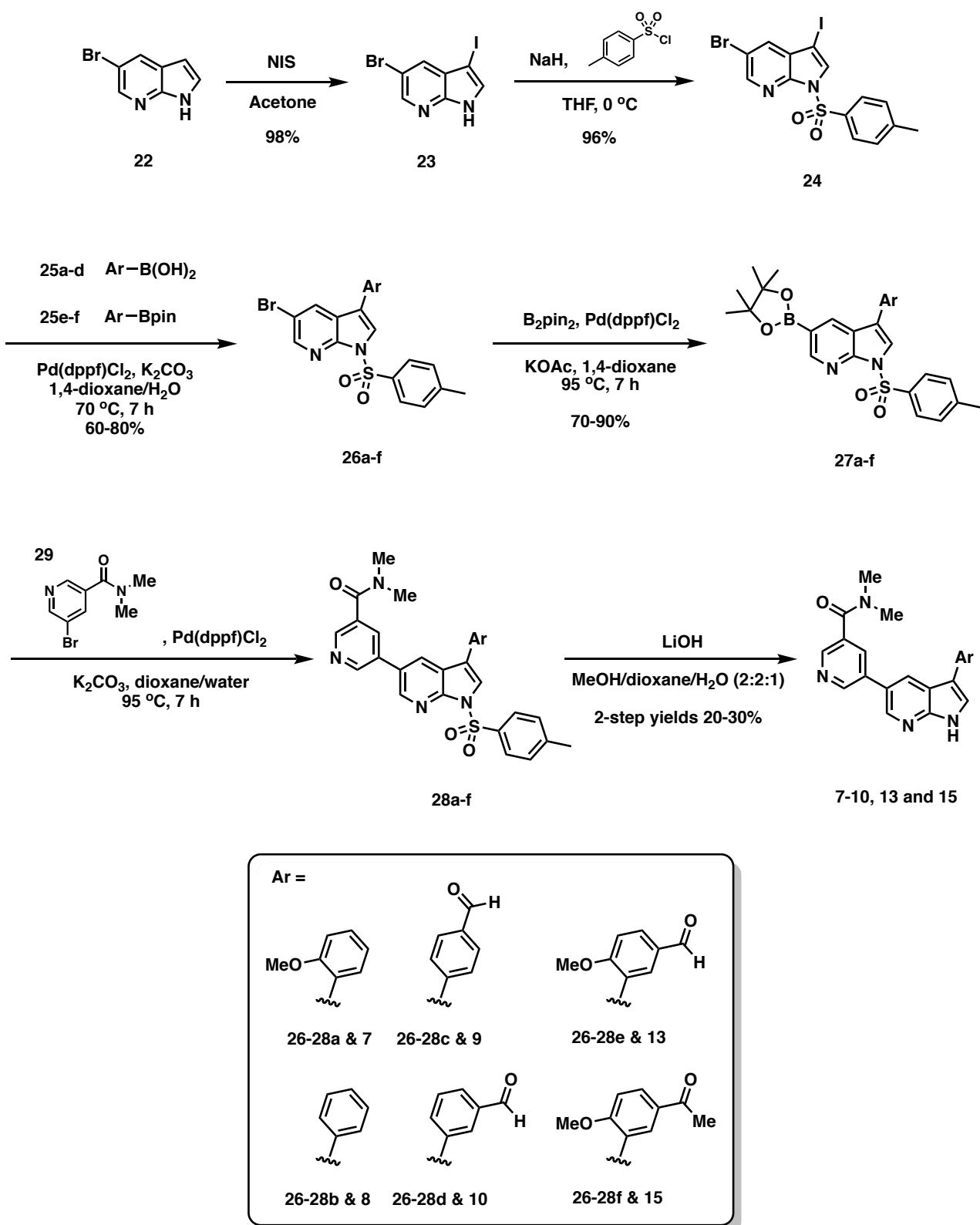
washed with brine, dried over Na_2SO_4 and evaporated under reduced pressure. The crude product was purified by flash chromatography ($\lambda_{max} = 260$ nm, hexane/EtOAc = 9:1) to give **20b** as a bright orange solid (363 mg, 70%). LC-MS: m/z 263.2 $[M+H]^+$, m/z 261.2 $[M-H]^-$. 1H NMR (400 MHz, $CDCl_3$) δ 12.06 (s, 1 H), 7.70 (d, $J = 7.9$ Hz, 1 H), 7.41 (s, 1 H), 7.29 (dd, $J = 2.9$ Hz, 1 H), 2.64 (s, 3 H), 1.35 (s, 12 H). ^{13}C NMR (101 MHz, $CDCl_3$) δ 204.70, 161.35, 129.60, 124.81, 124.44, 121.17, 84.30, 26.76, 24.84.

(2-Acetyl-5-(prop-2-yn-1-yloxy)phenyl)boronic acid (**5**)



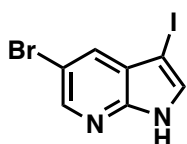
1-(4-Hydroxy-2-(4,4,5,5-tetramethyl-1,3,2-dioxaborolan-2-yl)phenyl)ethan-1-one **20b** (215 mg, 0.82 mmol) was dissolved in 6 mL of ACN/DMF (2:1), followed by addition of a solution of propargyl bromide (0.143 mL, 1.28 mmol, $\rho = 1.335$ g/mL, 80 wt. % in toluene), K_2CO_3 (177 mg, 1.28 mmol) and NaI (192 mg, 1.28 mmol). The mixture was then heated overnight for 16 h at 100 °C. The reaction was monitored by LC-MS and both boronic acid and boronic ester products were observed. The mixture was then cooled and the solvent was

evaporated under reduced pressure. The crude product **21b** was partitioned between EtOAc and water, and extracted using EtOAc (3 \times 20 mL). The combined organic extract was washed with brine, dried over Na_2SO_4 and evaporated under reduced pressure. The product was purified by flash column chromatography (Hexane/EtOAc 0% \rightarrow 30%). The solvent was evaporated under reduced pressure. (2-Methylpropyl)boronic acid (418 mg, 4.1 mmol) dissolved in 5 mL of ACN/1 M HCl (9:1) was added to the crude product. The deprotection was monitored by LC-MS for 24 h. Upon completion, the final product was purified by reverse-phase chromatography using 5% to 95% acetonitrile in H_2O with 0.1% formic acid ($\lambda_{max} = 254$ nm, eluted at 30% acetonitrile in water) to afford the pure product **5** as a white powder (50 mg, 28%). LC-MS: m/z 219.1 $[M+H]^+$. 1H NMR (400 MHz, $(CD_3)_2SO$) δ 8.26 (s, 2 H), 7.60 (s, 1 H), 7.52 (d, $J = 7.6$ Hz, 1 H), 7.46 (d, $J = 7.6$ Hz, 1 H), 4.93 (d, $J = 2.4$ Hz, 2 H), 3.62 (t, $J = 2.3$ Hz, 1 H), 2.54 (s, 3 H). ^{13}C NMR (101 MHz, $(CD_3)_2SO$) δ 199.18, 155.44, 129.87, 128.26, 126.80, 119.04, 78.89, 78.49, 56.08, 31.56.



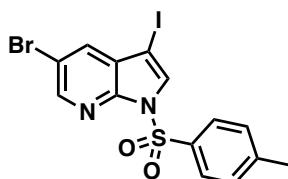
Scheme S3. Synthesis of ABL inhibitors 7, 8, 9, 10, 13 and 15.

5-Bromo-3-iodo-1*H*-pyrrolo[2,3-*b*]pyridine (**23**)



5-Bromo-1*H*-pyrrolo[2,3-*b*]pyridine **22** (4.50 g, 22.8 mmol) was dissolved in 125 mL of acetone which was stirred for about 20 min. *N*-Iodosuccinimide (6.16 g, 27.4 mmol) was added to the solution at room temperature and stirred for another 1 h. The mixture was then concentrated and extracted with EtOAc (3 × 30 mL). The combined organic layers were washed with saturated solution of Na₂S₂O₃ and brine, dried over Na₂SO₄ and evaporated under reduced pressure to afford the product **23** as an off-white solid (7.2 g, 98%). LC-MS: *m/z* 322.9 and 324.9 [M+H]⁺. ¹H NMR (400 MHz, (CD₃)₂SO) δ 12.34 (s, 1 H), 8.31 (d, *J* = 2.2 Hz, 1 H), 7.85 (d, *J* = 2.0 Hz, 1 H), 7.79 (d, *J* = 2.5 Hz, 1 H).

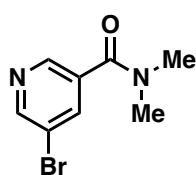
5-Bromo-3-iodo-1-tosyl-1*H*-pyrrolo[2,3-*b*]pyridine (**24**)



To a stirred solution of 5-bromo-3-iodo-1*H*-pyrrolo[2,3-*b*]pyridine **23** (6.46 g, 20 mmol) in 100 mL of anhydrous THF cooled to 0 °C in an ice bath was added NaH (1.2 g, 30 mmol, 60% dispersion in mineral oil). The reaction mixture was stirred for 20 min at 0 °C, after which *p*-toluenesulfonyl chloride (4.58 g, 24 mmol) was added. The resulting mixture was allowed to warm to room temperature over 1 h.

Upon completion as confirmed by LCMS and TLC, the reaction mixture was evaporated to dryness, quenched with water and filtered. The crude product was mixed with 150 mL of EtOAc and refluxed for 1 h, followed by precipitation with 75 mL of hexane. The product **24** was obtained as an off-white powder (9.18 g, 96%). LC-MS: *m/z* 476.9 and 478.9 [M+H]⁺. ¹H NMR (400 MHz, CDCl₃) δ 8.44 (d, *J* = 2.1 Hz, 1 H), 8.05 (dd, *J* = 2.8 Hz, 2 H), 7.86 (s, 1 H), 7.80 (d, *J* = 2.1 Hz, 1 H), 7.29 (d, *J* = 8.0 Hz, 2 H), 2.38 (s, 3 H).

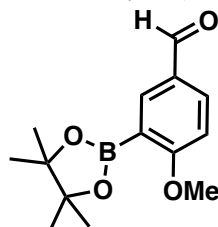
5-Bromo-*N,N*-dimethylnicotinamide (**29**)



To a solution of 5-bromonicotinic acid (2 g, 10 mmol) in 20 mL of DMF was added HATU (5.7 g, 15 mmol) and NEt₃ (4.18 mL, 30 mmol, ρ = 0.726 g/mL). The reaction mixture was stirred for 5 min, followed by addition of dimethylamine hydrochloride (1.22 g, 15 mmol) and K₂CO₃ (2.07 g, 15 mmol). The reaction was continuously stirred for another 3 h and the product formation was monitored and confirmed by LC-MS. Next,

saturated NaHCO₃ solution was added and the mixture was extracted with EtOAc (3 × 20 mL). The combined organic extract was washed with brine, dried over Na₂SO₄ and evaporated under reduced pressure. The crude product **29** was obtained as a brown oil (λ_{max} = 270 nm), and used directly in the next step without further purification. LC-MS: *m/z* 229 and 231 [M+H]⁺. ¹H NMR (400 MHz, (CD₃)₂SO) δ 8.77 (d, *J* = 2.2 Hz, 1 H), 8.60 (d, *J* = 1.7 Hz, 1 H), 7.95 (s, 1 H), 2.99 (br. s, 3 H), 2.92 (br. s, 3 H).

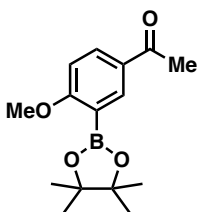
4-Methoxy-3-(4,4,5,5-tetramethyl-1,3,2-dioxaborolan-2-yl)benzaldehyde (**25e**)



A mixture of 3-bromo-4-methoxybenzaldehyde (645 mg, 3.0 mmol), B₂pin₂ (915 mg, 3.6 mmol), Pd(dppf)Cl₂·CH₂Cl₂ (245 mg, 0.3 mmol) and KOAc (884 mg, 9.0 mmol) was dissolved in 8 mL of dioxane and then stirred at 100 °C in a sealed tube for 7 h. The product formation was confirmed by TLC and LC-MS. Upon solvent evaporation, the crude product was partitioned between EtOAc and water, and extracted using EtOAc (3 × 20 mL). The combined organic extract was washed with brine, dried over Na₂SO₄ and evaporated under reduced pressure. The crude product was purified by flash chromatography (λ_{max} = 280 nm, hexane/EtOAc 0% → 10%) to give **25e** as a bright orange product (362 mg, 46%). LC-MS: *m/z* 263 [M+H]⁺.

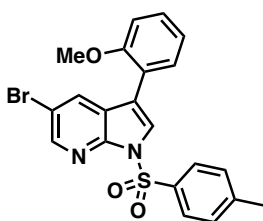
¹H NMR (400 MHz, CDCl₃) δ 9.88 (s, 1 H), 8.19 (d, *J* = 2.2 Hz, 1 H), 7.95 (dd, *J* = 3.6 Hz, 1 H), 6.96 (d, *J* = 8.6 Hz, 1 H), 3.91 (s, 3 H), 1.36 (s, 12 H). ¹³C NMR (101 MHz, CDCl₃) δ 190.99, 168.81, 139.94, 134.08, 129.27, 110.49, 83.90, 56.03, 24.77.

1-(4-Methoxy-3-(4,4,5,5-tetramethyl-1,3,2-dioxaborolan-2-yl)phenyl)ethan-1-one (25f)



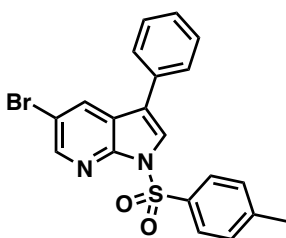
A mixture of 1-(3-bromo-4-methoxyphenyl)ethanone (550 mg, 2.4 mmol), B₂pin₂ (732 mg, 2.9 mmol), Pd(dppf)Cl₂.CH₂Cl₂ (195 mg, 0.24 mmol) and KOAc (707 mg, 7.2 mmol) was dissolved in 7 mL of dioxane and then stirred at 100 °C in a sealed tube for 16 h. The product formation was confirmed by TLC and LC-MS. Upon solvent evaporation, the crude product was partitioned between EtOAc and water, and extracted using EtOAc (3 × 20 mL). The combined organic extract was washed with brine, dried over Na₂SO₄ and evaporated under reduced pressure. The crude product was purified by flash chromatography (λ_{max} = 260 nm, hexane/EtOAc 0% → 30%) to give **25f** as a white product (225 mg, 34%). LC-MS: *m/z* 277.1 [M+H]⁺. ¹H NMR (400 MHz, CDCl₃) δ 8.26 (d, *J* = 2.2 Hz, 1 H), 8.05 (dd, *J* = 3.7 Hz, 1 H), 6.89 (d, *J* = 8.7 Hz, 1 H), 3.89 (s, 3 H), 2.57 (s, 3 H), 1.36 (s, 12 H). ¹³C NMR (101 MHz, CDCl₃) δ 196.96, 167.78, 137.75, 133.30, 129.76, 109.95, 83.80, 55.93, 24.80.

5-Bromo-3-(2-methoxyphenyl)-1-tosyl-1H-pyrrolo[2,3-b]pyridine (26a)



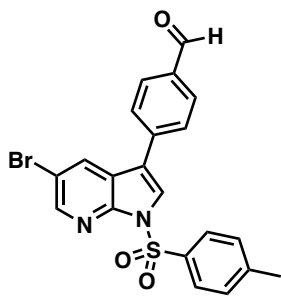
A mixture of 5-bromo-3-iodo-1-tosyl-1H-pyrrolo[2,3-b]pyridine **24** (500 mg, 1.05 mmol), 2-methoxyphenylboronic acid **25a** (160 mg, 1.05 mmol), Pd(dppf)Cl₂.CH₂Cl₂ (86 mg, 0.105 mmol) and K₂CO₃ (435 mg, 3.15 mmol) was dissolved in 7 mL of dioxane and 1 mL of water and then stirred at 70 °C in a sealed tube for 7 h. The product formation was confirmed by TLC and LC-MS. Upon solvent evaporation, the crude product was partitioned between EtOAc and water, and extracted using EtOAc (3 × 20 mL). The combined organic extract was washed with brine, dried over Na₂SO₄ and evaporated under reduced pressure. The crude product was purified by flash chromatography (λ_{max} = 250 nm, hexane/EtOAc 0% → 70% due to solubility issue) to give **26a** as a tan powder (341 mg, 71%). LC-MS: *m/z* 457 and 459 [M+H]⁺. ¹H NMR (400 MHz, (CD₃)₂SO) δ 8.50 (d, *J* = 2.1 Hz, 1 H), 8.14 (d, *J* = 2.2 Hz, 1 H), 8.07 (s, 1 H), 8.04 (dd, *J* = 2.8 Hz, 2 H), 7.54 (dd, *J* = 3.1 Hz, 1 H), 7.43 (dd, *J* = 4.0 Hz, 2 H), 7.40 (m, *J* = 2 Hz, 1 H), 7.16 (dd, *J* = 3.0 Hz, 1 H), 7.06 (td, *J* = 3.2 Hz, 1 H), 3.81 (s, 3 H), 2.34 (s, 3 H). ¹³C NMR (101 MHz, (CD₃)₂SO) δ 156.35, 145.92, 144.89, 144.79, 134.23, 132.33, 130.29, 130.13, 129.57, 127.68, 126.14, 123.40, 120.82, 119.69, 116.00, 114.98, 111.70, 55.38, 21.09.

5-Bromo-3-phenyl-1-tosyl-1H-pyrrolo[2,3-b]pyridine (26b)



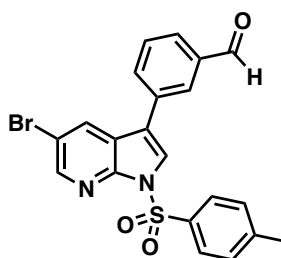
A mixture of 5-bromo-3-iodo-1-tosyl-1H-pyrrolo[2,3-b]pyridine **24** (500 mg, 1.05 mmol), phenylboronic acid **25b** (128 mg, 1.05 mmol), Pd(dppf)Cl₂.CH₂Cl₂ (86 mg, 0.105 mmol) and K₂CO₃ (435 mg, 3.15 mmol) was dissolved in 7 mL of dioxane and 1 mL of water and then stirred at 70 °C in a sealed tube for 7 h. The product formation was confirmed by TLC and LC-MS. Upon solvent evaporation, the crude product was partitioned between EtOAc and water, and extracted using EtOAc (3 × 20 mL). The combined organic extract was washed with brine, dried over Na₂SO₄ and evaporated under reduced pressure. The crude product was purified by flash chromatography (λ_{max} = 254 nm, hexane/EtOAc 0% → 70% due to solubility issue) to give **26b** as an off-white solid product (291 mg, 65%). LC-MS: *m/z* 427 and 429 [M+H]⁺. ¹H NMR (400 MHz, (CD₃)₂SO) δ 8.54 (d, *J* = 2.0 Hz, 1 H), 8.49 (d, *J* = 2.2 Hz, 1 H), 8.28 (s, 1 H), 8.04 (dd, *J* = 2.8 Hz, 2 H), 7.78 (m, *J* = 2.4 Hz, 2 H), 7.49 (td, *J* = 3.8 Hz, 2 H), 7.41 (m, *J* = 3.2 Hz, 3 H), 2.34 (s, 3 H). ¹³C NMR (101 MHz, (CD₃)₂SO) δ 145.94, 145.31, 145.24, 134.18, 131.45, 131.35, 130.12, 129.09, 127.82, 127.68, 127.38, 124.91, 122.28, 118.98, 115.45, 21.09.

4-(5-Bromo-1-tosyl-1*H*-pyrrolo[2,3-*b*]pyridin-3-yl)benzaldehyde (26c)



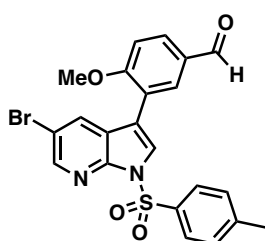
A mixture of 5-bromo-3-iodo-1-tosyl-1*H*-pyrrolo[2,3-*b*]pyridine **24** (500 mg, 1.05 mmol), 4-formylphenylboronic acid **25c** (157 mg, 1.05 mmol), Pd(dppf)Cl₂.CH₂Cl₂ (86 mg, 0.105 mmol) and K₂CO₃ (435 mg, 3.15 mmol) was dissolved in 7 mL of dioxane and 1 mL of water and then stirred at 70 °C in a sealed tube for 7 h. The product formation was confirmed by TLC and LC-MS. Upon solvent evaporation, the crude product was partitioned between EtOAc and water, and extracted using EtOAc (3 × 20 mL). The combined organic extract was washed with brine, dried over Na₂SO₄ and evaporated under reduced pressure. The crude product was purified by flash chromatography (λ_{max} = 300 nm, hexane/EtOAc 0% → 70% due to solubility issue) to give **26c** as a yellow powder (325 mg, 68%). LC-MS: *m/z* 455 and 457 [M+H]⁺. ¹H NMR (400 MHz, CDCl₃) δ 10.06 (s, 1 H), 8.52 (d, *J* = 2.1 Hz, 1 H), 8.24 (d, *J* = 2.2 Hz, 1 H), 8.11 (dd, *J* = 2.8 Hz, 2 H), 8.00 (m, *J* = 2.6 Hz, 3 H), 7.73 (dd, *J* = 2.7 Hz, 2 H), 7.32 (d, *J* = 4.3 Hz, 2 H), 2.40 (s, 3 H). ¹³C NMR (101 MHz, CDCl₃) δ 191.45, 146.14, 145.89, 145.71, 138.28, 135.52, 134.69, 130.98, 130.59, 129.85, 128.33, 127.69, 125.15, 122.46, 118.20, 115.79, 21.69.

3-(5-Bromo-1-tosyl-1*H*-pyrrolo[2,3-*b*]pyridin-3-yl)benzaldehyde (26d)



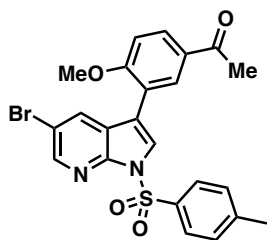
A mixture of 5-bromo-3-iodo-1-tosyl-1*H*-pyrrolo[2,3-*b*]pyridine **24** (500 mg, 1.05 mmol), 3-formylphenylboronic acid **25d** (157 mg, 1.05 mmol), Pd(dppf)Cl₂.CH₂Cl₂ (86 mg, 0.105 mmol) and K₂CO₃ (435 mg, 3.15 mmol) was dissolved in 7 mL of dioxane and 1 mL of water and then stirred at 70 °C in a sealed tube for 7 h. The product formation was confirmed by TLC and LC-MS. Upon solvent evaporation, the crude product was partitioned between EtOAc and water, and extracted using EtOAc (3 × 20 mL). The combined organic extract was washed with brine, dried over Na₂SO₄ and evaporated under reduced pressure. The crude product was purified by flash chromatography (λ_{max} = 254 nm, hexane/EtOAc 0% → 70% due to solubility issue) to give **26d** as a tan powder (359 mg, 75%). LC-MS: *m/z* 455 and 457 [M+H]⁺. ¹H NMR (400 MHz, CDCl₃) δ 10.10 (s, 1 H), 8.51 (d, *J* = 2.0 Hz, 1 H), 8.20 (d, *J* = 2.1 Hz, 1 H), 8.10 (d, *J* = 8.4 Hz, 2 H), 8.05 (t, *J* = 1.5 Hz, 1 H), 7.97 (s, 1 H), 7.89 (dt, *J* = 1.7 Hz, 1 H), 7.82 (dt, *J* = 1.5 Hz, 1 H), 7.67 (t, *J* = 7.7 Hz, 1 H), 7.31 (d, *J* = 8.0 Hz, 2 H), 2.40 (s, 3 H). ¹³C NMR (101 MHz, CDCl₃) δ 191.82, 146.08, 145.79, 145.67, 137.17, 134.78, 133.21, 133.12, 132.96, 130.78, 129.97, 129.83, 129.76, 129.48, 129.44, 128.27, 127.97, 127.85, 124.64, 122.64, 118.19, 115.70, 21.68.

3-(5-Bromo-1-tosyl-1*H*-pyrrolo[2,3-*b*]pyridin-3-yl)-4-methoxybenzaldehyde (26e)



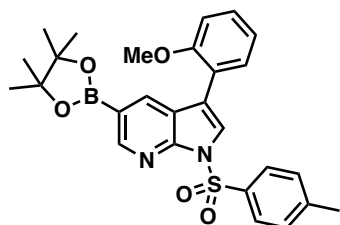
A mixture of 5-bromo-3-iodo-1-tosyl-1*H*-pyrrolo[2,3-*b*]pyridine **24** (1 g, 2.1 mmol), 4-methoxy-5-(4,4,5,5-tetramethyl-1,3,2-dioxaborolan-2-yl)benzaldehyde **25e** (550 mg, 2.1 mmol), Pd(dppf)Cl₂.CH₂Cl₂ (171 mg, 0.21 mmol) and K₂CO₃ (870 mg, 6.3 mmol) was dissolved in 7 mL of dioxane and 1 mL of water and then stirred at 70 °C in a sealed tube for 7 h. The product formation was confirmed by TLC and LC-MS. Upon solvent evaporation, the crude product was partitioned between EtOAc and water, and extracted using EtOAc (3 × 20 mL). The combined organic extract was washed with brine, dried over Na₂SO₄ and evaporated under reduced pressure. The crude product was purified by flash chromatography (λ_{max} = 254 nm, hexane/EtOAc 0% → 70% due to solubility issue) to give **26e** as a yellow solid (662 mg, 65%). LC-MS: *m/z* 485 and 487 [M+H]⁺. ¹H NMR (400 MHz, CDCl₃) δ 9.95 (s, 1 H), 8.48 (d, *J* = 2.0 Hz, 1 H), 8.10 (d, *J* = 8.4 Hz, 2 H), 7.99 (d, *J* = 2.2 Hz, 1 H), 7.97 (s, 1 H), 7.95 (d, *J* = 2.1 Hz, 1 H), 7.91 (dd, *J* = 3.5 Hz, 1 H), 7.31 (d, *J* = 9.2 Hz, 2 H), 7.15 (d, *J* = 8.5 Hz, 1 H), 3.96 (s, 3 H), 2.40 (s, 3 H). ¹³C NMR (101 MHz, CDCl₃) δ 190.50, 161.54, 145.61, 145.58, 145.27, 134.97, 132.26, 131.81, 131.21, 130.00, 129.78, 128.24, 126.57, 123.67, 121.87, 115.31, 114.51, 111.25, 56.00, 21.67.

1-(3-(5-Bromo-1-tosyl-1*H*-pyrrolo[2,3-*b*]pyridin-3-yl)-4-methoxyphenyl)ethan-1-one (26f)



A mixture of 5-bromo-3-iodo-1-tosyl-1*H*-pyrrolo[2,3-*b*]pyridine **24** (716 mg, 1.5 mmol), 1-(4-methoxy-3-(4,4,5,5-tetramethyl-1,3,2-dioxaborolan-2-yl)phenyl)ethan-1-one **25f** (414 mg, 1.5 mmol), Pd(dppf)Cl₂.CH₂Cl₂ (122 mg, 0.15 mmol) and K₂CO₃ (621 mg, 4.5 mmol) was dissolved in 7 mL of dioxane and 1 mL of water and then stirred at 70 °C in a sealed tube for 7 h. The product formation was confirmed by TLC and LC-MS. Upon solvent evaporation, the crude product was partitioned between EtOAc and water, and extracted using EtOAc (3 × 20 mL). The combined organic extract was washed with brine, dried over Na₂SO₄ and evaporated under reduced pressure. The crude product was purified by flash chromatography (λ_{max} = 250 nm, hexane/EtOAc 0% → 70%) to give **26f** as a yellow solid (484 mg, 65%). LC-MS: *m/z* 499 and 501 [M+H]⁺. ¹H NMR (400 MHz, CDCl₃) δ 8.47 (s, 1 H), 8.10 (d, *J* = 7.4 Hz, 2 H), 7.99 (m, *J* = 8.9 Hz, 4 H), 7.31 (d, *J* = 7.0 Hz, 2 H), 7.06 (d, *J* = 7.6 Hz, 1 H), 3.90 (s, 3 H), 2.60 (s, 3 H), 2.39 (s, 3 H). ¹³C NMR (101 MHz, CDCl₃) δ 196.44, 160.49, 145.55, 145.50, 145.31, 135.04, 131.90, 130.63, 130.49, 130.46, 129.76, 128.24, 126.37, 123.82, 121.09, 115.27, 115.00, 110.69, 55.85, 26.38, 21.66.

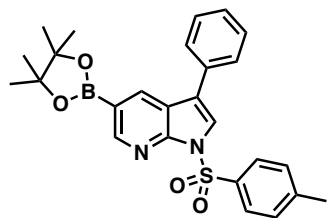
3-(2-Methoxyphenyl)-5-(4,4,5,5-tetramethyl-1,3,2-dioxaborolan-2-yl)-1-tosyl-1*H*-pyrrolo[2,3-*b*]pyridine (27a)



A mixture of 5-bromo-3-(2-methoxyphenyl)-1-tosyl-1*H*-pyrrolo[2,3-*b*]pyridine **26a** (640 mg, 1.4 mmol), B₂pin₂ (427 mg, 1.68 mmol), Pd(dppf)Cl₂.CH₂Cl₂ (114 mg, 0.14 mmol) and KOAc (413 mg, 4.2 mmol) was dissolved in 8 mL of dioxane and then stirred at 100 °C in a sealed tube for 7 h. The product formation was confirmed by LC-MS. Upon solvent evaporation, the crude product was partitioned between EtOAc and water, and extracted using EtOAc (3 × 20 mL). The combined organic extract was

washed with brine, dried over Na₂SO₄ and evaporated under reduced pressure. The crude product was purified by flash chromatography (λ_{max} = 254 nm, hexane/EtOAc 0% → 60%) to give **27a** as a viscous yellow foam (635 mg, 90%). LC-MS: *m/z* 505 [M+H]⁺. ¹H NMR (400 MHz, CDCl₃) δ 8.79 (d, *J* = 1.5 Hz, 1 H), 8.31 (d, *J* = 1.5 Hz, 1 H), 8.11 (d, *J* = 8.4 Hz, 2 H), 7.94 (s, 1 H), 7.50 (dd, *J* = 3.1 Hz, 1 H), 7.35 (td, *J* = 2.5 Hz, 1 H), 7.25 (d, *J* = 8 Hz, 2 H), 7.06 (td, *J* = 3.2 Hz, 1 H), 7.02 (d, *J* = 3.03 Hz, 1 H), 3.85 (s, 3 H), 2.36 (s, 3 H), 1.32 (s, 12 H). ¹³C NMR (101 MHz, CDCl₃) δ 156.80, 150.87, 148.77, 145.04, 136.27, 135.44, 130.44, 129.52, 128.88, 128.19, 124.75, 121.97, 121.29, 120.81, 116.31, 111.22, 83.99, 55.40, 24.79, 21.60.

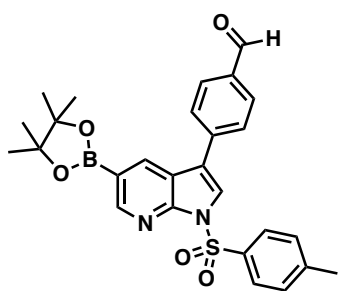
3-Phenyl-5-(4,4,5,5-tetramethyl-1,3,2-dioxaborolan-2-yl)-1-tosyl-1*H*-pyrrolo[2,3-*b*]pyridine (27b)



A mixture of 5-bromo-3-phenyl-1-tosyl-1*H*-pyrrolo[2,3-*b*]pyridine **26b** (641 mg, 1.5 mmol), B₂pin₂ (457 mg, 1.8 mmol), Pd(dppf)Cl₂.CH₂Cl₂ (122 mg, 0.15 mmol) and KOAc (442 mg, 4.5 mmol) was dissolved in 8 mL of dioxane and then stirred at 100 °C in a sealed tube for 7 h. The product formation was confirmed by LC-MS. Upon solvent evaporation, the crude product was

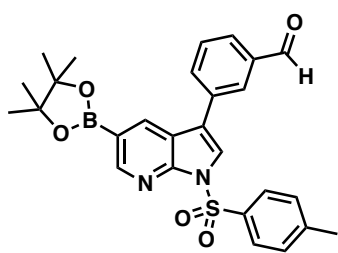
partitioned between EtOAc and water, and extracted using EtOAc (3 × 20 mL). The combined organic extract was washed with brine, dried over Na₂SO₄ and evaporated under reduced pressure. The crude product was purified by flash chromatography (λ_{max} = 250 nm, hexane/EtOAc 0% → 60%) to give **27b** as a viscous yellow foam (563 mg, 79%). LC-MS: *m/z* 475 [M+H]⁺. ¹H NMR (400 MHz, CDCl₃) δ 8.82 (d, *J* = 1.5 Hz, 1 H), 8.47 (d, *J* = 1.6 Hz, 1 H), 8.11 (d, *J* = 8.4 Hz, 2 H), 7.86 (s, 1 H), 7.61 (dd, *J* = 3.2 Hz, 2 H), 7.48 (t, *J* = 5.1 Hz, 2 H), 7.37 (t, *J* = 7.4 Hz, 1 H), 7.26 (d, *J* = 8 Hz, 2 H), 2.36 (s, 3 H), 1.34 (s, 12 H). ¹³C NMR (101 MHz, CDCl₃) δ 151.30, 149.16, 145.22, 135.46, 135.27, 132.60, 129.59, 129.03, 128.19, 127.66, 122.44, 121.02, 120.58, 84.13, 24.81, 21.61.

4-(5-(4,4,5,5-Tetramethyl-1,3,2-dioxaborolan-2-yl)-1-tosyl-1*H*-pyrrolo[2,3-*b*]pyridin-3-yl)benzaldehyde (27c)



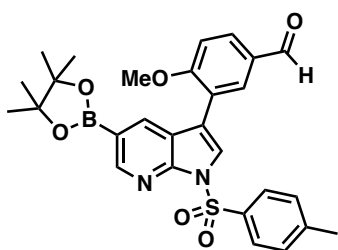
A mixture of 4-(5-bromo-1-tosyl-1*H*-pyrrolo[2,3-*b*]pyridin-3-yl)benzaldehyde **26c** (637 mg, 1.4 mmol), B₂pin₂ (427 mg, 1.68 mmol), Pd(dppf)Cl₂.CH₂Cl₂ (114 mg, 0.14 mmol) and KOAc (413 mg, 4.2 mmol) was dissolved in 8 mL of dioxane and then stirred at 100 °C in a sealed tube for 7 h. The product formation was confirmed by LC-MS. Upon solvent evaporation, the crude product was partitioned between EtOAc and water, and extracted using EtOAc (3 × 20 mL). The combined organic extract was washed with brine, dried over Na₂SO₄ and evaporated under reduced pressure. The crude product was purified by flash chromatography (λ_{max} = 250 nm, hexane/EtOAc 0% → 60%) to give **27c** as a viscous yellow foam (619 mg, 88%). LC-MS: *m/z* 503 [M+H]⁺. ¹H NMR (400 MHz, CDCl₃) δ 10.06 (s, 1 H), 8.85 (d, *J* = 1.5 Hz, 1 H), 8.49 (d, *J* = 1.5 Hz, 1 H), 8.14 (d, *J* = 2.8 Hz, 2 H), 7.99 (m, *J* = 4.2 Hz, 3 H), 7.80 (d, *J* = 2.7 Hz, 2 H), 7.28 (d, *J* = 8.1 Hz, 2 H), 2.37 (s, 3 H), 1.35 (s, 12 H). ¹³C NMR (101 MHz, CDCl₃) δ 191.59, 151.64, 149.09, 145.54, 138.99, 135.33, 135.30, 134.98, 130.50, 129.67, 128.36, 127.89, 123.68, 120.39, 119.11, 84.26, 24.81, 21.65.

3-(5-(4,4,5,5-Tetramethyl-1,3,2-dioxaborolan-2-yl)-1-tosyl-1*H*-pyrrolo[2,3-*b*]pyridin-3-yl)benzaldehyde (27d)



A mixture of 3-(5-bromo-1-tosyl-1*H*-pyrrolo[2,3-*b*]pyridin-3-yl)benzaldehyde **26d** (637 mg, 1.4 mmol), B₂pin₂ (427 mg, 1.68 mmol), Pd(dppf)Cl₂.CH₂Cl₂ (114 mg, 0.14 mmol) and KOAc (413 mg, 4.2 mmol) was dissolved in 8 mL of dioxane and then stirred at 100 °C in a sealed tube for 7 h. The product formation was confirmed by LC-MS. Upon solvent evaporation, the crude product was partitioned between EtOAc and water, and extracted using EtOAc (3 × 20 mL). The combined organic extract was washed with brine, dried over Na₂SO₄ and evaporated under reduced pressure. The crude product was purified by flash chromatography (λ_{max} = 250 nm, hexane/EtOAc 0% → 60%) to give **27d** as a viscous orange foam (640 mg, 91%). LC-MS: *m/z* 503 [M+H]⁺. ¹H NMR (400 MHz, CDCl₃) δ 10.11 (s, 1 H), 8.85 (d, *J* = 1.5 Hz, 1 H), 8.43 (d, *J* = 1.5 Hz, 1 H), 8.13 (d, *J* = 2.8 Hz, 2 H), 8.09 (t, *J* = 1.5 Hz, 1 H), 7.93 (s, 1 H), 7.89 (dd, *J* = 3.1 Hz, 2 H), 7.66 (t, *J* = 7.6 Hz, 1 H), 7.28 (d, *J* = 8.1 Hz, 2 H), 2.37 (s, 3 H), 1.34 (s, 12 H). ¹³C NMR (101 MHz, CDCl₃) δ 192.06, 151.59, 149.03, 145.44, 137.07, 135.08, 133.82, 133.49, 129.80, 129.66, 128.89, 128.51, 128.28, 123.13, 120.59, 119.14, 84.24, 24.81, 21.64.

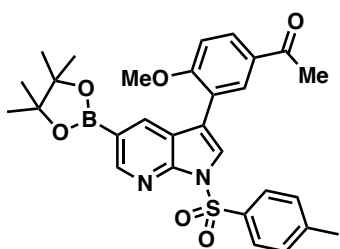
4-Methoxy-3-(5-(4,4,5,5-tetramethyl-1,3,2-dioxaborolan-2-yl)-1-tosyl-1*H*-pyrrolo[2,3-*b*]pyridin-3-yl)benzaldehyde (27e)



A mixture of 3-(5-bromo-1-tosyl-1*H*-pyrrolo[2,3-*b*]pyridin-3-yl)-4-methoxybenzaldehyde **26e** (728 mg, 1.5 mmol), B₂pin₂ (457 mg, 1.8 mmol), Pd(dppf)Cl₂.CH₂Cl₂ (122 mg, 0.15 mmol) and KOAc (442 mg, 4.5 mmol) was dissolved in 8 mL of dioxane and then stirred at 100 °C in a sealed tube for 7 h. The product formation was confirmed by LC-MS. Upon solvent evaporation, the crude product was partitioned between EtOAc and water, and extracted using EtOAc (3 × 20 mL). The combined organic extract was washed with brine, dried over Na₂SO₄ and evaporated under reduced pressure. The crude product was purified by flash chromatography (λ_{max} = 250 nm, hexane/EtOAc 0% → 60%) to give **27e** as a viscous yellow foam (680 mg, 85%). LC-MS: *m/z* 533 [M+H]⁺. ¹H NMR (400 MHz, CDCl₃) δ 9.95 (s, 1 H), 8.24 (d, *J* = 1.6 Hz, 1 H), 8.12 (d, *J* = 8.4 Hz, 2 H), 8.09 (d, *J* = 8.5 Hz, 1 H), 7.98 (d, *J* = 2.1 Hz, 1 H), 7.93 (s, 1 H), 7.90 (dd, *J* = 3.5 Hz, 1 H), 7.27 (d, *J* = 7.6 Hz, 2 H), 7.14 (d, *J* = 8.5 Hz, 1 H), 3.94 (s, 3 H), 2.37 (s, 3 H),

1.34 (12 H). ^{13}C NMR (101 MHz, CDCl_3) δ 190.74, 161.77, 151.15, 145.26, 135.99, 135.25, 131.94, 131.66, 129.87, 129.60, 129.53, 128.24, 128.13, 125.09, 122.39, 121.63, 115.17, 111.20, 84.10, 24.82, 21.62.

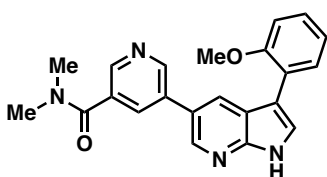
1-(4-Methoxy-3-(5-(4,4,5,5-tetramethyl-1,3,2-dioxaborolan-2-yl)-1-tosyl-1H-pyrrolo[2,3-b]pyridin-3-yl)phenyl)ethan-1-one (27f)



A mixture of 1-(3-(5-bromo-1-tosyl-1H-pyrrolo[2,3-b]pyridin-3-yl)-4-methoxyphenyl)ethan-1-one **26f** (499 mg, 1 mmol), B_2pin_2 (330 mg, 1.3 mmol), $\text{Pd}(\text{dppf})\text{Cl}_2 \cdot \text{CH}_2\text{Cl}_2$ (81 mg, 0.1 mmol) and KOAc (294 mg, 3 mmol) was dissolved in 7 mL of dioxane and then stirred at 100 °C in a sealed tube for 7 h. The product formation was confirmed by LC-MS. Upon solvent evaporation, the crude product was partitioned between EtOAc and water, and extracted using EtOAc (3×20 mL). The combined organic extract was

washed with brine, dried over Na_2SO_4 and evaporated under reduced pressure. The crude product was purified by flash chromatography ($\lambda_{\text{max}} = 250$ nm, hexane/EtOAc 0% \rightarrow 40%) to give **27f** as a viscous yellow foam (197 mg, 36%). LC-MS: m/z 547 $[\text{M}+\text{H}]^+$. ^1H NMR (400 MHz, CDCl_3) δ 8.80 (s, 1 H), 8.24 (s, 1 H), 8.12 (d, $J = 7.9$ Hz, 2 H), 8.07 (s, 1 H), 8.00 (d, $J = 8.6$ Hz, 1 H), 7.91 (s, 1 H), 7.27 (d, $J = 6.9$ Hz, 2 H), 7.05 (d, $J = 8.6$ Hz, 1 H), 3.91 (s, 3 H), 2.60 (s, 3 H), 2.37 (s, 3 H), 1.32 (s, 12 H). ^{13}C NMR (101 MHz, CDCl_3) δ 196.64, 160.72, 151.06, 148.65, 145.20, 136.10, 135.32, 131.05, 132.32, 130.08, 129.57, 128.24, 124.86, 121.75, 121.58, 115.65, 110.65, 84.05, 75.02, 24.82, 21.61.

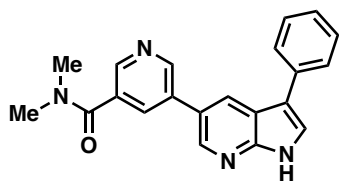
5-(3-(2-Methoxyphenyl)-1H-pyrrolo[2,3-b]pyridin-5-yl)-N,N-dimethylnicotinamide (7)



A mixture of 3-(2-methoxyphenyl)-5-(4,4,5,5-tetramethyl-1,3,2-dioxaborolan-2-yl)-1-tosyl-1H-pyrrolo[2,3-b]pyridine **27a** (505 mg, 1.0 mmol), 5-bromo-N,N-dimethylnicotinamide **29** (344 mg, 1.5 mmol), $\text{Pd}(\text{dppf})\text{Cl}_2 \cdot \text{CH}_2\text{Cl}_2$ (82 mg, 0.1 mmol) and K_2CO_3 (414 mg, 3.0 mmol) was dissolved in 7 mL of dioxane and 1 mL of water and then stirred at 100 °C in a sealed tube for 7 h.

The product formation was confirmed by TLC and LC-MS. Upon solvent evaporation, the crude product was partitioned between EtOAc and water, and extracted using EtOAc (3×20 mL). The combined organic extract was washed with brine, dried over Na_2SO_4 and evaporated under reduced pressure. The crude product was purified by flash chromatography ($\lambda_{\text{max}} = 254$ nm, DCM/MeOH 0% \rightarrow 5%) to give **28a** as an orange viscous crude oil. To a solution of the crude product in 5 mL of MeOH/dioxane/ H_2O (2:2:1) was added LiOH (120 mg, 5 mmol). The reaction mixture was then stirred continuously and monitored by LC-MS until the conversion was complete. The crude product was partitioned between EtOAc and water, and extracted using EtOAc (3×20 mL). The combined organic extract was washed with brine, dried over Na_2SO_4 and evaporated under reduced pressure. The final product was dissolved in methanol or DMSO, filtered and purified by reverse-phase chromatography using 5% to 95% acetonitrile in H_2O with 0.1% formic acid ($\lambda_{\text{max}} = 254$ nm, eluted at 40% acetonitrile in water) to afford the pure product **7** as a tan powder (95.2 mg, 26%). LC-MS: m/z 373 $[\text{M}+\text{H}]^+$, m/z 371 $[\text{M}-\text{H}]^-$. ^1H NMR (400 MHz, $(\text{CD}_3)_2\text{SO}$) δ 12.00 (s, 1 H), 9.01 (d, $J = 2.2$ Hz, 1 H), 8.63 (d, $J = 2.1$ Hz, 1 H), 8.59 (d, $J = 1.9$ Hz, 1 H), 8.30 (d, $J = 2.1$ Hz, 1 H), 8.19 (t, $J = 2.1$ Hz, 1 H), 7.78 (d, $J = 2.5$ Hz, 1 H), 7.65 (dd, $J = 3.0$ Hz, 1 H), 7.30 (app. td, $J = 4.3$ Hz, 1 H), 7.13 (d, $J = 7.7$ Hz, 1 H), 7.05 (td, $J = 3.1$ Hz, 1 H), 3.83 (s, 3 H), 3.03 (br. s, 3 H), 2.99 (br. s, 3 H). ^{13}C NMR (101 MHz, $(\text{CD}_3)_2\text{SO}$) δ 167.81, 156.17, 148.41, 148.37, 145.83, 141.62, 134.31, 132.65, 132.43, 129.71, 127.40, 126.81, 126.60, 124.53, 123.08, 120.74, 118.46, 111.58, 111.28, 55.27, 34.80.

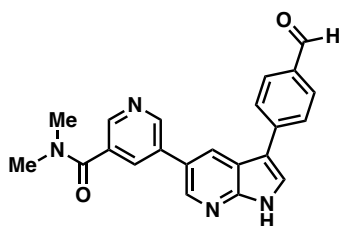
***N,N*-Dimethyl-5-(3-phenyl-1*H*-pyrrolo[2,3-*b*]pyridin-5-yl)nicotinamide (8)**



A mixture of 3-phenyl-5-(4,4,5,5-tetramethyl-1,3,2-dioxaborolan-2-yl)-1-tosyl-1*H*-pyrrolo[2,3-*b*]pyridine **27b** (570 mg, 1.2 mmol), 5-bromo-*N,N*-dimethylnicotinamide **29** (412 mg, 1.8 mmol), Pd(dppf)Cl₂.CH₂Cl₂ (98 mg, 0.12 mmol) and K₂CO₃ (497 mg, 3.0 mmol) was dissolved in 7 mL of dioxane and 1 mL of water and then stirred at 100 °C in a sealed tube for 7 h. The

product formation was confirmed by TLC and LC-MS. Upon solvent evaporation, the crude product was partitioned between EtOAc and water, and extracted using EtOAc (3 × 20 mL). The combined organic extract was washed with brine, dried over Na₂SO₄ and evaporated under reduced pressure. The crude product was purified by flash chromatography ($\lambda_{\text{max}} = 254$ nm, DCM/MeOH 0% → 5%) to give **28b** as an orange viscous crude oil. To a solution of the crude product in 5 mL of MeOH/dioxane/H₂O (2:2:1) was added LiOH (144 mg, 5 mmol). The reaction mixture was then stirred continuously and monitored by LC-MS until the conversion was complete. The crude product was partitioned between EtOAc and water, and extracted using EtOAc (3 × 20 mL). The combined organic extract was washed with brine, dried over Na₂SO₄ and evaporated under reduced pressure. The final product was dissolved in methanol or DMSO, filtered and purified by reverse-phase chromatography using 5% to 95% acetonitrile in H₂O with 0.1% formic acid ($\lambda_{\text{max}} = 254$ nm, eluted at 45% acetonitrile in water) to afford **8** as a white powder (74 mg, 18%). LC-MS: *m/z* 343 [M+H]⁺, *m/z* 341 [M-H]⁻. ¹H NMR (400 MHz, (CD₃)₂SO) δ 12.09 (s, 1 H), 9.07 (d, *J* = 2.2 Hz, 1 H), 8.65 (d, *J* = 2.1 Hz, 1 H), 8.60 (d, *J* = 1.9 Hz, 1 H), 8.57 (d, *J* = 2.0 Hz, 1 H), 8.23 (t, *J* = 2.1 Hz, 1 H), 7.95 (d, *J* = 2.6 Hz, 1 H), 7.83 (d, *J* = 4.1 Hz, 2 H), 7.45 (t, *J* = 7.7 Hz, 2 H), 7.27 (t, *J* = 7.4 Hz, 1 H), 3.04 (br. s, 3 H), 2.99 (br. s, 3 H). ¹³C NMR (101 MHz, (CD₃)₂SO) δ 167.85, 148.99, 148.51, 145.85, 142.01, 134.70, 134.12, 132.79, 132.46, 128.89, 126.52, 126.17, 125.80, 124.99, 124.91, 117.34, 114.93, 34.80.

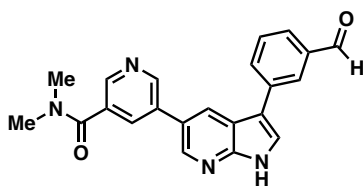
5-(3-(4-Formylphenyl)-1*H*-pyrrolo[2,3-*b*]pyridin-5-yl)-*N,N*-dimethylnicotinamide (9)



A mixture of 4-(5-(4,4,5,5-tetramethyl-1,3,2-dioxaborolan-2-yl)-1-tosyl-1*H*-pyrrolo[2,3-*b*]pyridin-3-yl)benzaldehyde **27c** (503 mg, 1.0 mmol), 5-bromo-*N,N*-dimethylnicotinamide **29** (344 mg, 1.5 mmol), Pd(dppf)Cl₂.CH₂Cl₂ (82 mg, 0.1 mmol) and K₂CO₃ (414 mg, 3.0 mmol) was dissolved in 7 mL of dioxane and 1 mL of water and then stirred at 100 °C in a sealed tube for 7 h. The

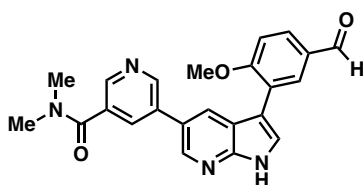
product formation was confirmed by TLC and LC-MS. Upon solvent evaporation, the crude product was partitioned between EtOAc and water, and extracted using EtOAc (3 × 20 mL). The combined organic extract was washed with brine, dried over Na₂SO₄ and evaporated under reduced pressure. The crude product was purified by flash chromatography ($\lambda_{\text{max}} = 254$ nm, DCM/MeOH 0% → 5%) to obtain **28c** as an orange viscous crude oil. To a solution of the crude product in 5 mL of MeOH/dioxane/H₂O (2:2:1) was added LiOH (120 mg, 5 mmol). The reaction mixture was then stirred continuously and monitored by LC-MS until the conversion was complete. The crude product was partitioned between EtOAc and water, and extracted using EtOAc (3 × 20 mL). The combined organic extract was washed with brine, dried over Na₂SO₄ and evaporated under reduced pressure. The final product was dissolved in methanol or DMSO, filtered and purified by reverse-phase chromatography using 5% to 95% acetonitrile in H₂O with 0.1% formic acid ($\lambda_{\text{max}} = 254$ nm, eluted at 45% acetonitrile in water) to afford **9** as an off-white powder (25.7 mg, 6.9%). LC-MS: *m/z* 371 [M+H]⁺, *m/z* 369 [M-H]⁻. ¹H NMR (400 MHz, (CD₃)₂SO) δ 12.37 (br. s, 1 H), 10.00 (s, 1 H), 9.10 (d, *J* = 2.2 Hz, 1 H), 8.70 (m, *J* = 2.0 Hz, 2 H), 8.62 (d, *J* = 1.9 Hz, 1 H), 8.29 (t, *J* = 2.0 Hz, 1 H), 8.22 (s, 1 H), 8.11 (d, *J* = 8.2 Hz, 2 H), 7.97 (d, *J* = 8.3 Hz, 2 H), 3.05 (br. s, 3 H), 3.00 (br. s, 3 H). ¹³C NMR (101 MHz, (CD₃)₂SO) δ 192.31, 167.84, 149.17, 148.59, 145.98, 142.43, 141.14, 133.99, 133.50, 132.86, 132.46, 130.28, 127.13, 126.46, 125.52, 117.16, 113.74, 34.80.

5-(3-(3-Formylphenyl)-1H-pyrrolo[2,3-b]pyridin-5-yl)-N,N-dimethylnicotinamide (10)



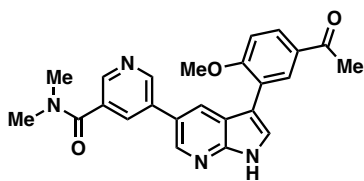
A mixture of 3-(5-(4,4,5,5-tetramethyl-1,3,2-dioxaborolan-2-yl)-1-tosyl-1H-pyrrolo[2,3-b]pyridin-3-yl)benzaldehyde **27d** (503 mg, 1.0 mmol), 5-bromo-N,N-dimethylnicotinamide **29** (344 mg, 1.5 mmol), Pd(dppf)Cl₂.CH₂Cl₂ (82 mg, 0.1 mmol) and K₂CO₃ (414 mg, 3.0 mmol) was dissolved in 7 mL of dioxane and 1 mL of water and then stirred at 100 °C in a sealed tube for 7 h. The product formation was confirmed by TLC and LC-MS. Upon solvent evaporation, the crude product was partitioned between EtOAc and water, and extracted using EtOAc (3 × 20 mL). The combined organic extract was washed with brine, dried over Na₂SO₄ and evaporated under reduced pressure. The crude product was purified by flash chromatography (λ_{max} = 254 nm, DCM/MeOH 0% → 5%) to obtain **28d** as an orange viscous crude oil. To a solution of the crude product in 5 mL of MeOH/dioxane/H₂O (2:2:1) was added LiOH (120 mg, 5 mmol). The reaction mixture was then stirred continuously and monitored by LC-MS until the conversion was complete. The crude product was partitioned between EtOAc and water, and extracted using EtOAc (3 × 20 mL). The combined organic extract was washed with brine, dried over Na₂SO₄ and evaporated under reduced pressure. The final product was dissolved in methanol or DMSO, filtered and purified by reverse-phase chromatography using 5% to 95% acetonitrile in H₂O with 0.1% formic acid (λ_{max} = 254 nm, eluted at 45% acetonitrile in water) to afford **10** as an off-white powder (17.4 mg, 4.7%). LC-MS: m/z 371 [M+H]⁺, m/z 369 [M-H]⁻. ¹H NMR (400 MHz, (CD₃)₂SO) δ 12.23 (br. s, 1 H), 10.12 (s, 1 H), 9.08 (d, J = 2.2 Hz, 1 H), 8.68 (d, J = 2.0 Hz, 1 H), 8.65 (d, J = 2.0 Hz, 1 H), 8.61 (d, J = 1.9 Hz, 1 H), 8.33 (s, 1 H), 8.26 (t, J = 2.1 Hz, 1 H), 8.20 (d, J = 3.9 Hz, 1 H), 8.11 (d, J = 2.6 Hz, 1 H), 7.79 (d, J = 7.6 Hz, 1 H), 7.68 (t, J = 7.6 Hz, 1 H), 3.04 (br. s, 3 H), 3.00 (br. s, 3 H). ¹³C NMR (101 MHz, (CD₃)₂SO) δ 193.55, 167.83, 148.99, 148.59, 142.30, 136.88, 135.72, 132.84, 132.44, 132.34, 129.79, 128.19, 126.14, 125.77, 117.18, 113.69, 34.81.

5-(3-(5-Formyl-2-methoxyphenyl)-1H-pyrrolo[2,3-b]pyridin-5-yl)-N,N-dimethylnicotinamide (13)

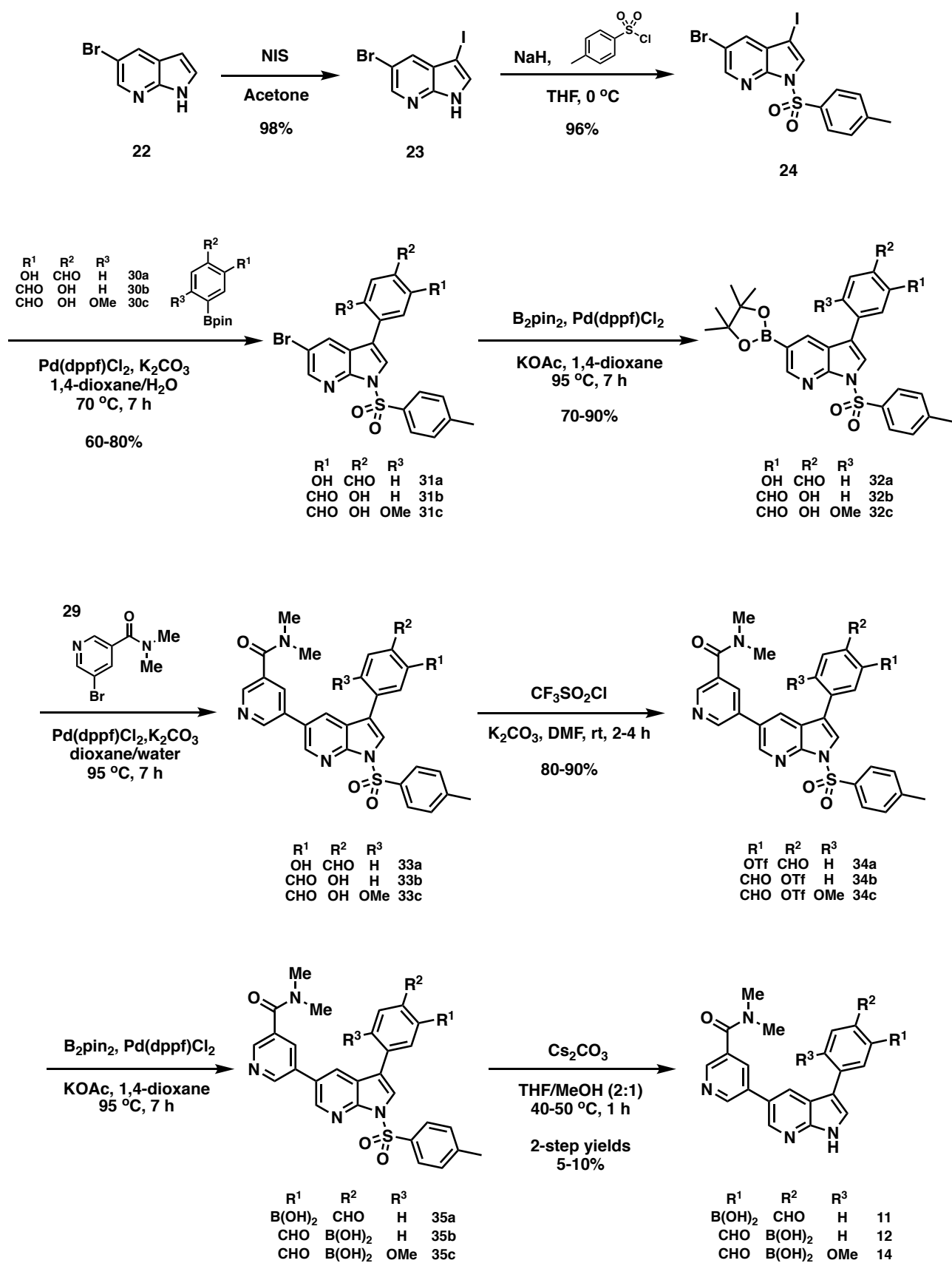


A mixture of 4-methoxy-3-(5-(4,4,5,5-tetramethyl-1,3,2-dioxaborolan-2-yl)-1-tosyl-1H-pyrrolo[2,3-b]pyridin-3-yl)benzaldehyde **27e** (586 mg, 1.1 mmol), 5-bromo-N,N-dimethylnicotinamide **29** (378 mg, 1.65 mmol), Pd(dppf)Cl₂.CH₂Cl₂ (90 mg, 0.11 mmol) and K₂CO₃ (456 mg, 3.3 mmol) was dissolved in 7 mL of dioxane and 1 mL of water and then stirred at 100 °C in a sealed tube for 7 h. The product formation was confirmed by TLC and LC-MS. Upon solvent evaporation, the crude product was partitioned between EtOAc and water, and extracted using EtOAc (3 × 20 mL). The combined organic extract was washed with brine, dried over Na₂SO₄ and evaporated under reduced pressure. The crude product was purified by flash chromatography (λ_{max} = 254 nm, DCM/MeOH 0% → 5%) to obtain crude **28e** as an orange viscous crude oil. To a solution of the crude product in 5 mL of MeOH/dioxane/H₂O (2:2:1) was added LiOH (132 mg, 5 mmol). The reaction mixture was then stirred continuously and monitored by LC-MS until the conversion was complete. The crude product was partitioned between EtOAc and water, and extracted using EtOAc (3 × 20 mL). The combined organic extract was washed with brine, dried over Na₂SO₄ and evaporated under reduced pressure. The final product was dissolved in methanol or DMSO, filtered and purified by reverse-phase chromatography using 5% to 95% acetonitrile in H₂O with 0.1% formic acid (λ_{max} = 262 nm, eluted at 40% acetonitrile in water) to afford **13** as a white powder (28.3 mg, 6.5%). LC-MS: m/z 399 [M+H]⁺, m/z 401 [M-H]⁻. ¹H NMR (400 MHz, (CD₃)₂SO) δ 12.11 (s, 1 H), 9.98 (s, 1 H), 9.01 (d, J = 1.9 Hz, 1 H), 8.65 (d, J = 1.7 Hz, 1 H), 8.59 (d, J = 1.4 Hz, 1 H), 8.35 (d, J = 1.6 Hz, 1 H), 8.19 (s, 1 H), 8.13 (d, J = 1.7 Hz, 1 H), 7.89 (app. dd, J = 3.5 Hz, 2 H), 7.35 (d, J = 8.6 Hz, 1 H), 3.96 (s, 3 H), 3.03 (br. s, 3 H), 2.99 (br. s, 3 H). ¹³C NMR (101 MHz, (CD₃)₂SO) δ 191.79, 167.80, 161.12, 148.42, 145.95, 141.91, 134.17, 132.69, 132.41, 131.31, 129.65, 129.49, 127.17, 126.77, 124.75, 123.89, 118.34, 111.94, 110.21, 55.95, 34.83.

5-(3-(5-Acetyl-2-methoxyphenyl)-1H-pyrrolo[2,3-b]pyridin-5-yl)-N,N-dimethylnicotinamide (15)

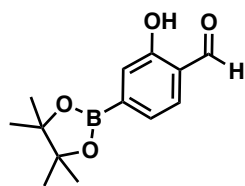


A mixture of 1-(4-methoxy-3-(5-(4,4,5,5-tetramethyl-1,3,2-dioxaborolan-2-yl)-1-tosyl-1H-pyrrolo[2,3-b]pyridin-3-yl)phenyl)ethan-1-one **27f** (404 mg, 0.74 mmol), 5-bromo-*N,N*-dimethylnicotinamide **29** (254 mg, 1.11 mmol), Pd(dppf)Cl₂.CH₂Cl₂ (60 mg, 0.074 mmol) and K₂CO₃ (306 mg, 2.22 mmol) was dissolved in 6 mL of dioxane and 1 mL of water and then stirred at 100 °C in a sealed tube for 5 h. The product formation was confirmed by TLC and LC-MS. Upon solvent evaporation, the crude product was partitioned between EtOAc and water, and extracted using EtOAc (3 × 20 mL). The combined organic extract was washed with brine, dried over Na₂SO₄ and evaporated under reduced pressure. The crude product was purified by flash chromatography (λ_{max} = 250 nm, DCM/MeOH 0% → 5%) to obtain crude **28f** as an orange viscous crude oil. To a solution of the crude product in 2.5 mL of MeOH/dioxane/H₂O (2:2:1) was added LiOH (89 mg, 3.7 mmol). The reaction mixture was then stirred continuously and monitored by LC-MS until the conversion was complete. The crude product was partitioned between EtOAc and water, and extracted using EtOAc (3 × 20 mL). The combined organic extract was washed with brine, dried over Na₂SO₄ and evaporated under reduced pressure. The final product was dissolved in methanol or DMSO, filtered and purified by reverse-phase chromatography using 5% to 95% acetonitrile in H₂O with 0.1% formic acid (λ_{max} = 260 nm) to afford **15** as a white powder (55 mg, 18%). LC-MS: *m/z* 415 [M+H]⁺, *m/z* 413 [M-H]⁻. ¹H NMR (400 MHz, (CD₃)₂SO) δ 12.10 (s, 1 H), 9.00 (s, 1 H), 8.65 (s, 1 H), 8.59 (s, 1 H), 8.31 (s, 1 H), 8.18 (s, 1 H), 8.14 (s, 1 H), 7.95 (d, *J* = 4.3 Hz, 1 H), 7.85 (s, 1 H), 7.25 (s, *J* = 8.7 Hz, 1 H), 3.92 (s, 3 H), 3.03 (s, 3 H), 2.99 (s, 3 H), 2.59 (s, 3 H). ¹³C NMR (101 MHz, (CD₃)₂SO) δ 196.59, 167.77, 160.07, 148.44, 148.33, 145.97, 141.83, 134.16, 132.61, 132.41, 130.02, 129.89, 128.52, 126.94, 126.74, 124.63, 123.18, 118.44, 111.27, 110.71, 55.76, 34.82, 26.54.



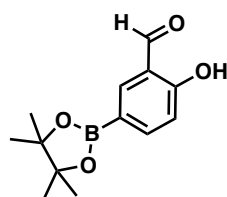
Scheme S4. Synthesis of carbonyl boronic acid inhibitors **11**, **12** and **14**.

2-Hydroxy-4-(4,4,5,5-tetramethyl-1,3,2-dioxaborolan-2-yl)benzaldehyde (30a)



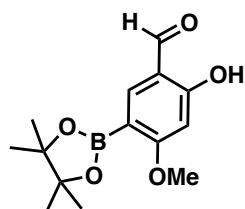
A mixture of 4-bromo-2-hydroxybenzaldehyde (500 mg, 2.49 mmol), B₂pin₂ (822 mg, 3.24 mmol), Pd(dppf)Cl₂.CH₂Cl₂ (203 mg, 0.249 mmol) and KOAc (733 mg, 7.47 mmol) were dissolved in 8 mL of dioxane and then stirred at 100 °C in a sealed tube for 7 h. The product formation was confirmed by TLC and LC-MS. Upon solvent evaporation, the crude product was partitioned between EtOAc and water, and extracted using EtOAc (3 × 20 mL). The combined organic extract was washed with brine, dried over Na₂SO₄ and evaporated under reduced pressure. The crude product was purified by flash chromatography (λ_{max} = 260 nm, hexane/EtOAc = 50:1) to give **30a** as yellow crystals (297 mg, 48%). LC-MS: *m/z* 249.2 [M+H]⁺, *m/z* 247.1 [M-H]⁻. ¹H NMR (400 MHz, CDCl₃) δ 10.82 (s, 1 H), 9.92 (s, 1 H), 7.54 (d, *J* = 8.1 Hz, 1 H), 7.42 (s, 1 H), 7.41 (dd, *J* = 7.8 Hz, 1 H), 1.35 (s, 12 H). ¹³C NMR (101 MHz, CDCl₃) δ 196.79, 160.57, 132.59, 125.36, 123.83, 121.99, 84.41, 24.83.

2-Hydroxy-5-(4,4,5,5-tetramethyl-1,3,2-dioxaborolan-2-yl)benzaldehyde (30b)



A mixture of 5-bromo-2-hydroxybenzaldehyde (500 mg, 2.49 mmol), B₂pin₂ (822 mg, 3.24 mmol), Pd(dppf)Cl₂.CH₂Cl₂ (203 mg, 0.249 mmol) and KOAc (733 mg, 7.47 mmol) were dissolved in 8 mL of dioxane and then stirred at 100 °C in a sealed tube for 7 h. The product formation was confirmed by TLC and LC-MS. Upon solvent evaporation, the crude product was partitioned between EtOAc and water, and extracted using EtOAc (3 × 20 mL). The combined organic extract was washed with brine, dried over Na₂SO₄ and evaporated under reduced pressure. The crude product was purified by flash chromatography (λ_{max} = 254 nm, hexane/EtOAc = 50:1) to give **30b** as a bright orange product (315 mg, 51%). LC-MS: *m/z* 249.2 [M+H]⁺, *m/z* 247.1 [M-H]⁻. ¹H NMR (400 MHz, CDCl₃) δ 11.22 (s, 1 H), 9.92 (s, 1 H), 8.04 (d, *J* = 1.6 Hz, 1 H), 7.94 (dd, *J* = 3.3 Hz, 1 H), 6.97 (d, *J* = 8.4 Hz, 1 H), 1.35 (s, 12 H). ¹³C NMR (101 MHz, CDCl₃) δ 196.92, 163.98, 143.19, 141.39, 120.39, 117.05, 84.06, 24.85.

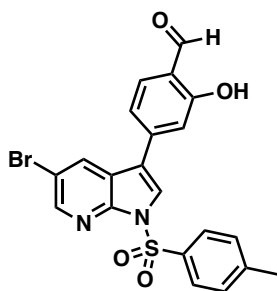
2-Hydroxy-4-methoxy-5-(4,4,5,5-tetramethyl-1,3,2-dioxaborolan-2-yl)benzaldehyde (30c)



A mixture of 5-bromo-2-hydroxy-4-methoxybenzaldehyde (693 mg, 3.0 mmol), B₂pin₂ (915 mg, 3.6 mmol), Pd(dppf)Cl₂.CH₂Cl₂ (245 mg, 0.3 mmol) and KOAc (884 mg, 9.0 mmol) were dissolved in 8 mL of dioxane and then stirred at 100 °C in a sealed tube for 7 h. The product formation was confirmed by TLC and LC-MS. Upon solvent evaporation, the crude product was partitioned between EtOAc and water, and extracted using EtOAc (3 × 20 mL). The combined organic extract was washed with

brine, dried over Na₂SO₄ and evaporated under reduced pressure. The crude product was purified by flash chromatography (λ_{max} = 280 nm, hexane/EtOAc 0% → 10%) to give **30c** as a bright orange product (459 mg, 55%). LC-MS: *m/z* 279 [M+H]⁺. ¹H NMR (400 MHz, CDCl₃) δ 9.73 (s, 1 H), 7.91 (s, 1 H), 6.37 (s, 1 H), 3.87 (s, 3 H), 1.34 (s, 12 H). ¹³C NMR (101 MHz, CDCl₃) δ 194.71, 171.17, 166.86, 144.27, 114.98, 98.46, 83.61, 56.14, 24.75.

4-(5-Bromo-1-tosyl-1*H*-pyrrolo[2,3-*b*]pyridin-3-yl)-2-hydroxybenzaldehyde (31a)

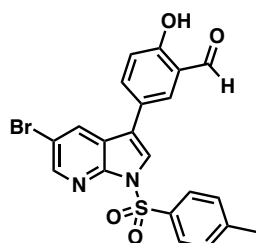


A mixture of 5-bromo-3-iodo-1-tosyl-1*H*-pyrrolo[2,3-*b*]pyridine **24** (500 mg, 1.05 mmol), 2-hydroxy-4-(4,4,5,5-tetramethyl-1,3,2-dioxaborolan-2-yl)benzaldehyde **30a** (261 mg, 1.05 mmol), Pd(dppf)Cl₂.CH₂Cl₂ (86 mg, 0.105 mmol) and K₂CO₃ (435 mg, 3.15 mmol) was dissolved in 7 mL of dioxane and 1 mL of water and then stirred at 70 °C in a sealed tube for 7 h. The product formation was confirmed by TLC and LC-MS. Upon solvent evaporation, the crude product was partitioned between EtOAc and water, and extracted using EtOAc (3 × 20 mL). The combined organic extract was washed with brine, dried over Na₂SO₄ and evaporated under

reduced pressure. The crude product was purified by flash chromatography (λ_{max} = 300 nm, hexane/EtOAc

0% → 70% due to solubility issue) to give **31a** as an off-white solid product (356 mg, 72%). LC-MS: m/z 471 and 473 $[M+H]^+$. 1H NMR (400 MHz, $CDCl_3$) δ 11.19 (s, 1 H), 9.93 (s, 1 H), 8.51 (d, $J = 2.0$ Hz, 1 H), 8.26 (d, $J = 2.2$ Hz, 1 H), 8.10 (d, $J = 2.8$ Hz, 2 H), 8.02 (s, 1 H), 7.66 (d, $J = 8.0$ Hz, 1 H), 7.32 (d, $J = 8.8$ Hz, 2 H), 7.22 (dd, $J = 3.2$ Hz, 1 H), 7.18 (d, $J = 1.6$ Hz, 1 H), 2.40 (s, 3 H). ^{13}C NMR (101 MHz, $CDCl_3$) δ 195.77, 162.12, 146.19, 145.94, 145.68, 140.87, 134.62, 134.50, 131.10, 129.86, 128.36, 128.29, 125.60, 122.28, 119.80, 118.67, 117.88, 115.86, 115.66, 21.70.

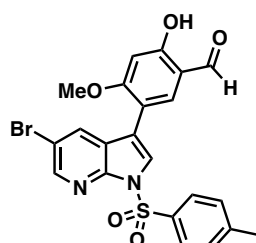
5-(5-Bromo-1-tosyl-1*H*-pyrrolo[2,3-*b*]pyridin-3-yl)-2-hydroxybenzaldehyde (**31b**)



A mixture of 5-bromo-3-iodo-1-tosyl-1*H*-pyrrolo[2,3-*b*]pyridine **24** (500 mg, 1.05 mmol), 2-hydroxy-5-(4,4,5,5-tetramethyl-1,3,2-dioxaborolan-2-yl)benzaldehyde **30b** (261 mg, 1.05 mmol), $Pd(dppf)Cl_2 \cdot CH_2Cl_2$ (86 mg, 0.105 mmol) and K_2CO_3 (435 mg, 3.15 mmol) was dissolved in 7 mL of dioxane and 1 mL of water and then stirred at 70 °C in a sealed tube for 7 h. The product formation was confirmed by TLC and LC-MS. Upon solvent evaporation, the crude product was partitioned between EtOAc and water, and extracted using EtOAc (3 × 20 mL). The combined organic extract

was washed with brine, dried over Na_2SO_4 and evaporated under reduced pressure. The crude product was purified by flash chromatography ($\lambda_{max} = 254$ nm, hexane/EtOAc 0% → 70% due to solubility issue) to give **31b** as a pale orange solid (396 mg, 80%). LC-MS: m/z 471 and 473 $[M+H]^+$. 1H NMR (400 MHz, $CDCl_3$) δ 11.07 (s, 1 H), 10.00 (s, 1 H), 8.50 (d, $J = 2.1$ Hz, 1 H), 8.13 (d, $J = 2.2$ Hz, 1 H), 8.10 (dd, $J = 2.8$ Hz, 2 H), 7.86 (s, 1 H), 7.71 (s, 1 H), 7.70 (dd, $J = 4.2$, 1 H), 7.31 (d, $J = 3.0$ Hz, 2 H), 7.13 (d, $J = 8.2$ Hz, 1 H), 2.40 (s, 3 H). ^{13}C NMR (101 MHz, $CDCl_3$) δ 196.31, 161.28, 145.98, 145.73, 145.60, 135.95, 134.85, 132.20, 130.62, 129.81, 128.23, 124.05, 123.83, 122.85, 120.89, 118.78, 117.91, 115.57, 21.68.

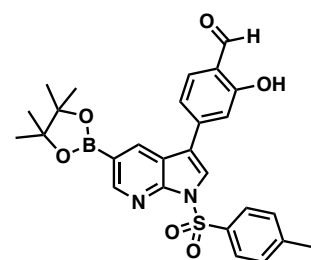
5-(5-Bromo-1-tosyl-1*H*-pyrrolo[2,3-*b*]pyridin-3-yl)-2-hydroxy-4-methoxybenzaldehyde (**31c**)



A mixture of 5-bromo-3-iodo-1-tosyl-1*H*-pyrrolo[2,3-*b*]pyridine **24** (883 mg, 1.85 mmol), 2-hydroxy-4-methoxy-5-(4,4,5,5-tetramethyl-1,3,2-dioxaborolan-2-yl)benzaldehyde **30c** (513 mg, 1.85 mmol), $Pd(dppf)Cl_2 \cdot CH_2Cl_2$ (151 mg, 0.185 mmol) and K_2CO_3 (766 mg, 5.54 mmol) was dissolved in 7 mL of dioxane and 1 mL of water and then stirred at 70 °C in a sealed tube for 7 h. The product formation was confirmed by TLC and LC-MS. Upon solvent evaporation, the crude product was partitioned between EtOAc and water, and extracted using EtOAc (3 × 20 mL). The

combined organic extract was washed with brine, dried over Na_2SO_4 and evaporated under reduced pressure. The crude product was purified by flash chromatography ($\lambda_{max} = 254$ nm, hexane/EtOAc 0% → 70% due to solubility issue) to give **31c** as a yellow solid (529 mg, 57%). LC-MS: m/z 501 and 503 $[M+H]^+$. 1H NMR (400 MHz, $CDCl_3$) δ 11.59 (s, 1 H), 9.79 (s, 1 H), 8.47 (d, $J = 2.0$ Hz, 1 H), 8.10 (d, $J = 8.4$ Hz, 2 H), 7.93 (d, $J = 2.2$ Hz, 1 H), 7.86 (s, 1 H), 7.53 (s, 1 H), 7.31 (d, $J = 8.0$ Hz, 2 H), 6.58 (s, 1 H), 3.90 (s, 3 H), 2.40 (s, 3 H). ^{13}C NMR (101 MHz, $CDCl_3$) δ 194.34, 164.44, 163.85, 145.57, 145.52, 145.25, 135.06, 135.02, 131.60, 129.75, 128.29, 128.23, 125.87, 123.92, 115.22, 114.86, 114.27, 114.06, 99.73, 56.15, 21.67.

2-Hydroxy-4-(5-(4,4,5,5-tetramethyl-1,3,2-dioxaborolan-2-yl)-1-tosyl-1*H*-pyrrolo[2,3-*b*]pyridin-3-yl)benzaldehyde (**32a**)

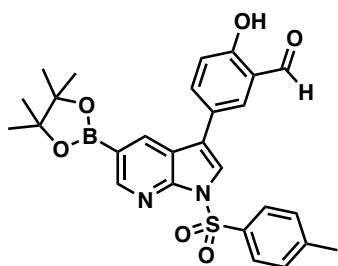


A mixture of 4-(5-bromo-1-tosyl-1*H*-pyrrolo[2,3-*b*]pyridin-3-yl)-2-hydroxybenzaldehyde **31a** (707 mg, 1.5 mmol), B_2pin_2 (457 mg, 1.8 mmol), $Pd(dppf)Cl_2 \cdot CH_2Cl_2$ (122 mg, 0.15 mmol) and $KOAc$ (442 mg, 4.5 mmol) was dissolved in 8 mL of dioxane and then stirred at 100 °C in a sealed tube for 7 h. The product formation was confirmed by LC-MS. Upon solvent evaporation, the crude product was partitioned between EtOAc and water, and extracted using EtOAc (3 × 20 mL). The combined organic extract was washed with brine, dried

over Na_2SO_4 and evaporated under reduced pressure. The crude product was purified by flash

chromatography ($\lambda_{\max} = 250$ nm, hexane/EtOAc 0% \rightarrow 60%) to give **32a** as a viscous yellow foam (653 mg, 84%). LC-MS: m/z 519 [M+H]⁺. ¹H NMR (400 MHz, CDCl₃) δ 11.20 (s, 1 H), 9.91 (s, 1 H), 8.83 (d, $J = 1.5$ Hz, 1 H), 8.50 (d, $J = 1.4$ Hz, 1 H), 8.12 (d, $J = 8.4$ Hz, 2 H), 7.99 (s, 1 H), 7.65 (d, $J = 7.9$ Hz, 1 H), 7.28 (m, $J = 2.2$ Hz, 4 H), 2.37 (s, 3 H), 1.34 (s, 12 H). ¹³C NMR (101 MHz, CDCl₃) δ 195.81, 162.02, 151.64, 149.01, 145.59, 141.63, 135.45, 134.88, 134.36, 129.67, 128.36, 124.20, 120.19, 119.63, 119.00, 118.81, 115.79, 84.28, 24.80, 21.64.

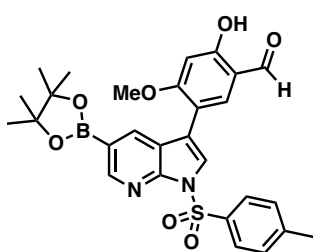
2-Hydroxy-5-(5-(4,4,5,5-tetramethyl-1,3,2-dioxaborolan-2-yl)-1-tosyl-1H-pyrrolo[2,3-b]pyridin-3-yl)benzaldehyde (32b)



A mixture of 5-(5-bromo-1-tosyl-1H-pyrrolo[2,3-b]pyridin-3-yl)-2-hydroxybenzaldehyde **31b** (707 mg, 1.5 mmol), B₂pin₂ (457 mg, 1.8 mmol), Pd(dppf)Cl₂.CH₂Cl₂ (122 mg, 0.15 mmol) and KOAc (442 mg, 4.5 mmol) was dissolved in 8 mL of dioxane and then stirred at 100 °C in a sealed tube for 7 h. The product formation was confirmed by LC-MS. Upon solvent evaporation, the crude product was partitioned between EtOAc and water, and extracted using EtOAc (3 \times 20 mL). The combined organic extract was

washed with brine, dried over Na₂SO₄ and evaporated under reduced pressure. The crude product was purified by flash chromatography ($\lambda_{\max} = 250$ nm, hexane/EtOAc 0% \rightarrow 60%) to give **32b** as a viscous yellow foam (692 mg, 89%). LC-MS: m/z 519 [M+H]⁺. ¹H NMR (400 MHz, CDCl₃) δ 11.06 (s, 1 H), 10.00 (s, 1 H), 8.84 (d, $J = 1.5$ Hz, 1 H), 8.38 (d, $J = 1.5$ Hz, 1 H), 8.12 (d, $J = 8.4$ Hz, 2 H), 7.83 (s, 1 H), 7.77 (s, 1 H), 7.76 (dd, $J = 3.6$ Hz, 1 H), 7.27 (d, $J = 8.8$ Hz, 2 H), 7.12 (dd, $J = 4.8$ Hz, 1 H), 2.37 (s, 3 H), 1.34 (s, 12 H). ¹³C NMR (101 MHz, CDCl₃) δ 196.52, 161.10, 151.53, 148.98, 145.38, 136.30, 135.14, 134.94, 132.42, 129.63, 128.25, 124.72, 122.29, 120.84, 120.76, 118.81, 118.55, 84.24, 24.81, 21.64.

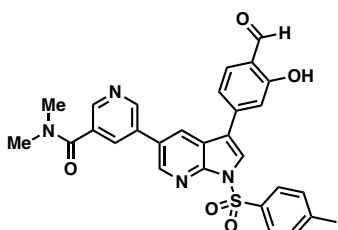
2-Hydroxy-4-methoxy-5-(5-(4,4,5,5-tetramethyl-1,3,2-dioxaborolan-2-yl)-1-tosyl-1H-pyrrolo[2,3-b]pyridin-3-yl)benzaldehyde (32c)



A mixture of 5-(5-bromo-1-tosyl-1H-pyrrolo[2,3-b]pyridin-3-yl)-2-hydroxy-4-methoxy benzaldehyde **31c** (655 mg, 1.31 mmol), B₂pin₂ (398 mg, 1.57 mmol), Pd(dppf)Cl₂.CH₂Cl₂ (107 mg, 0.131 mmol) and KOAc (386 mg, 3.93 mmol) was dissolved in 8 mL of dioxane and then stirred at 100 °C in a sealed tube for 7 h. The product formation was confirmed by LC-MS. Upon solvent evaporation, the crude product was partitioned between EtOAc and water, and extracted using EtOAc (3 \times 20 mL). The combined organic extract was

washed with brine, dried over Na₂SO₄ and evaporated under reduced pressure. The crude product was purified by flash chromatography ($\lambda_{\max} = 250$ nm, hexane/EtOAc 0% \rightarrow 60%) to give **32c** as a viscous yellow foam (661 mg, 92%). LC-MS: m/z 549 [M+H]⁺. ¹H NMR (400 MHz, CDCl₃) δ 11.57 (s, 1 H), 9.79 (s, 1 H), 8.80 (d, $J = 1.5$ Hz, 1 H), 8.19 (d, $J = 1.5$ Hz, 1 H), 8.12 (d, $J = 8.4$ Hz, 2 H), 7.84 (s, 1 H), 7.59 (s, 1 H), 7.27 (d, $J = 8$ Hz, 2 H), 6.57 (s, 1 H), 3.89 (s, 3 H), 2.37 (s, 3 H), 1.32 (s, 12 H). ¹³C NMR (101 MHz, CDCl₃) δ 194.51, 164.20, 164.09, 151.12, 145.21, 135.73, 135.30, 135.24, 129.57, 128.24, 124.50, 121.82, 114.76, 114.67, 99.6, 84.11, 24.82, 21.62.

5-(3-(4-Formyl-3-hydroxyphenyl)-1-tosyl-1H-pyrrolo[2,3-b]pyridin-5-yl)-N,N-dimethylnicotinamide (33a)

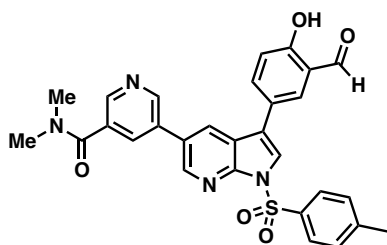


A mixture of 2-hydroxy-4-(5-(4,4,5,5-tetramethyl-1,3,2-dioxaborolan-2-yl)-1-tosyl-1H-pyrrolo[2,3-b]pyridin-3-yl)benzaldehyde **32a** (570 mg, 1.1 mmol), 5-bromo-N,N-dimethylnicotinamide **29** (378 mg, 1.65 mmol), Pd(dppf)Cl₂.CH₂Cl₂ (90 mg, 0.11 mmol) and K₂CO₃ (456 mg, 3.3 mmol) was dissolved in 7 mL of dioxane and 1 mL of water and then stirred at 100 °C in

a sealed tube for 7 h. The product formation was confirmed by TLC and LC-MS. Upon solvent evaporation,

the crude product was partitioned between EtOAc and water, and extracted using EtOAc (3 × 20 mL). The combined organic extract was washed with brine, dried over Na₂SO₄ and evaporated under reduced pressure. The crude product was purified by flash chromatography ($\lambda_{\text{max}} = 254 \text{ nm}$, DCM/MeOH 0% → 5%) to give **33a** as a viscous orange oil (428 mg, 72%). The intermediate was used in the next step without further purification. LC-MS: m/z 541 [M+H]⁺, m/z 539 [M-H]⁻.

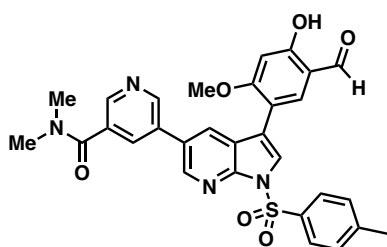
5-(3-(3-Formyl-4-hydroxyphenyl)-1-tosyl-1*H*-pyrrolo[2,3-*b*]pyridin-5-yl)-*N,N*-dimethylnicotinamide (33b)



A mixture of 2-hydroxy-5-(5-(4,4,5,5-tetramethyl-1,3,2-dioxaborolan-2-yl)-1-tosyl-1*H*-pyrrolo[2,3-*b*]pyridin-3-yl)benzaldehyde **32b** (570 mg, 1.1 mmol), 5-bromo-*N,N*-dimethylnicotinamide **29** (378 mg, 1.65 mmol), Pd(dppf)Cl₂.CH₂Cl₂ (90 mg, 0.11 mmol) and K₂CO₃ (456 mg, 3.3 mmol) was dissolved in 7 mL of dioxane and 1 mL of water and then stirred at 100 °C in a sealed tube for 7 h. The product formation was confirmed by TLC and LC-MS. Upon solvent evaporation, the crude product was

partitioned between EtOAc and water, and extracted using EtOAc (3 × 20 mL). The combined organic extract was washed with brine, dried over Na₂SO₄ and evaporated under reduced pressure. The crude product was purified by flash chromatography ($\lambda_{\text{max}} = 254 \text{ nm}$, DCM/MeOH 0% → 5%) to give **33b** as a viscous yellow oil (464 mg, 78%). The intermediate was used in the next step without further purification. LC-MS: m/z 541 [M+H]⁺, m/z 539 [M-H]⁻.

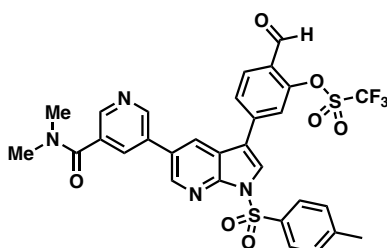
5-(3-(5-Formyl-4-hydroxy-2-methoxyphenyl)-1-tosyl-1*H*-pyrrolo[2,3-*b*]pyridin-5-yl)-*N,N*-dimethylnicotinamide (33c)



A mixture of 2-hydroxy-4-methoxy-5-(5-(4,4,5,5-tetramethyl-1,3,2-dioxaborolan-2-yl)-1-tosyl-1*H*-pyrrolo[2,3-*b*]pyridin-3-yl)benzaldehyde **32c** (318 mg, 0.58 mmol), 5-bromo-*N,N*-dimethylnicotinamide **29** (200 mg, 0.87 mmol), Pd(dppf)Cl₂.CH₂Cl₂ (48 mg, 0.11 mmol) and K₂CO₃ (241 mg, 1.74 mmol) was dissolved in 7 mL of dioxane and 1 mL of water and then stirred at 100 °C in a sealed tube for 7 h. The product formation was confirmed by TLC and LC-MS. Upon solvent evaporation,

the crude product was partitioned between EtOAc and water, and extracted using EtOAc (3 × 20 mL). The combined organic extract was washed with brine, dried over Na₂SO₄ and evaporated under reduced pressure. The crude product was purified by flash chromatography ($\lambda_{\text{max}} = 250 \text{ nm}$, DCM/MeOH 0% → 5%) to give **33c** as a viscous yellow oil (276 mg, 83%). The intermediate was used in the next step without further purification. LC-MS: m/z 571 [M+H]⁺, m/z 569 [M-H]⁻.

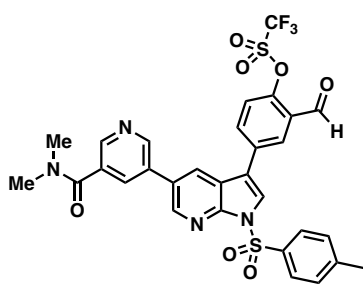
5-(5-(5-(Dimethylcarbamoyl)pyridin-3-yl)-1-tosyl-1*H*-pyrrolo[2,3-*b*]pyridin-3-yl)-2-formylphenyl trifluoromethanesulfonate (34a)



To a solution of 5-(3-(4-formyl-3-hydroxyphenyl)-1-tosyl-1*H*-pyrrolo[2,3-*b*]pyridin-5-yl)-*N,N*-dimethylnicotinamide **33a** (321 mg, 0.59 mmol) in anhydrous DMF (5 mL) was added K₂CO₃ (327 mg, 2.36 mmol). The mixture was then stirred gently at 0 °C for 5 min and CF₃SO₂Cl (0.252 mL, 2.36 mmol, $\rho = 1.583 \text{ g/mL}$) was added. The reaction was monitored using LC-MS. The crude product was partitioned

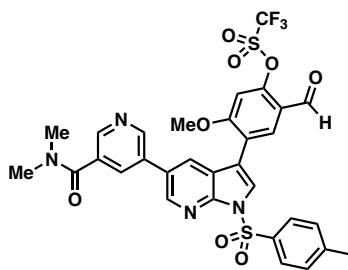
between EtOAc and saturated NaHCO₃, and extracted using EtOAc (3 × 20 mL). pH was adjusted to 8. The combined organic extract was washed with brine, dried over Na₂SO₄ and evaporated under reduced pressure. The crude product was purified by flash chromatography ($\lambda_{\text{max}} = 250 \text{ nm}$, DCM/MeOH 0% → 5%) to give **34a** as a viscous reddish-brown oil (317 mg, 80%). LC-MS: m/z 673 [M+H]⁺. The product was used in the next step without further purification.

4-(5-(5-(Dimethylcarbamoyl)pyridin-3-yl)-1-tosyl-1*H*-pyrrolo[2,3-*b*]pyridin-3-yl)-2-formylphenyl trifluoromethanesulfonate (**34b**)



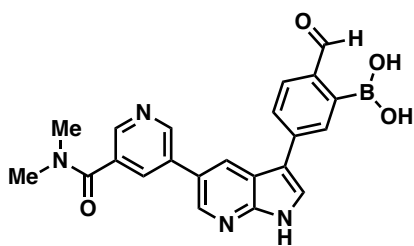
To a solution of 5-(3-(3-formyl-4-hydroxyphenyl)-1-tosyl-1*H*-pyrrolo[2,3-*b*]pyridin-5-yl)-*N,N*-dimethylnicotinamide **33b** (230 mg, 0.43 mmol) in anhydrous DMF (5 mL) was added K_2CO_3 (237 mg, 1.72 mmol). The mixture was then stirred gently at 0 °C for 5 min and CF_3SO_2Cl (0.181 mL, 1.72 mmol, $\rho = 1.583$ g/mL) was added. The reaction was monitored using LC-MS. The crude product was partitioned between EtOAc and saturated $NaHCO_3$, and extracted using EtOAc (3 \times 20 mL). *pH* was adjusted to 8. The combined organic extract was washed with brine, dried over Na_2SO_4 and evaporated under reduced pressure. The crude product was purified by flash chromatography ($\lambda_{max} = 250$ nm, DCM/MeOH 0% \rightarrow 5%) to obtain **34b** as a viscous reddish brown oil (283 mg, 98%). LC-MS: *m/z* 673 $[M+H]^+$. The product was used in the next step without further purification.

4-(5-(5-(Dimethylcarbamoyl)pyridin-3-yl)-1-tosyl-1*H*-pyrrolo[2,3-*b*]pyridin-3-yl)-2-formyl-5-methoxyphenyl trifluoromethanesulfonate (**34c**)



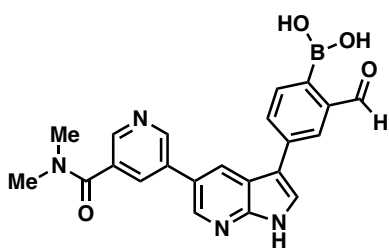
To a solution of 5-(3-(5-formyl-4-hydroxy-2-methoxyphenyl)-1-tosyl-1*H*-pyrrolo[2,3-*b*]pyridin-5-yl)-*N,N*-dimethylnicotinamide **33c** (276 mg, 0.45 mmol) in anhydrous DMF (5 mL) was added K_2CO_3 (248 mg, 1.8 mmol). The mixture was then stirred gently at 0 °C for 5 min and CF_3SO_2Cl (0.192 mL, 1.8 mmol, $\rho = 1.583$ g/mL) was added. The reaction was monitored using LC-MS. The crude product was partitioned between EtOAc and saturated $NaHCO_3$, and extracted using EtOAc (3 \times 20 mL). *pH* was adjusted to 8. The combined organic extract was washed with brine, dried over Na_2SO_4 and evaporated under reduced pressure. The crude product was purified by flash chromatography ($\lambda_{max} = 250$ nm, pure DCM) to obtain **34c** as a viscous reddish brown oil (174 mg, 55%). LC-MS: *m/z* 703 $[M+H]^+$. The product was used in the next step without further purification.

(5-(5-(5-(Dimethylcarbamoyl)pyridin-3-yl)-1*H*-pyrrolo[2,3-*b*]pyridin-3-yl)-2-formylphenyl)boronic acid (**11**)



A mixture of 5-(5-(5-(dimethylcarbamoyl)pyridin-3-yl)-1-tosyl-1*H*-pyrrolo[2,3-*b*]pyridin-3-yl)-2-formylphenyl trifluoromethanesulfonate **34a** (336 mg, 0.5 mmol), B_2pin_2 (152 mg, 0.6 mmol), $Pd(dppf)Cl_2 \cdot CH_2Cl_2$ (41 mg, 0.05 mmol) and KOAc (148 mg, 1.5 mmol) was dissolved in 6 mL of dioxane and then stirred at 100 °C in a sealed tube for 7 h. The product formation was confirmed by LC-MS. Upon solvent evaporation, the crude product was partitioned between EtOAc and water, and extracted using EtOAc (3 \times 20 mL). The combined organic extract was washed with brine, dried over Na_2SO_4 and evaporated under reduced pressure. To a solution of the crude product **35a** in THF/MeOH (2:1) was added Cs_2CO_3 (489 mg, 1.5 mmol, 0.5 M).^[3] The reaction mixture was then stirred continuously at 40 °C for 30 min and monitored by LC-MS until the deprotection was complete. The solvent was evaporated under reduced pressure. The final product was re-dissolved in methanol or DMSO, filtered and purified by reverse-phase chromatography using 5% to 95% acetonitrile in H_2O with 0.1% formic acid ($\lambda_{max} = 250$ nm, eluted at 30% acetonitrile in water) to afford **11** as a yellow powder (11.6 mg, 5.6%). LC-MS: *m/z* 415 $[M+H]^+$, 413 $[M-H]^-$. 1H NMR (400 MHz, $(CD_3)_2SO$) δ 12.32 (s, 1 H), 10.15 (s, 1 H), 9.08 (d, $J = 2.2$ Hz, 1 H), 8.68 (s, 2 H), 8.62 (d, $J = 1.8$ Hz, 1 H), 8.39 (s, 2 H), 8.26 (t, $J = 2.0$ Hz, 1 H), 8.19 (d, $J = 2.5$ Hz, 1 H), 8.05 (app. m, $J = 4.4$ Hz, 2 H), 7.95 (d, $J = 8$ Hz, 1 H). ^{13}C NMR (101 MHz, $(CD_3)_2SO$) δ 193.32, 167.78, 149.12, 148.54, 146.00, 142.35, 139.45, 136.56, 134.01, 132.79, 132.42, 130.55, 129.99, 126.74, 126.39, 126.31, 125.40, 117.24, 114.01, 34.79.

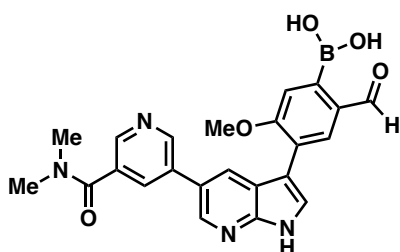
(4-(5-(5-(Dimethylcarbamoyl)pyridin-3-yl)-1*H*-pyrrolo[2,3-*b*]pyridin-3-yl)-2-formylphenyl)boronic acid (12)



A mixture of 4-(5-(5-(dimethylcarbamoyl)pyridin-3-yl)-1-tosyl-1*H*-pyrrolo[2,3-*b*]pyridin-3-yl)-2-formylphenyl trifluoromethanesulfonate **34b** (283 mg, 0.42 mmol), B₂pin₂ (130 mg, 0.51 mmol), Pd(dppf)Cl₂.CH₂Cl₂ (35 mg, 0.042 mmol) and KOAc (125 mg, 1.26 mmol) was dissolved in 6 mL of dioxane and then stirred at 100 °C in a sealed tube for 7 h. The product formation was confirmed by LC-MS. Upon solvent evaporation, the crude product was partitioned between

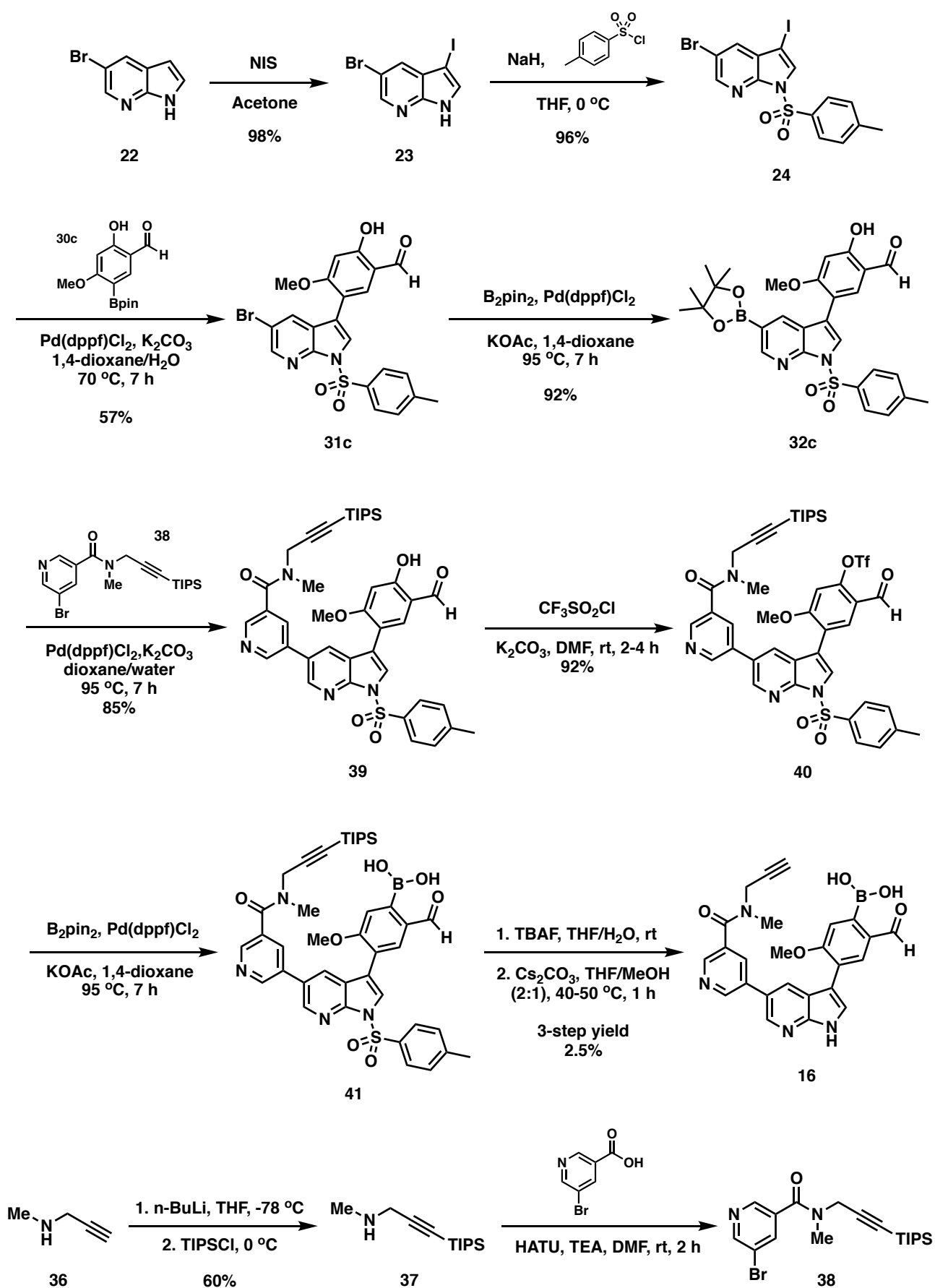
EtOAc and water, and extracted using EtOAc (3 × 20 mL). The combined organic extract was washed with brine, dried over Na₂SO₄ and evaporated under reduced pressure. To a solution of the crude product **35b** in THF/MeOH (2:1) was added Cs₂CO₃ (411 mg, 1.26 mmol, 0.5 M). The reaction mixture was then stirred continuously at 40 °C for 30 min and monitored by LC-MS until the deprotection was complete. The solvent was evaporated under reduced pressure. The final product was re-dissolved in methanol or DMSO, filtered and purified by reverse-phase chromatography using 5% to 95% acetonitrile in H₂O with 0.1% formic acid ($\lambda_{\text{max}} = 250$ nm, eluted at 30% acetonitrile in water) to afford **12** as a pale yellow powder (18 mg, 10.3%). LC-MS: *m/z* 415 [M+H]⁺, 413 [M-H]⁻. ¹H NMR (400 MHz, (CD₃)₂SO) δ 12.27 (s, 1 H), 10.25 (s, 1 H), 9.14 (d, *J* = 1.9 Hz, 1 H), 8.68 (app. m, *J* = 4.9 Hz, 4 H), 8.39 (d, *J* = 1.8 Hz, 1 H), 8.28 (d, *J* = 1.6 Hz, 1 H), 8.13 (m, *J* = 2.3 Hz, 3 H), 7.71 (d, *J* = 7.6 Hz, 1 H), 3.05 (br. s, 3 H), 3.01 (br. s, 3 H). ¹³C NMR (101 MHz, (CD₃)₂SO) δ 194.75, 167.29, 148.96, 147.35, 144.79, 142.23, 140.09, 135.26, 134.69, 134.04, 132.92, 130.68, 127.44, 126.33, 125.78, 124.75, 117.25, 113.88, 34.82.

(4-(5-(5-(Dimethylcarbamoyl)pyridin-3-yl)-1*H*-pyrrolo[2,3-*b*]pyridin-3-yl)-2-formyl-5-methoxyphenyl)boronic acid (14)



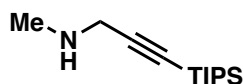
A mixture of 4-(5-(5-(dimethylcarbamoyl)pyridin-3-yl)-1-tosyl-1*H*-pyrrolo[2,3-*b*]pyridin-3-yl)-2-formyl-5-methoxyphenyl trifluoromethanesulfonate **34c** (174.2 mg, 0.25 mmol), B₂pin₂ (76.2 mg, 0.3 mmol), Pd(dppf)Cl₂.CH₂Cl₂ (20 mg, 0.025 mmol) and KOAc (74 mg, 0.75 mmol) was dissolved in 4 mL of dioxane and then stirred at 100 °C in a sealed tube for 7 h. The product formation was confirmed by LC-MS. Upon solvent evaporation, the crude product was partitioned

between EtOAc and water, and extracted using EtOAc (3 × 10 mL). The combined organic extract was washed with brine, dried over Na₂SO₄ and evaporated under reduced pressure. To a solution of the crude product **35c** in THF/MeOH (2:1) was added Cs₂CO₃ (244 mg, 0.75 mmol, 0.5 M). The reaction mixture was then stirred continuously at 40 °C for 30 min and monitored by LC-MS until the deprotection was complete. The solvent was evaporated under reduced pressure. The final product was re-dissolved in methanol or DMSO, filtered and purified by reverse-phase chromatography using 5% to 95% acetonitrile in H₂O with 0.1% formic acid ($\lambda_{\text{max}} = 262$ nm, eluted at 35% acetonitrile in water) to afford **14** as a pale yellow powder (9.5 mg, 8.6%). LC-MS: *m/z* 445 [M+H]⁺, 443 [M-H]⁻. ¹H NMR (400 MHz, (CD₃)₂SO) δ 12.13 (s, 1 H), 10.14 (s, 1 H), 9.01 (d, *J* = 2.1 Hz, 1 H), 8.65 (d, *J* = 2.0 Hz, 1 H), 8.60 (d, *J* = 1.8 Hz, 1 H), 8.50 (br. s, 2 H), 8.32 (d, *J* = 2.0 Hz, 1 H), 8.18 (t, *J* = 2.0 Hz, 1 H), 8.14 (s, 1 H), 7.88 (d, *J* = 2.5 Hz, 1 H), 7.36 (s, 1 H), 3.96 (s, 3 H), 3.04 (br. s, 3 H), 3.00 (br. s, 3 H). ¹³C NMR (101 MHz, (CD₃)₂SO) δ 193.22, 167.75, 159.66, 148.42, 148.38, 145.97, 141.90, 134.17, 132.75, 132.65, 132.40, 131.39, 127.17, 126.66, 124.73, 123.60, 118.31, 115.89, 110.22, 55.74, 34.81.



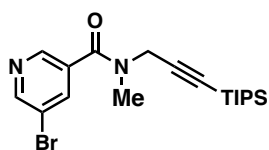
Scheme S5. Synthesis of an alkynylated aldehyde boronic acid ABL-targeting probe **16**.

***N*-Methyl-3-(triisopropylsilyl)prop-2-yn-1-amine (37)**



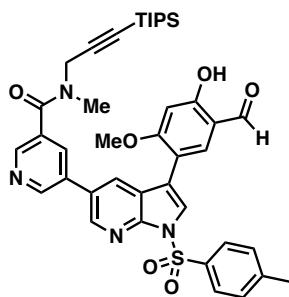
A solution of *N*-methylpropargylamine **36** (1.52 mL, 18 mmol, $\rho = 0.819$ g/mL) in 50 mL of anhydrous THF was cooled to -78 °C. *n*-BuLi (10 mL, 19.8 mmol, $\rho = 0.775$ g/mL, 2 M in cyclohexane) was added dropwise. The solution was stirred for 15 min at -78 °C and then warmed to 0 °C. Triisopropylsilyl chloride (4.62 mL, 21.6 mmol, $\rho = 0.901$ g/mL) was added dropwise. The reaction mixture was stirred for another 4 h and saturated NaHCO₃ solution was added. The product was extracted with EtOAc (3 × 20 mL). The combined organic extract was washed with brine, dried over Na₂SO₄ and evaporated under reduced pressure. The product was purified with hexane/EtOAc (4:1) and **37** was obtained as a yellow oil (2.43 g, 60%). ¹H NMR (400 MHz, CDCl₃) δ 3.43 (s, 2 H), 2.49 (s, 3 H), 1.06 (m, 21 H).

5-Bromo-*N*-methyl-*N*-(3-(triisopropylsilyl)prop-2-yn-1-yl)nicotinamide (38)



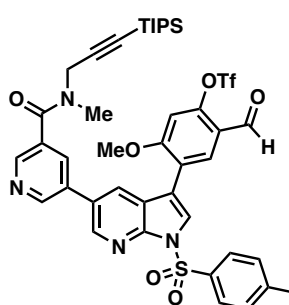
To a solution of 5-bromonicotinic acid (1.2 g, 5.94 mmol) in 20 mL of DMF was added HATU (3.4 g, 8.91 mmol) and NEt₃ (2.5 mL, 17.8 mmol, $\rho = 0.726$ g/mL). The reaction mixture was stirred for 5 minutes and *N*-methyl-3-(triisopropylsilyl)prop-2-yn-1-amine **37** (2 g, 8.91 mmol) was added. The reaction was stirred for another 3 h and the product was monitored and confirmed by LC-MS. To the mixture, saturated NaHCO₃ solution was added, and the mixture was extracted with EtOAc (3 × 20 mL). The combined organic extract was washed with brine, dried over Na₂SO₄ and evaporated under reduced pressure, providing the crude product **38** as a red oil ($\lambda_{\max} = 270$ nm), which was used in the next step without further purification. LC-MS: m/z 409 and 411 [M+H]⁺. ¹H NMR (400 MHz, (CD₃)₂SO) δ 8.82 (d, $J = 2.2$ Hz, 1 H), 8.63 (br. s, 1 H), 8.10 (s, 1 H), 4.39 (br. s, 1 H), 4.16 (br. s, 1 H), 3.34 (s, 3 H), 1.06 (m, 21 H).

5-(3-(5-Formyl-4-hydroxy-2-methoxyphenyl)-1-tosyl-1*H*-pyrrolo[2,3-*b*]pyridin-5-yl)-*N*-methyl-*N*-(3-(triisopropylsilyl)prop-2-yn-1-yl)nicotinamide (39)



A mixture of 2-hydroxy-4-methoxy-5-(5-(4,4,5,5-tetramethyl-1,3,2-dioxaborolan-2-yl)-1-tosyl-1*H*-pyrrolo[2,3-*b*]pyridin-3-yl)benzaldehyde **32c** (661 mg, 1.21 mmol), 5-bromo-*N*-methyl-*N*-(3-(triisopropylsilyl)prop-2-yn-1-yl)nicotinamide **38** (741 mg, 1.81 mmol), Pd(dppf)Cl₂·CH₂Cl₂ (98 mg, 0.121 mmol) and K₂CO₃ (500 mg, 3.62 mmol) was dissolved in 7 mL of dioxane and 1 mL of water and then stirred at 100 °C in a sealed tube for 7 h. The product formation was confirmed by TLC and LC-MS. Upon solvent evaporation, the crude product was partitioned between EtOAc and water, and extracted using EtOAc (3 × 20 mL). The combined organic extract was washed with brine, dried over Na₂SO₄ and evaporated under reduced pressure. The crude product was purified by flash chromatography ($\lambda_{\max} = 250$ nm, DCM/MeOH 0% → 5%) to obtain **39** as a viscous red foam (772 mg, 85%). LC-MS: m/z 751 [M+H]⁺, m/z 749 [M-H]⁻. The intermediate was used in the next step without further purification.

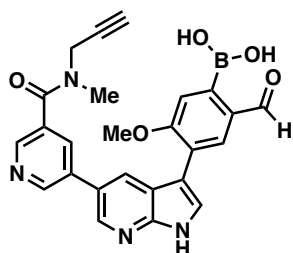
2-Formyl-5-methoxy-4-(5-(5-(methyl(3-(triisopropylsilyl)prop-2-yn-1-yl)carbamoyl)pyridin-3-yl)-1-tosyl-1*H*-pyrrolo[2,3-*b*]pyridin-3-yl)phenyl trifluoromethanesulfonate (40)



To a solution of 5-(3-(5-formyl-4-hydroxy-2-methoxyphenyl)-1-tosyl-1*H*-pyrrolo[2,3-*b*]pyridin-5-yl)-*N*-methyl-*N*-(3-(triisopropylsilyl)prop-2-yn-1-yl)nicotinamide **39** (981 mg, 1.31 mmol) in anhydrous DMF (5 mL) was added NEt₃ (0.73 mL, 5.24 mmol, $\rho = 0.726$ g/mL). The mixture was then stirred gently at 0 °C for 5 min and CF₃SO₂Cl (0.558 mL, 5.24 mmol, $\rho = 1.583$ g/mL) was added. The reaction was monitored using LC-MS. The crude product was partitioned between EtOAc and saturated NaHCO₃, and extracted using EtOAc (3 × 20 mL). *pH* was adjusted to 8. The combined organic extract was washed with brine, dried over Na₂SO₄ and evaporated under reduced pressure. The crude product was purified by flash

chromatography ($\lambda_{\max} = 250$ nm, DCM/MeOH 0% \rightarrow 5%) to obtain **40** as a viscous reddish brown oil (1.063 g, 92%). LC-MS: m/z 883 $[M+H]^+$. The product was used in the next step without further purification.

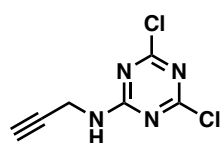
(2-Formyl-5-methoxy-4-(5-(5-(methyl(prop-2-yn-1-yl)carbamoyl)pyridin-3-yl)-1H-pyrrolo[2,3-b]pyridin-3-yl)phenyl)boronic acid (16)



A mixture of 2-formyl-5-methoxy-4-(5-(5-(methyl(3-(triisopropylsilyl)prop-2-yn-1-yl)carbamoyl)pyridin-3-yl)-1-tosyl-1H-pyrrolo[2,3-b]pyridin-3-yl)phenyl trifluoromethane sulfonate **40** (1.16 g, 1.31 mmol), B_2pin_2 (400 mg, 1.57 mmol), $Pd(dppf)Cl_2 \cdot CH_2Cl_2$ (107 mg, 0.131 mmol) and KOAc (386 mg, 3.93 mmol) was dissolved in 8 mL of dioxane and then stirred at 100 °C in a sealed tube for 7 h. The product formation was confirmed by LC-MS. Upon solvent evaporation, the crude product was partitioned between EtOAc and water, and extracted using

EtOAc (3 \times 10 mL). The combined organic extract was washed with brine, dried over Na_2SO_4 and evaporated under reduced pressure. To a solution of the crude product **41** in 4 mL of anhydrous THF and 4 mL of tetrabutylammonium fluoride (TBAF) 1.0 M in THF (4 mmol, 3 equiv.). The reaction mixture was then stirred continuously at 40 °C and monitored by LC-MS until the conversion was complete. The crude product was partitioned between EtOAc (20 mL) and a dilute solution of NaCl (180 mL), and extracted using dilute NaCl solution (20 \times 180 mL) to remove TBA completely. The organic extract was washed with brine, dried over Na_2SO_4 and evaporated under reduced pressure. To a solution of the crude product in THF/MeOH (2:1) was added Cs_2CO_3 (1.28 g, 3.93 mmol, 0.5 M). The reaction mixture was then stirred continuously at 40 °C for 30 min and monitored by LC-MS until the deprotection was complete. Upon solvent evaporation, the final product was re-dissolved in methanol or DMSO, filtered and purified by reverse-phase chromatography using 5% to 95% acetonitrile in H_2O with 0.1% formic acid ($\lambda_{\max} = 266$ nm, eluted at 35% acetonitrile in water) to afford **16** as a bright yellow powder (15 mg, 2.5%). LC-MS: m/z 469 $[M+H]^+$, 467 $[M-H]^-$. 1H NMR (400 MHz, $(CD_3)_2SO$) δ 12.14 (s, 1 H), 10.11 (s, 1 H), 9.04 (s, 1 H), 8.66 (d, $J = 1.5$ Hz, 1 H), 8.63 (d, $J = 1.8$ Hz, 1 H), 8.36 (s, 2 H), 8.33 (d, $J = 1.9$ Hz, 1 H), 8.19 (br. s, 1 H), 8.14 (s, 1 H), 7.89 (d, $J = 2.5$ Hz, 1 H), 7.35 (s, 1 H), 4.35 (br. s, 1 H), 4.14 (br. s, 1 H), 3.96 (s, 3 H), 3.06 (br. s, 4 H). ^{13}C NMR (101 MHz, $(CD_3)_2SO$) δ 193.16, 163.10, 159.67, 148.88, 148.44, 145.99, 141.93, 140.10, 134.29, 132.65, 132.36, 131.65, 131.57, 127.18, 126.70, 124.64, 123.55, 118.31, 115.81, 110.23, 79.10, 55.76.

4,6-Dichloro-N-(prop-2-yn-1-yl)-1,3,5-triazin-2-amine (17)



The intermediate was synthesized following the reported procedure.^[4]

A solution of cyanuric chloride (0.553 g, 3 mmol) in 10 mL of THF/DCM (2:8 v/v) was cooled in an ice bath to 0 °C. A solution of propargyl amine (0.192 mL, 3 mmol) and N,N -diisopropylethylamine (DIPEA) (0.871 mL, 5 mmol) in 8 mL of THF/DCM (2:1 v/v) was added slowly and the reaction was stirred for 90 min at 0 °C. The reaction mixture was then allowed to warm to room temperature and stirred for another 2 h. Upon solvent evaporation, the product was purified by flash chromatography using dichloromethane as an eluent to obtain **17** as an off-white solid product (554 mg, 91%). LC-MS: m/z 204 $[M+H]^+$. 1H NMR (400 MHz, $CDCl_3$) δ 6.15 (br. s, 1 H), 4.29 (dd, $J = 2.7$ Hz, 2 H), 2.32 (t, $J = 2.5$ Hz, 1 H).

3. Other Experimental Details

3.1. Modeling Methodology

The X-ray structure of ABL1 complexed with PPY-A (1) (PDB ID: 2QOH) was downloaded from the protein data bank (www.rcsb.org). The structure was prepared using the protein preparation wizard in Maestro release 2016-2 (www.schrodinger.com) with standard settings. This included bond assignments, protonation state assignment, optimization of the hydrogen bond network and constrained minimization.

Protein-inhibitor complexes were modeled in two ways. First, it was to investigate the molecular recognition/complementarity between kinase binding-site and unreacted inhibitor. Secondly, the probability of a covalent reaction between the warhead and the evolutionary conserved lysine K271 was accessed. Inhibitors were modeled in the active site using the co-crystallized inhibitor 7 as a template. The aldehyde and boronic acid groups were added and the resulting compounds 9-14 were minimized inside the active site using Macromodel release 2016-2 (www.schrodinger.com) with the protein constrained but otherwise standard settings. No significant clashes between inhibitor and protein atoms were observed. This complex was used to model the covalently attached inhibitor. The sidechain of the conserved lysine was rotated so that the basic nitrogen was coordinating with the boron atom and in plane of the phenyl ring. The imine was then built and the resulting covalent complex was minimized using constraints on protein residues more than 9 Å from the inhibitor (i.e. the binding site residues were also minimized). Modeling results are shown in **Figure S1**. Upon obtaining the X-ray structure, we observed the inhibitors binding in the same orientation as modeling had predicted. Results are shown in **Figure 2B**.

3.2. Biochemical Assay

Phosphorylated peptides have shorter retention time compared to that of unphosphorylated peptides due to the negative charge carried by the phosphate group. Phosphorylated and unphosphorylated peptides were separated in an electric field by their charge/mass ratio using the Caliper's microfluidic mobility shift technology. IC₅₀ values were determined from percent inhibition values at various concentrations of compounds by non-linear regression analysis.

Buffer composition

Reconstitution buffer (RA): 10 mM HEPES/NaOH pH 7.5, 0.003% Brij® L23, 0.004% TWEEN® 20 / *Substrate buffer*: 245 mM HEPES/NaOH pH 7.5, 0.003% Brij® L23, 0.004% TWEEN® 20, 26 mM MgCl₂ / *Termination buffer*: 100mM HEPES/NaOH pH 7.3, 0.022% Brij® L23, 5.6% DMSO, 0.16% CR3, 11.2 mM EDTA pH 8.0 / *Separation buffer*: 100 mM HEPES/NaOH pH 7.3, 0.015% Brij® L23, 5% DMSO, 0.1% CR3, 1 mM EDTA pH 8.0

Procedure

80 µL of RA buffer (DTT) + 10% DMSO was added into all wells from row B onwards. Next, 90 µL of RA buffer (DTT) was added into wells in row A of the dilution plate. 10 µL of stock compound (1 mM) was then added into wells in row A containing 90 µL of RA buffer (DTT). A serial dilution was performed by diluting 40 µL of compounds into the subsequent wells containing the 80 µL of RA buffer (DTT + 10% DMSO) to obtain 12 different concentrations of 100, 33.33, 11.11, 3.704, 1.235, 0.412, 0.137, 0.0457, 0.0152, 0.00508, 0.00169 and 0.000565 µM.

The enzyme master mix was prepared by diluting stock enzyme (full-length ABL (Cat. No. 08-001), full-length ABL^{T315I} (Cat. No. 08-093) and full-length ABL^{E255K} (Cat. No. 08-094) from Carna Biosciences, Inc.) with RA buffer (DTT). 6 µL of the enzyme master mix was added into all wells of the reaction plate. 10 µL of compounds was transferred from the dilution plate to the reaction plate containing 6 µL of the enzyme master mix each. After that, 10 µL of RA buffer (DTT) + 10% DMSO was transferred to the wells for positive and negative controls. The incubation time was adjusted according to the experimental design (0 min, 15 min, 3 h, 6 h, 12 h and 24 h). 10 µL of the prepared negative control mix (substrate buffer + water + peptide 5-FAM-EAIYAAPFAKKK-CONH₂ 3.9 µM)

was added to all wells for the negative control. Similarly, 10 μL of substrate master mix (Substrate buffer + DTT + ATP 36.4 μM + peptide 3.9 μM) was added to all wells for compounds and positive control. The reaction plate was incubated for 1 hour (cover the assay plate with aluminum foil). 45 μL of termination buffer was added into each well and the plate content was centrifuged to remove any air bubbles. The assay plate was transferred to the Caliper workstations (LabChip EZ Reader) for reading. Results are shown in **Figures 2C, S2 and S3**.

Final concentrations in 26 μL of reaction mixture

[ABL] = 1 nM; [peptide] = 1.5 μM , [ATP] = 14 μM

[Compound] = 38.46, 12.82, 4.274, 1.425, 0.4748, 0.1583, 0.05276, 0.01759, 0.005862, 0.001964, 0.0006513 and 0.0002171 μM

3.3. Kinetic Assay

40 μL of RA buffer (DTT) + 10% DMSO was added into all wells from row B to row L of the dilution plate. 90 μL of RA buffer (DTT) was into wells in row A of the dilution plate. 10 μL of stock compound (520 μM) was then added into wells in row A containing 90 μL of RA buffer (DTT). A serial dilution was performed by adding 40 μL of compounds to the subsequent wells containing the 40 μL of RA buffer (DTT + 10% DMSO) to obtain 12 different concentrations of 52, 26, 13, 6.5, 3.25, 1.625, 0.8125, 0.40625, 0.203125, 0.1015625, 0.05078125 and 0 μM .

The enzyme master mix was prepared by diluting stock enzyme (full-length ABL (Cat. No. 08-001), Carna Biosciences, Inc.) with RA buffer (DTT) and 12 μL of the enzyme master mix was subsequently added into all wells of the reaction plate. 20 μL of compounds was transferred from the dilution plate to the reaction plate containing 12 μL of the enzyme master mix each. 20 μL of substrate master mix (Substrate buffer + DTT + ATP 1.3 mM + peptide 5-FAM-EAIYAAPFAKKK-CONH₂ 3.9 μM) was immediately added to all wells. The assay plate was then transferred to the Caliper workstations (LabChip EZ Reader) for reading. Data was collected for up to 120 cycles. Results are shown in **Figure S4**.

Final concentrations in 52 μL of reaction mixture

[ABL] = 0.25 nM; [peptide] = 1.5 μM , [ATP] = 500 μM

[Compound] = 20, 10, 5, 2.5, 1.25, 0.625, 0.3125, 0.15625, 0.078125, 0.0390625, 0.01953125 and 0 μM

3.4. Protein Mass Spectrometry

10- μL samples of ABL kinase domain (30 μM) were incubated with a probe or inhibitor (1 mM) for 1 h and transferred to a 96-well plate. Two water samples were added between samples. LC-MS was performed on an Agilent capillary LC system coupled to an Agilent TOF6224 mass spectrometer equipped with an electrospray probe operated in the positive ionization mode. 5 μL of each sample was injected into an Agilent Poroshell 300SB-C₈, 2.1 mm \times 75 mm, 5 μm column. The mobile phase was 0.1% formic acid in water (A) and 0.1% formic acid in acetonitrile (B). The separation was performed by a gradient elution at a flow rate of 20 $\mu\text{L}/\text{min}$. During the first 8 min, the percentage of mobile phase B was increased from 10% to 90% than maintained at 90% for another 6 min, followed by column equilibration at 10% for the last 7 min. A column oven was used to maintain the temperature at 45 $^{\circ}\text{C}$. Mass spectrometer source condition were as follows: VCap 4000V, Fragmentor 180 V, gas temperature 325 $^{\circ}\text{C}$, scan range 110 to 2000 amu. Results are shown in **Figures 2A and S5**.

3.5. Protein Purification for ABL kinase domain 229-510

The gene encoding for the bacterial construct of ABL was cloned using NcoI/XhoI restriction sites into a pET28a vector (Novagen), yielding a tobacco etch virus (TEV) protease cleavable N-terminal hexahistidine tag. A YopH gene encoding the tyrosine phosphatase protein (from *Yersinia enterocolitica* EC 3.1.3.48) was cloned into a pCDFDuetTM-1 vector.^[5] The kinase domain (KD) of human ABL was co-expressed in *E. coli*

with YopH protein tyrosine phosphatase. Cells were grown at 37 °C in TB (terrific broth) medium (10% v/v K₃PO₄) up to an OD₆₀₀ of 1.7 when the overexpression of ABL protein was induced with 0.5 mM isopropyl- β -D-thiogalactopyranoside (IPTG). The incubation continued at 18 °C for 16 h before harvesting. The cell pellets were resuspended in lysis buffer comprised of 20 mM Tris buffer pH 7.3, 500 mM NaCl, 10 mM imidazole, 2 mM dithiothreitol (DTT), 10% (v/v) glycerol and cOmpleteTM protease inhibitor cocktail (1 tablet for every 50 mL of lysis buffer). Cell pellets were lysed using a probe sonicator with amplification of 40% for 30 min. The lysate was clarified via centrifugation at 14000 rpm for 45 min at 4 °C and the cell debris was removed. Soluble portion of the cell lysate was purified with a HisTrap HP 1 ml immobilized metal ion affinity chromatography (IMAC) column and the ABL protein was eluted in a buffer comprised of 20 mM Tris buffer pH 7.5, 500 mM NaCl, 250 mM imidazole, 10% (v/v) glycerol and 2 mM DTT. The proteins were further purified with a Superdex 200 size exclusion column using a running buffer comprised of in 20 mM TrisHCl pH 7.3, 25 mM NaCl, and 2 mM DTT. Fractions containing the ABL protein were identified by Coomassie blue staining and further purified with a HiTrap Q HP anion exchange chromatography column (His-tag ABL protein has a theoretical *pI* of around 5.0) using ion exchange buffer A comprised of 20 mM Tris buffer pH 7.3, 25 mM NaCl and 2 mM DTT and ion exchange buffer B comprised of 20 mM Tris buffer pH 7.5, 1 M NaCl and 2 mM DTT. The ABL protein was concentrated to 4.5 mg/mL. The purity was determined by Coomassie blue staining and mass spectrometry. The His-tag ABL kinase domain was used for in-gel fluorescence experiments. Results are shown in **Figure S5**.

3.6. X-ray Crystallography

The above construct was also used for structure biology and MS studies after cleaving the His tag using TEV protease. A brief method is described here. To the supernatant in 100-mL bottle was added 8 mL of Nickel NTA Agarose Resin which was then stirred gently for 45 min at 4 °C. The ABL protein was eluted using 500 mM imidazole. The affinity chromatography result was confirmed by Coomassie blue staining for the supernatant, pellet, 'flow-through' sample, 'wash' sample and eluate. A rough protein concentration was determined by NanoDrop and TEV protease was added to the combined eluent (1:20) to remove the *N*-terminal hexa-histidine tag. The eluate was then dialysed at 4 °C overnight against 2 L of dialysis buffer containing 50 mM Tris buffer pH 8, 500 mM NaCl, 5% glycerol and 1 mM DTT (high salt to prevent protein precipitation but cleaved protein was unexpectedly not precipitating even at 50 mM NaCl). Another 8 mL of Nickel NTA Agarose Resin was added to the fraction pool and stirred gently for 45 min at 4 °C. The flow-through fraction which contained tag-free ABL protein was collected. Cleavage efficiency was determined by Coomassie blue staining. The ABL protein (with >95% purity) was further purified with a HiTrap Q HP anion exchange chromatography column (Untagged ABL protein has a theoretical *pI* of around 5.56) using ion exchange buffer A comprised of 20 mM Tris buffer pH 8, 50 mM NaCl, 5% glycerol and 2 mM DTT and ion exchange buffer B comprised of 20 mM Tris buffer pH 8, 1 M NaCl, 5% glycerol and 2 mM DTT. The desired fractions were confirmed by Coomassie blue staining and further purified with a Superdex 75 size exclusion column using the running buffer comprised of 20 mM Tris buffer pH 8, 100 mM NaCl, 5% glycerol and 4 mM DTT. The untagged ABL protein (residues 229-510) was concentrated to 5 mg/mL before crystallization trials. The purity was determined by Coomassie blue staining and mass spectrometry. Results are shown in **Figure S5**.

Purified untagged ABL kinase domain was mixed with 1 mM of inhibitor and incubated at 4 °C for a minimum of 4 h and concentrated to 30 mg/mL. The complex was then spun down to remove the precipitates and used for crystallization. Crystals of ABL KD-inhibitor complex were grown in hanging drops containing 1:1 (v/v) ratio of protein to reservoir solution (ABL KD-**12** complex: 7 % w/v Polyethylene glycol 8000, 100 mM MES pH 6.5, 20 % v/v Ethylene glycol; ABL KD-**14** complex: 20% w/v Polyethylene glycol 3350, 1% Tryptone, 0.05 M HEPES sodium pH 7) at 4 °C. Crystals were harvested after a week and flash-frozen in liquid nitrogen after cryo-protection with mother liquor supplemented with 30% v/v glycerol. The X-ray diffraction data was collected at the MX2 beamline at the Australian Synchrotron.^[6] Processing and scaling of the data were done using the program XDS.^[7] The ABL KD-PPY-A complex (PDB: 2QOH) was used as a

search model for the molecular replacement method in PHASER in PHENIX to determine the structure of the ABL KD-inhibitor complex.^[8] Subsequently, the model building and iterative refinement were carried out using COOT and PHENIX, respectively.^[9,10] Results are shown in **Figures 2B & S6-S9**, as well as **Tables S2 & S3**.

3.7. KINOMEScan[®]

Inhibitors that bind to the ATP-binding pocket prevent kinase from binding to the immobilized ligand and therefore, reduce the amount of kinase captured on the solid support. However, molecules that do not bind to the kinase have no effects on the amount of kinase captured on the solid support. Screening hits are identified by measuring the amount of kinase captured in test samples against control samples by using a quantitative, precise and ultra-sensitive *q*PCR method that detects the associated DNA label. Selectivity Score (S-score) is calculated by dividing the number of hits at certain percent control (%Ctrl) by the total number of kinases being tested. The assay was carried out by the Eurofins Discovery. Results are shown in **Figure 2E** and **Table S4**.

3.8. Cell Culture

K562 cells (ATCC[®] CCL-243[™]) were cultured in the Iscove's Modified Dulbecco's Medium (IMDM, Gibco[™], Thermo Fisher Scientific) containing 10% (v/v) of fetal bovine serum (FBS, Gibco[™], Thermo Fisher Scientific) and 1% (v/v) of penicillin-streptomycin (Sigma-Aldrich) in a humidified 37 °C incubator with 5% CO₂. Ba/F3 cells transfected with BCR-ABL^{WT} (Creative Biogene) were similarly cultured in RPMI 1640 medium (Gibco[™], Thermo Fisher Scientific) containing 10% (v/v) of FBS and 1 µg/mL puromycin (Sigma-Aldrich). 3 × 10⁶ cells were transferred to a T25 flask containing 10 mL of pre-warmed culture medium for every passage. Cells were counted using the NucleoCounter[®] (Chemometec).

3.9. Anti-Proliferation Assay

Day 1 Seeding 2500 cells were seeded in a 96-well plate. The media were topped up to 50 µL if necessary. The plate was placed overnight in the incubator (37 °C, 5% CO₂).

Day 2 Treatment 297 µL of culture medium was added to row A of the dilution plate. 3 µL of stock solution (10 mM) was then added into wells in row A. Next, 120 µL of culture medium + 1% DMSO was added into all wells from row B onwards. A serial dilution was performed by diluting 30 µL of compounds into the subsequent wells containing 120 µL of culture medium 1% DMSO) to obtain 10 different concentrations of 100, 20, 4, 0.8, 0.16, 0.032, 0.0064, 0.00128, 0.000256 and 0.0000512 µM. 50 µL of the serial diluted compounds was added to each row and the plate was labeled accordingly and left in the incubator. Final concentrations of the compound were 50, 10, 2, 0.4, 0.08, 0.016, 0.0032, 0.00064, 0.000128 and 0.0000256 µM.

Day 5 Reading CellTiter-Glo (CTG) reagent was thawed out for at least 1 hr at room temperature. It was wrapped in the aluminum foil due to light sensitivity. The plate was removed from the incubator and left on the lab bench for 10 min. 100 µL of CTG reagent from the Promega CellTiter-Glo Luminescent Cell Viability Assay kit (#G7572) was added into each well. The plate was covered with aluminum foil and placed on the shaker for 0.5 h. The plate was read using Tecan Safire II Multi-Mode Plate Reader. Results are shown in **Figure 2F**.

3.10. Caco-2 Test

The Caco-2 cells were plated on a 96-well plate at the cell density of 12000 cells/well and allowed to grow for 21 d in the Dulbecco's Modified Eagle's Medium (DMEM) with media changed every 2 d. On the 21st day, transepithelial/transendothelial electrical resistance (TEER) was checked using EVOM (World Precision Instruments) and wells showing TEER above 230 ohm cm² were selected for the assay. Assays were carried out in Hanks Balanced Salt Solution (HBSS) containing 25 mM HEPES (pH 7.4). 10 µM of the test compound was prepared in the HEPES buffer (1% DMSO) followed by adding 75 µL of it to the apical

chamber against 250 μL of blank buffer (1% DMSO) in the basal chamber for A-B direction. For B-A direction, 250 μL of 10 μM test compound prepared in buffer (1% DMSO) was added to the basal chamber against 75 μL of blank buffer (1% DMSO) in the apical chamber. For incubation with an inhibitor, the respective buffers (with and without compound) were prepared with added inhibitors. Samples were crashed in acetonitrile containing an internal standard after an incubation period of 120 min, centrifuged and the supernatant was analyzed using LC-MS/MS. The assays were performed by GVK BIO and results are shown in **Tables S5 & S6**.

3.11. In-Gel Fluorescence Scanning Analysis

For in-gel fluorescence scanning analysis, pellets of K562 cells (ATCC[®] CCL-243[™]) or Ba/F3 cells transfected with BCR-ABL^{WT} (Creative Biogene) were thawed on ice and 300 μL of cold 1 \times PBS (with 0.1% Triton added) was added, followed by PMSF protease inhibitor (100 μM). The cells were lysed using a probe sonicator and the lysate was fractionated by centrifugation at 13,200 rpm for 8 min. The supernatant (soluble proteome) was transferred to a separate microcentrifuge tube. The protein concentrations of all samples were determined using the Pierce[™] BCA Protein Assay Kit and then normalized to 1 mg/mL. Click chemistry was performed on each sample using the final concentrations of rhodamine azide (25 μM), tris(3-hydroxypropyltriazolylmethyl)amine (THPTA) (100 μM), tris(2-carboxyethyl)phosphine (TCEP) (1 mM) and CuSO₄ (1 mM). The samples were incubated at room temperature for 1 h, followed by addition of 6 \times SDS loading buffer. 20 μL of the samples were then loaded and resolved on a NuPAGE[™] 4-12% Bis-Tris protein gel and imaged using the GE Healthcare Typhoon 9410 scanner (Cy3 and Cy5 laser channels). Fluorescence images were shown in gray scale. Results are shown in **Figures 3A-C & S10**.

Protocol 1: Pure proteins (His-tag ABL kinase domain)

The His-tag ABL kinase domain (residues 201-510) was diluted in 1 \times PBS buffer to a desired concentration of 0.2 μM in a volume of 49 μL . Samples were treated with a probe (1 μL of 50 \times stock in DMSO), mixed by agitation, centrifuged and incubated at 37 $^{\circ}\text{C}$ for 1 h. Click chemistry was then carried out as described above in a total volume of 52 μL . The samples were incubated at room temperature for 1 h, followed by the addition of 10.4 μL of 6 \times SDS loading buffer. 20 μL of the samples were then loaded and resolved on a NuPAGE[™] 4-12% Bis-Tris protein gel and imaged.

Protocol 2: Cell lysates (K562 and Ba/F3)

Soluble protein samples were obtained as described above and normalized to a concentration of 1 mg/mL in a volume of 49 μL . Samples were treated with inhibitor or probe (1 μL of 50 \times stock in DMSO), mixed by agitation, centrifuged and incubated at 37 $^{\circ}\text{C}$ for 1 h. Click chemistry was then carried out as described above in a total volume of 52 μL . The samples were incubated at room temperature for 1 h, followed by the addition of 10.4 μL of 6 \times SDS loading buffer. 20 μL of the samples were then loaded and resolved on a NuPAGE[™] 4-12% Bis-Tris protein gel and imaged.

Protocol 3: Competition Assay

The His-tag ABL kinase domain (residues 201-510) were diluted in 1 \times PBS buffer to a desired concentration of 0.2 μM in a volume of 48 μL . Samples were treated with inhibitor (1 μL of 50 \times stock in DMSO), mixed by agitation and incubated at 37 $^{\circ}\text{C}$ for 1 h. Samples were then treated with alkynylated probe (1 μL of 50 \times stock in DMSO), mixed by agitation, centrifuged and incubated at 37 $^{\circ}\text{C}$ for another 1 h. Click chemistry was then carried out as described above in a total volume of 52 μL . The samples were incubated at room temperature for 1 h, followed by the addition of 10.4 μL of 6 \times SDS loading buffer. 20 μL of the samples were then loaded and resolved on a NuPAGE[™] 4-12% Bis-Tris protein gel and imaged.

Protocol 4: Reduction of iminoboronate C=N by NaBH₃CN

Soluble protein samples were obtained as described above and adjusted to a concentration of 6-8 mg/mL in a volume of 48 μ L. Samples of soluble proteome were treated with inhibitor or probe (1 μ L of 50 \times stock in DMSO), followed by NaBH₃CN (1 μ L of 50 \times stock in water), mixed by agitation, centrifuged and incubated at 37 $^{\circ}$ C for 24 h. Next, 200 μ L of pre-chilled acetone was added and protein precipitation was carried out for 1 h. Pellets were then washed thoroughly with cold acetone (\times 2) and cold methanol (\times 2), centrifuged at 13,200 rpm for 8 min at 4 $^{\circ}$ C and re-dissolved in 50 μ L of PBS (with 1% SDS) via sonication. Click chemistry was performed on each sample using the final concentrations of rhodamine azide (25 μ M), tris(3-hydroxypropyltriazolymethyl)amine (THPTA) (100 μ M), tris(2-carboxyethyl)phosphine (TCEP) (1 mM) and CuSO₄ (1 mM). The samples were incubated at room temperature for 1 h, followed by addition of 6 \times SDS loading buffer. 20 μ L of the samples were then loaded and resolved on a NuPAGETM 4-12% Bis-Tris protein gel and imaged using the GE Healthcare Typhoon 9410 scanner (Cy3 and Cy5 laser channels). Fluorescence images were shown in gray scale.

3.12. Chemoproteomics and Off-Target Identification (ID)

3.12.1. Large-Scale Pull-Down (PD)

Soluble proteomes were obtained as described above and adjusted to a concentration of 8 mg/mL in a volume of 47 μ L. In an attempt to capture the greatest number of potential off-targets as previously reported,^[11,12] samples were treated with 10 μ M of probe **16** or DMSO (1 μ L of 500 μ M stock in DMSO), followed by NaBH₃CN (1 μ L of 10 M stock), topped up with 1 μ L of PBS buffer, mixed by agitation, centrifuged and incubated at 37 $^{\circ}$ C for 24 h. High concentrations of known covalent kinase inhibitors such as ibrutinib and afatinib (1-10 μ M) have been used by Taunton's and Cravatt's research groups for mass spectrometry despite nanomolar potency due to the well-known variability and sensitivity of mass spectrometry, and efficiency of pull-down experiments.^[11,12] In the competition study using inhibitor **14**, 1 μ L of 25 mM stock in DMSO, was added first, followed by NaBH₃CN (1 μ L of 10 M stock) and incubated for 1 h at 37 $^{\circ}$ C. 10 μ M of probe **16** was then added and the mixture was incubated at 37 $^{\circ}$ C for 24 h. Click chemistry was performed on each sample using the final concentrations of azide-PEG3-biotin (25 μ M), tris(3-hydroxypropyltriazolymethyl)amine (THPTA) (100 μ M), tris(2-carboxyethyl)phosphine (TCEP) (1 mM) and CuSO₄ (1 mM). The sample was incubated at room temperature for 1 h. Next, 200 μ L of pre-chilled acetone was added and protein precipitation was carried out for 1 h. Pellets were then washed thoroughly with cold acetone (\times 2) and cold methanol (\times 2), centrifuged at 13,200 rpm for 8 min at 4 $^{\circ}$ C and re-dissolved in 50 μ L of PBS (with 1% SDS) via sonication. 100 μ L of NeutrAvidin agarose resins were added and the mixture was shaken for another 3 h at room temperature or 4 $^{\circ}$ C overnight. The supernatant was removed and resins were washed thoroughly using PBS (with 1% SDS) for 6-7 times. Another 50 μ L of PBS (with 1% SDS) was added, followed by 6 \times SDS loading buffer. The samples were then boiled at 95 $^{\circ}$ C for 15-20 min and spun down for 30 s.

For Western blotting, 10 μ L of the samples were then loaded and resolved on a NuPAGETM 4-12% Bis-Tris protein gel. Each sample was run on a NuPAGETM 4-12% Bis-Tris protein gel in MES buffer using MagicMark XP Western and Novex Sharp Pre-stained protein standards. Protein was transferred onto a PVDF membrane (soaked in methanol for 5 min beforehand) in Transfer buffer (voltage 30 V for 2 h). Blots were blocked with 5% milk in Tris-buffered saline with 0.1% Tween (TBST) for 1 h at room temperature. Blots were incubated with rolling at 4 $^{\circ}$ C overnight with the primary antibody (c-ABL antibody #2862 from Cell Signaling Technology) in 5% BSA in TBST (1:1000). After incubation, blots were rinsed once and washed three times for 15 min each with TBST. Next, blots were then incubated with the secondary antibody (*anti-rabbit IgG*, HRP-linked antibody (#7074 from Cell Signaling Technology) in 5% BSA in TBST (1:10000) for 1 h at room temperature. Blots were then rinsed once and washed three times for 15 min each with TBST. Amersham ECL Western Blotting detection reagent (from GE Healthcare Life Sciences) was used as the HRP substrate (5-min incubation). Bands were detected using the FluorChemTM E system (ProteinSimple). Next, blots were incubated with another primary antibody (GADPH antibody) in 5% BSA

in TBST (1:10000). After incubation, blots were rinsed once and washed three times for 5 min each with TBST. Next, blots were then incubated with the secondary antibody (*anti*-mouse IgG) in 5% BSA in TBST (1:5000) for 30 min at room temperature. Blots were then rinsed once and washed three times for 15 min each with TBST. Amersham ECL Western Blotting detection reagent (from GE Healthcare Life Sciences) was used as the HRP substrate (5-min incubation). Bands were detected using the FluorChemTM E system (ProteinSimple). Results are shown in **Figure 3C**.

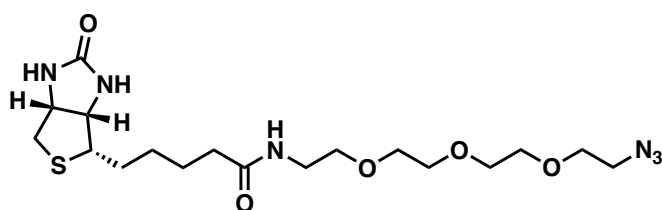
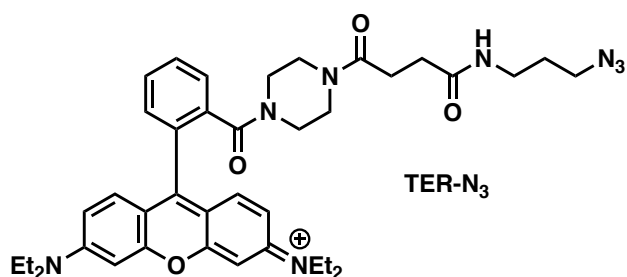
For proteomic mass spectrometry sample preparation, 20 μL of the samples were then loaded and resolved on a NuPAGETM 4-12% Bis-Tris protein gel. Each lane of the Coomassie-stained gel was cut into $3 \times 1 \text{ mm}^2$ cubes with a razor blade. The gel particles were collected and destained with 1 mL of 25 mM ammonium bicarbonate (ABC) in 50% ACN (0.5 mL of 25 mM of ABC and 0.5 mL of ACN) at 37 °C for several times until the blue color of the gel disappeared completely. The gel cubes were dehydrated with 500 μL of ACN for 5-10 min (the gel cubes would shrink and become white and crinkle). ACN was then removed completely and the cubes were dried by Speedvac for 30 min. 1 M DTT stock was prepared in water and diluted to 10 mM with 25 mM ammonium bicarbonate (ABC) buffer. Next, 0.5 mL of the diluted DTT solution was added to each tube which was incubated at 60 °C for 60 min using a thermo mixer. The volume of the solution should be enough to immerse all the gel cubes. (After 1 h, it was checked whether the gel cubes were dried. More 10 mM DTT solution should be added and the tubes were incubated for another 10-20 min). The DTT solution was then removed completely. 0.5 M IAA was prepared in water and diluted to 50 mM with 25 mM ABC. 600 μL of the diluted solution was then added to each tube which was incubated at room temperature for 45 min in the dark. The iodoacetamide (IAA) solution was then removed. Gel cubes were then washed with 100 mM ABC 50% ACN solution (5 mL of 100 mM ABC and 5 mL of 100% ACN) for 2-3 times. The DTT and IAA should be washed completely or they would affect the following trypsin digestion.

The particles were dehydrated with ACN for 5 – 10 min followed by drying using Speedvac for 20 – 30 min (water should be removed completely so that the particles could be more readily absorbed by the trypsin solution for digestion). 1 pack of trypsin was diluted (20 μg) with 20 μL 50 mM acetic acid (3.3 μL acetic acid in 1 mL H₂O). The final concentration of trypsin was 1 $\mu\text{g}/\mu\text{L}$. The amount of trypsin added was in the approximate ratio of 1:20 (trypsin/protein in gel). In all, 120 μL of trypsin solution was diluted to 8.4 mL of 25 mM ABC solution from which 700 μL was added to each tube. Incubation was done for 30 min at room temperature. If the gel cubes were dried (the gel should absorb most of the solution), more 25 mM ABC solution should be added to immerse the gel cubes completely. The mixture was then incubated at 37 °C overnight. The solution in the digestion tube was transferred to another 2 mL tube. The gel cubes were washed with 500 μL 50% ACN 1% formic acid solution twice. The washing solutions were combined together and the solvent was evaporated in Speedvac completely. Peptides in each tube were dissolved in 0.5 mL 1% formic acid (no ACN). The C₁₈ column (50 mg) was first washed with 1 mL methanol followed by 1 mL 1% formic acid. 500 μL sample was added to the column, and the solution was drained and the peptide would be absorbed onto the column. The column was washed with 1% formic acid for 6 to 8 times to remove the salt in sample. The peptide was eluted with 0.9 mL of 70% ACN 1% formic acid in water. The eluents were evaporated in Speedvac.

3.12.2. Protein Mass Spectrometry Analysis and Data Analysis

For each sample, three biological replicates were performed. The samples were dissolved in 10 μL of H₂O and centrifuged at 15000 rpm/4 °C for 30 min. 8 μL of the supernatant was collected. The LC-MS/MS experiment was performed on an UltiMate 3000 Nano HPLC system coupled to an Orbitrap Fusion Lumos (Thermo Fisher Scientific). A volume of 3 μL of each sample was injected into a trap column (0.3 mm \times 5 mm, C₁₈, 5 μm , 100 Å, 160454) and an Acclaim PepMap C₁₈ RSLC 50 μm ID \times 15 cm separation column in an EASY-SprayTM setting. Peptides were separated with an 60-min gradient (buffer A: 0.1% formic acid in deionized water; buffer B: 0.08% formic acid in 80% acetonitrile with a flow rate of 0.3

$\mu\text{L}/\text{min}$: 5 min of 4% B, 35 min of 4–30 % B, 5 min of 30–80% B, 5 min of 80% B, 5 min of 80–4% B, 5 min of 4% B). Separated peptides were then directly analyzed on the Orbitrap Fusion-Lumos in a data-dependent manner. Peptides were ionized by using spray voltage of 2.4 kV and the ion transfer tube temperature was 320 °C, with automatic switching between MS and MS/MS scans using exclusion duration 60 s. Mass spectra were acquired at a resolution of 60,000 with a target value of 4×10^5 ions or a maximum integration time of 50 ms. The scan range was limited from 350 to 1500 m/z. Peptide fragmentation was performed via higher-energy collision dissociation (HCD) with the energy set to 30%. The MS/MS spectra were acquired at a resolution of 15,000 with a target value of 5×10^4 ions or a maximum integration time of 30 ms. The fixed first m/z was 110, and the isolation window was 1.6 m/z. Data processing was performed on Proteome Discoverer 2.4 software (Thermo Fisher Scientific) with label free quantification (LFQ) mode, and peptide sequences were determined by matching protein databases with the acquired fragmentation pattern by SEQUEST HT algorithm. The precursor mass tolerance was set to 10 ppm and fragment ion mass tolerance was set to 0.6 Da. Two missed cleavage site of trypsin was allowed. Carbamidomethyl (C) was used as a fixed modification; oxidation (M) and deamination (N, Q) were used as variable modifications. All spectra were searched against protein database (Uniprot, Human, 2019.05.06) using a target false discovery rate (FDR) of 1%. The peptide spectrum matches (PSMs) value of each identified protein target was an average of three individual experiments. The normalized LFQ abundance ratio under different conditions were extracted, the max value of the LFQ abundance ratio value was set to be 100. The proteins identified were additionally filtered by including two or three valid abundance ratio values in three replicates, and more than two unique peptides. Further statistical analysis was performed on Perseus software (version 1.5.1.6.).^[13] Prior to analysis, for proteins whose ratio values were all 100, one of the ratio values was changed from 100 to be 99.9. The abundance ratio values were \log_2 transformed and performed two-sample Student's *t*-test including Benjamini-Hochberg multiple testing correction (FDR = 0.05) on Perseus. The Proteins with an abundance ratio > 2 ($\log_2(x) > 1$) and $-\log_{10}$ t-test p-value > 1.3 were considered as high-confidence hits. Results are summarized in **Figures 3D-3F, S11-12** and **Table S7**. Full data are provided in excel format as SI_II.



4. Results and Discussion

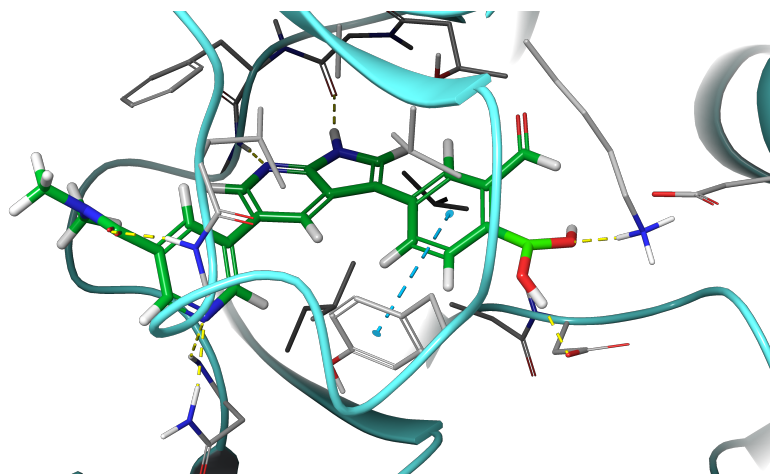


Figure S1. Structure-based design of BCR-ABL inhibitor targeting the catalytic lysine K271. A covalent inhibitor was modeled into the active site by using the co-crystallized inhibitor 7 as a template.

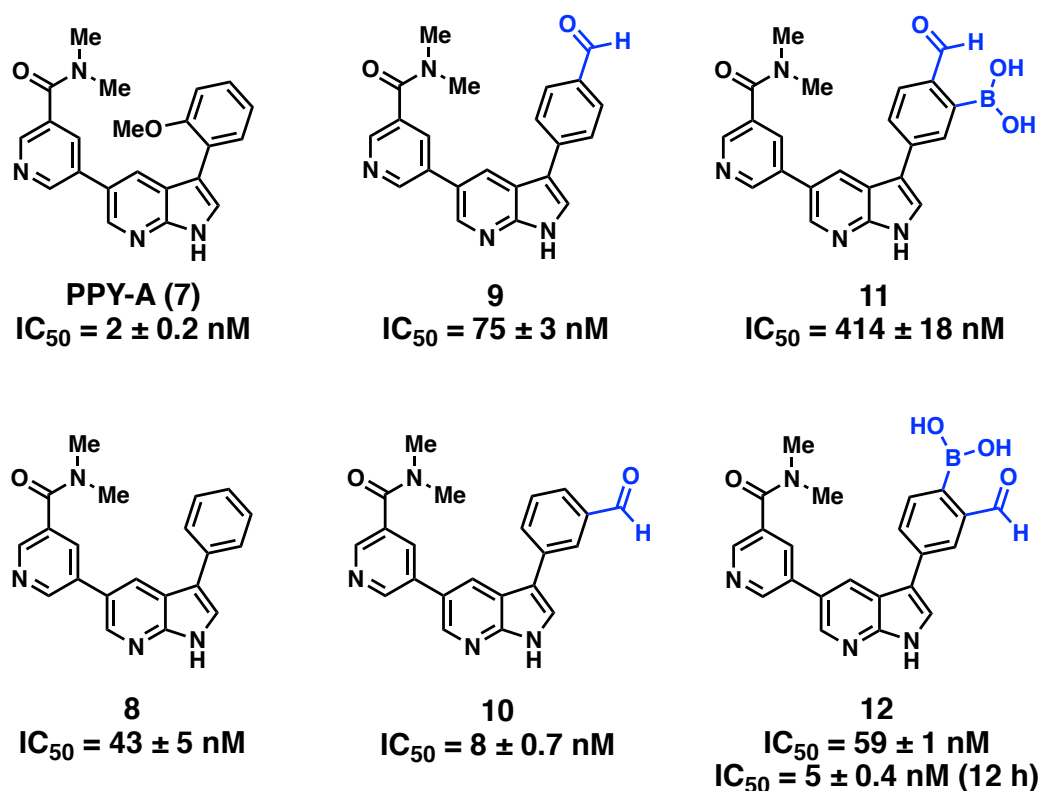
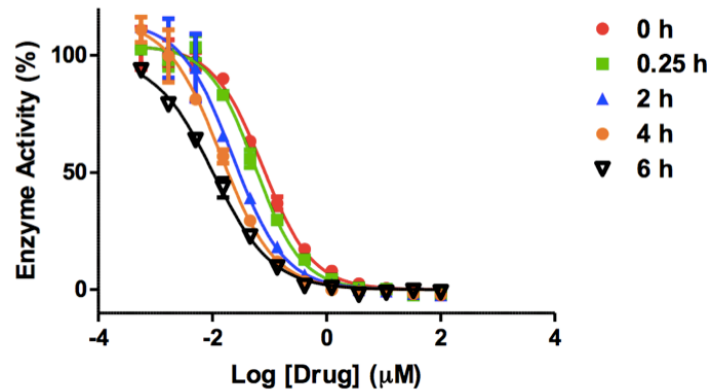


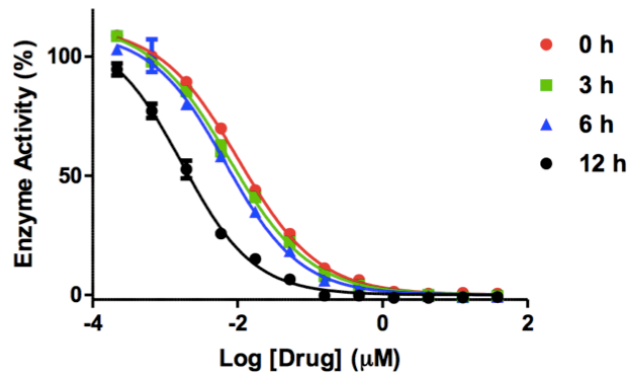
Figure S2. Comparison of ABL inhibition of different analogs using the IC_{50} biochemical assay after 15 minutes of incubation.

A

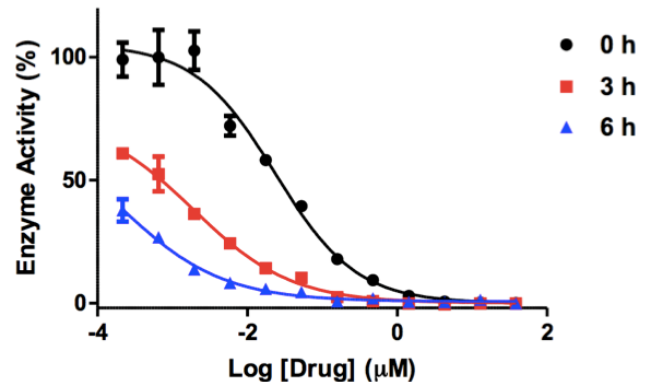
Time (h)	Potency IC ₅₀ (nM)	
	Compound 12	Compound 10
0	83 ± 2	7 ± 0.3
0.25	59 ± 1	8 ± 0.1
2	27 ± 4	8 ± 0.2
4	18 ± 1	7 ± 0.2
6	10 ± 2	ND
8	7 ± 0.2	ND
12	5 ± 0.4	ND

**B**

T (h)	Potency IC ₅₀ (nM)	
	Compound 14	Compound 13
0	13 ± 0.3	3 ± 0.1
3	10 ± 0.9	4 ± 0.2
6	6 ± 0.2	3 ± 0.2
12	1.7 ± 0.2	3 ± 0.1

**C**

T (h)	Potency IC ₅₀ (nM)	
	Compound 14	Compound 13
0	25 ± 1	4 ± 0.2
3	1.8 ± 1	4 ± 0.3
6	0.1 ± 0.02	3 ± 0.1

**D**

T (h)	Potency IC ₅₀ (nM)	
	Compound 14	Compound 13
0	43 ± 2	9 ± 0.1
3	28 ± 3	8 ± 0.2
6	13 ± 0.1	10 ± 0.2
12	0.5 ± 0.03	8 ± 0.1

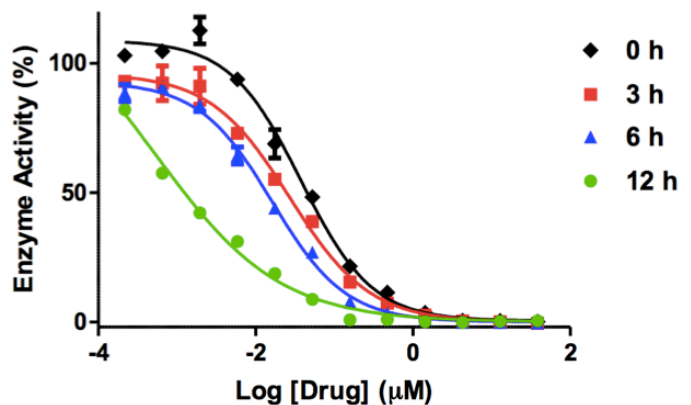


Figure S3. (A) Time-dependent IC₅₀ values of compound 12 against ABL^{WT}. (B) Time-dependent IC₅₀ values of compound 14 against ABL^{WT}. (C) Time-dependent IC₅₀ values of 14 against ABL^{T315I}. (D) Time-dependent IC₅₀ values of 14 against ABL^{E255K} (ND – Not determined).

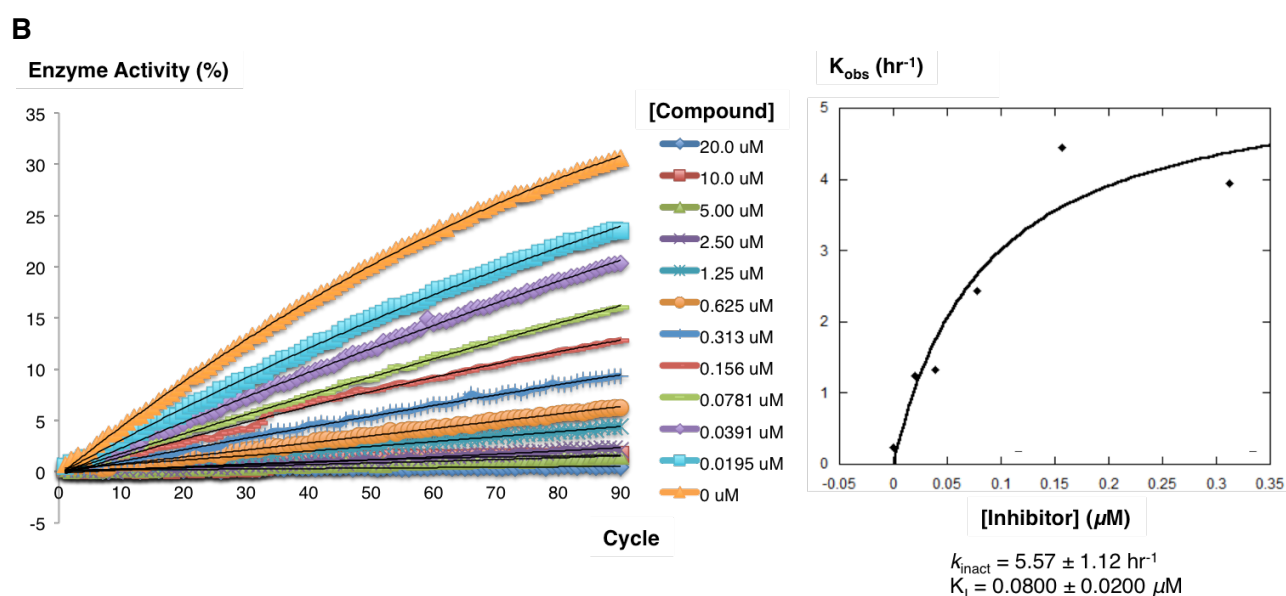
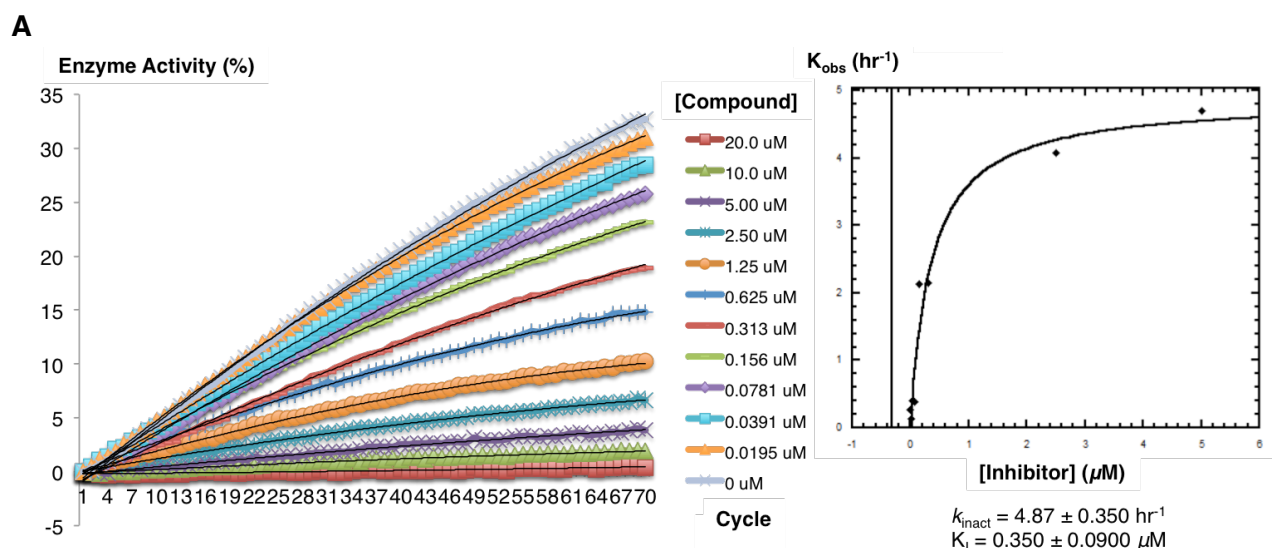


Figure S4. (A) Kinetic study of compound **12**. (B) Kinetic study of compound **14**. The average values of duplicates were reported.

The kinetic analysis was performed using the mathematical model used for irreversible covalent inhibitors; however, we observed longer incubation time taken to reach binding equilibrium in the biochemical assays. One of the possible reasons could be because of the reversibility nature of this covalent warhead which included a dissociation rate constant k_{off} . An attempt to determine this value using surface plasmon resonance did not produce reproducible results. Similar models and results were reported by Taunton and co-workers in their studies of cysteine-targeting, reversible covalent inhibitors of kinases,^[14] where the authors concluded that the limitation of the current analysis model for reversible covalent inhibitors, that is, the actual residence time did not directly correlate with k_{inact} , K_{I} or $k_{\text{inact}}/K_{\text{I}}$.

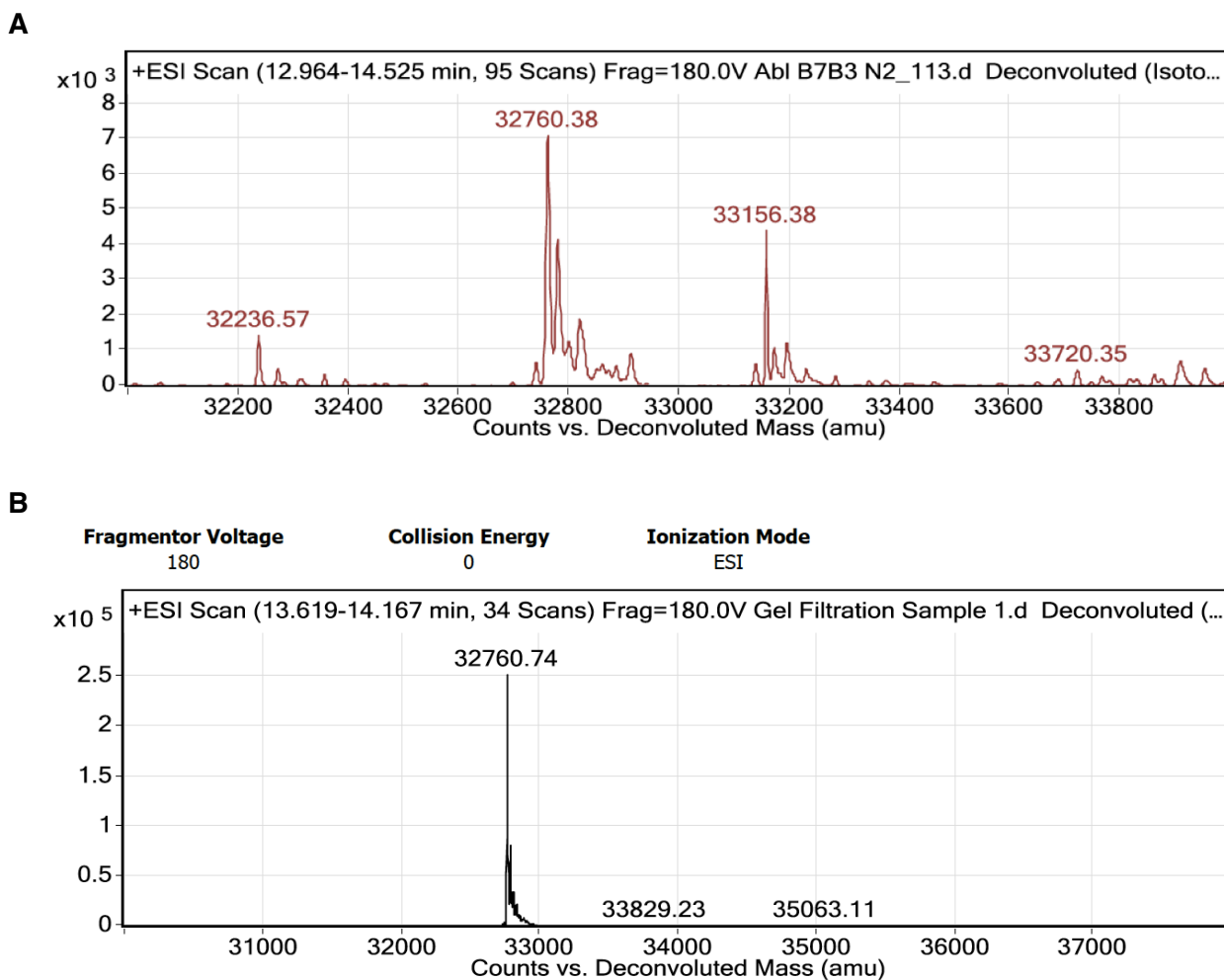


Figure S5. Mass spectrometric analysis. (A) Untagged ABL kinase domain + **12**. (B) Untagged ABL kinase domain.

In another attempt to determine the specificity of this warhead towards the catalytic lysine residue, we purified the mutant forms of ABL kinase domains ABL^{K271A}, ABL^{K271R} and ABL^{K271N} lead to unstable ABL kinase proteins probably due to the disruption of the salt bridge. Nevertheless, mass spectrometry and X-ray crystallography data for the first time showed that both **12** and **14** interacted with K271 covalently and not with any other lysine residues in the ABL kinase domain which has 19 lysine residues in total.

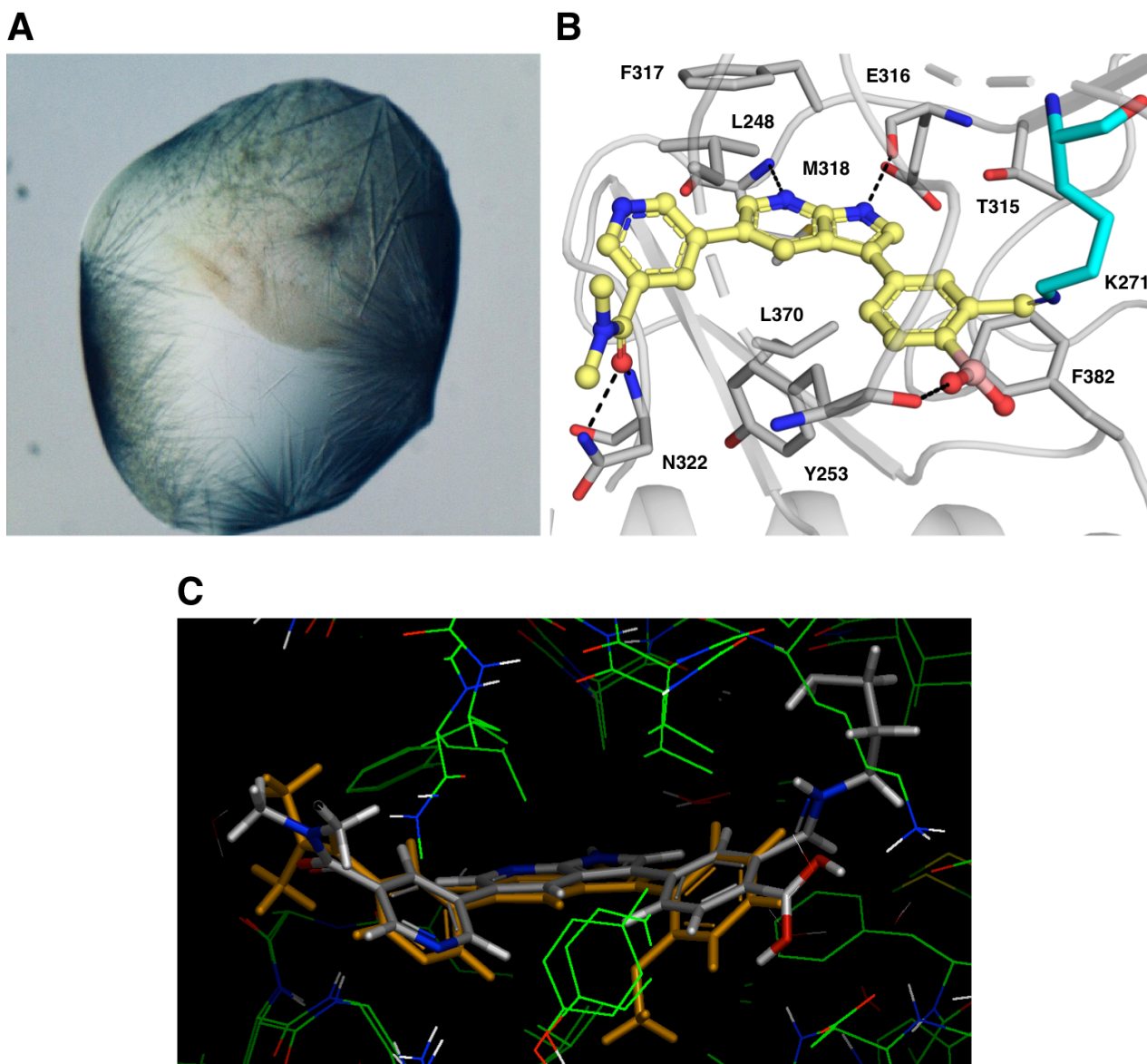


Figure S6. (A) Needle-shaped crystals of ABL kinase domain complex-**12**. (B) Co-crystal structure of ABL kinase domain-**12** complex (PDB ID: 7CC2). (C) Overlaid crystal structures of **7** (orange) (PDB ID: 2QOH) and **12** (grey) with the ABL kinase domain.

Table S2. X-Ray data collection and refinement statistics for ABL KD-12 complex

	ABL-12
Wavelength	0.9537
Resolution range	47.39 - 2.723 (2.82 - 2.723)
Space group	P 21 21 2
Unit cell	116.489 127.939 56.76 90 90 90
Total reflections	46608 (4487)
Unique reflections	23349 (2265)
Multiplicity	2.0 (2.0)
Completeness (%)	99.59 (99.17)
Mean I/sigma(I)	9.08 (2.04)
Wilson B-factor	43.74
R-merge	0.050 (0.284)
R-meas	0.071 (0.402)
R-pim	0.050 (0.284)
CC1/2	0.996 (0.8)
CC*	0.999 (0.943)
Reflections used in refinement	23342 (2265)
Reflections used for R-free	2000 (194)
R-work	0.192 (0.252)
R-free	0.241 (0.344)
CC(work)	0.949 (0.847)
CC(free)	0.921 (0.678)
Number of non-hydrogen atoms	4348
macromolecules	4303
solvent	45
Protein residues	529
RMS(bonds)	0.003
RMS(angles)	0.64
Ramachandran favored (%)	96.12
Ramachandran allowed (%)	3.88
Ramachandran outliers (%)	0.00
Rotamer outliers (%)	0.00
Clashscore	4.76
Average B-factor	46.13
macromolecules	46.24
solvent	34.99

*Statistics for the highest-resolution shell are shown in parentheses. ^a $R_{merge} = \sum_h \sum_i |I_{hi} - \langle I_h \rangle| / \sum_h \sum_i I_{hi}$, where I_{hi} is the i th observation of the reflection h , while $\langle I_h \rangle$ is its mean intensity. ^bR-factor = $\sum ||F_{obs}| - |F_{calc}|| / \sum |F_{obs}|$. ^cR-free was calculated with 5% of reflections excluded from the whole refinement procedure.

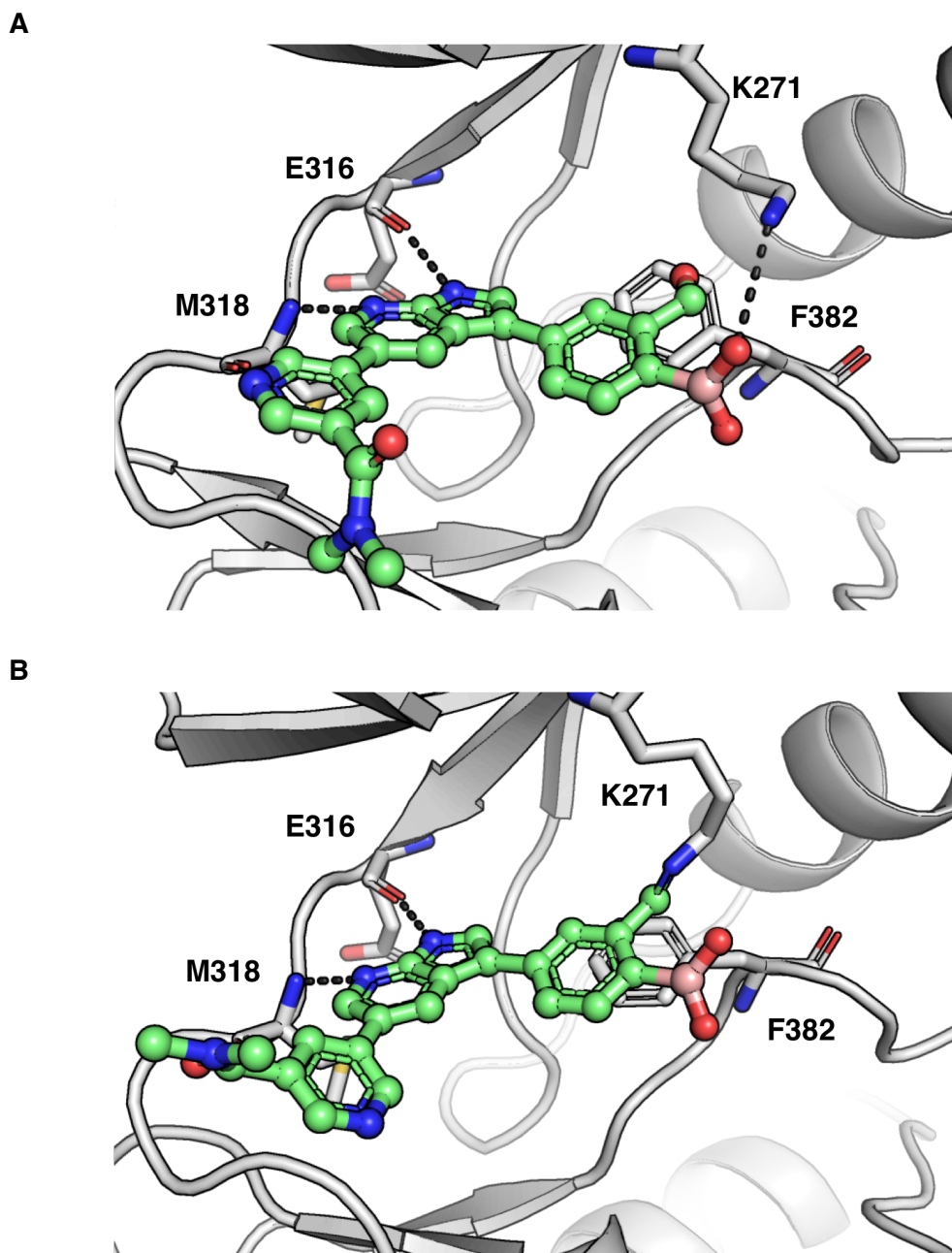


Figure S7. Two ABL kinase domains in a crystal unit of ABL kinase domain-12 complex, (A) without covalent interaction, and (B) with covalent interaction.

Every crystal unit contains two ABL kinase domains. One molecule of **12** is bound to ABL KD non-covalently whereas another molecule of **12** binds to the second ABL kinase domain both non-covalently and covalently via the K271 residue. As shown in **Figure S5**, the non-covalently bound **12** forms a hydrogen bond between the catalytic lysine residue and boronic acid. A careful examination of **Figure S7** shows that the lysine is ideally positioned for a nucleophilic attack on the adjacent aldehyde carbonyl, suggesting that this may be an intermediate in the imine formation between **12** and ABL kinase.

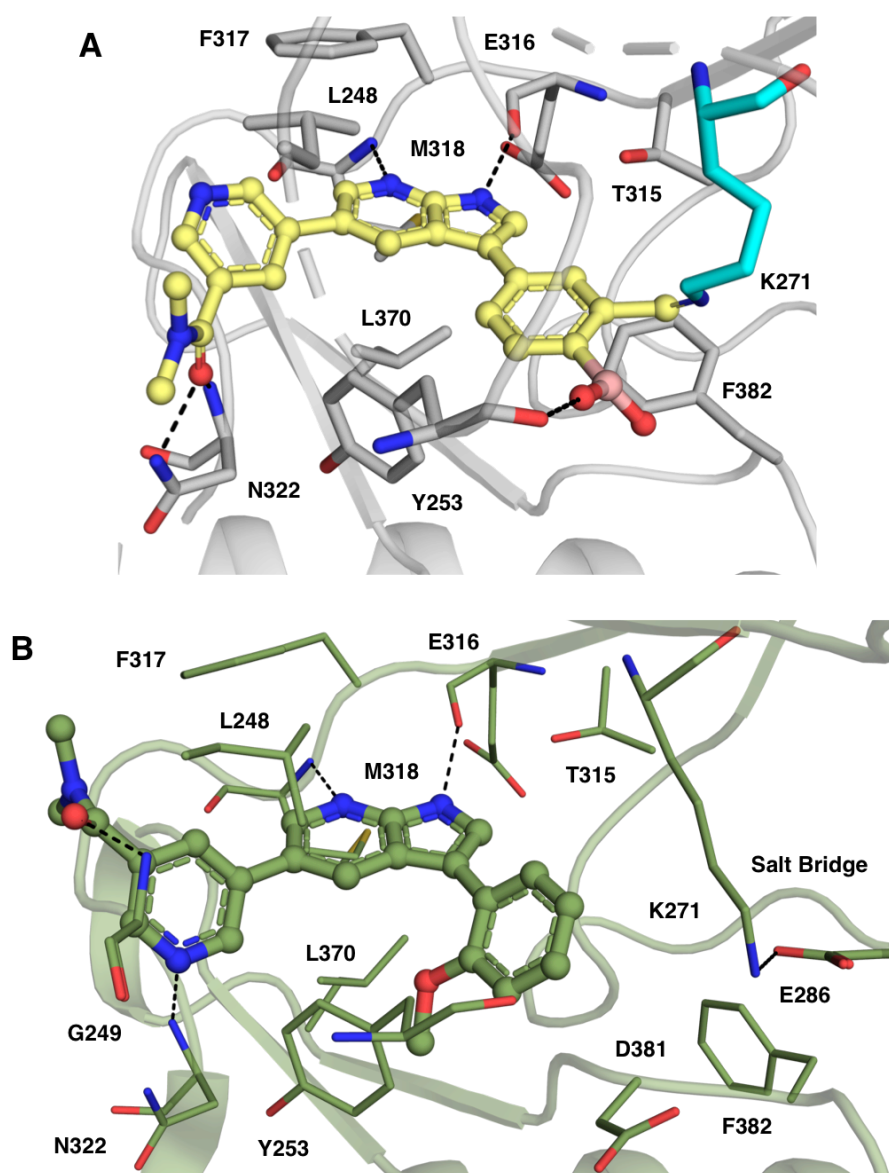


Figure S8. Comparison between ABL kinase domain-12 complex (PDB ID: 7CC2) and ABL kinase domain-PPY-A (7) complex (PDB ID: 2QOH). (A) ABL KD-12 complex. (B) ABL KD-7 complex.

Figure S8 shows the difference between the ABL kinase domain-12 complex (PDB ID: 7CC2) and the ABL kinase domain-PPY-A (7) complex (PDB ID: 2QOH). Two major differences can be observed. First, the *N,N*-dimethylnicotinamide structural unit is flipped upside down in 7CC2 and there are major differences pertinent to DFG motif and α C helix between two crystal structures. Nevertheless, both proteins adopt a DFG-Asp in conformation. Attempts to mutate the catalytic lysine residue to alanine and glycine residues using a similar purification procedure were unsuccessful probably due to the importance of this residue in the protein structure and function of ABL kinase.

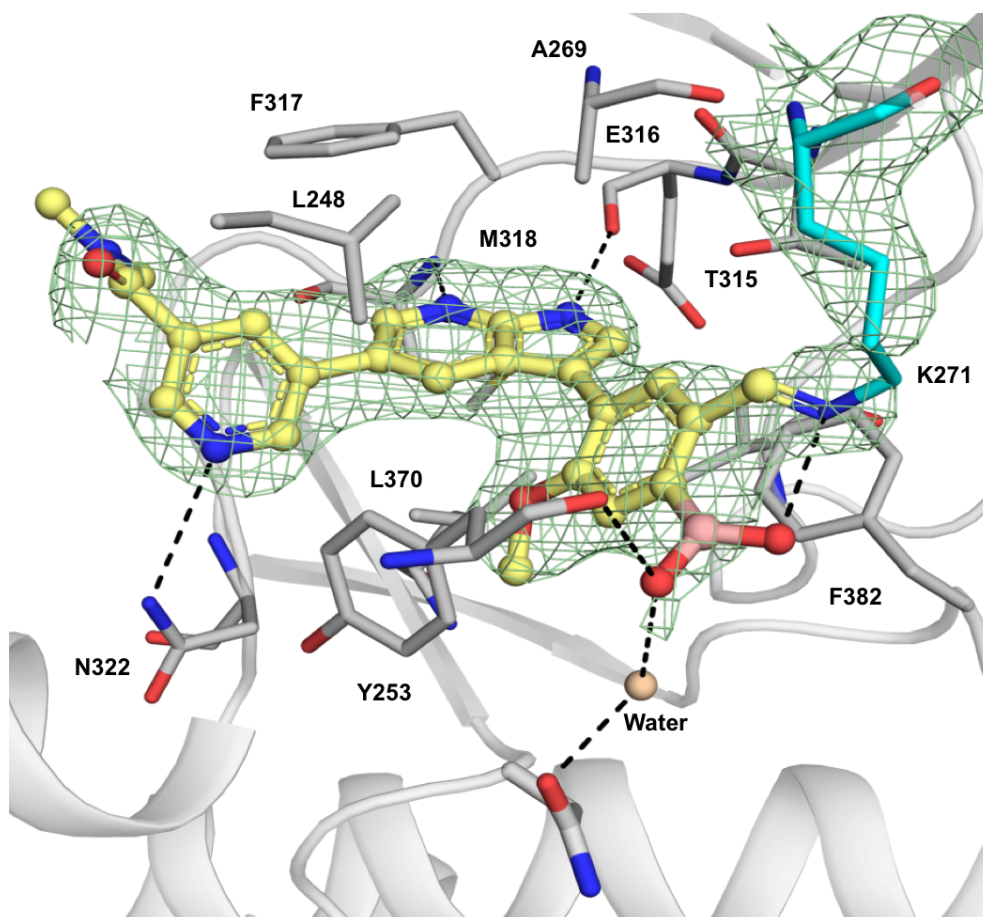


Figure S9. Co-crystal structure of ABL kinase domain-**14** complex (PDB ID: 7DT2).

The X-ray co-crystal structure of compound **14** and the ABL kinase domain was solved up to 2.3 Å resolution. The continuous electron density from K271 to compound **14** suggests that the imine product was formed; however, the formation of the expected dative bond between the imine nitrogen and the boron atom was not observed (**Figure S9**). The imine nitrogen appears to be oriented away from the boron atom. Compound **14** displayed a similar mode of binding compared to that of **12** in the DFG-Asp in kinase conformation. Two hinge-region hydrogen bonds occurred between the carbonyl oxygen of E316 and amide nitrogen of M318 with N1 and N7 of the 7-azaindole, respectively. Another hydrogen bond formed between pyridine N and the N322 residue. The position of OMe group in the 3-dimensional binding site was similar to that of **7** which was believed to occupy a small but important pocket in the ATP-binding site.¹ The boronic acid O atoms formed extensive hydrogen bonding with NH of nearby residues and there was also a hydrogen bond formed between C=N of the imine and the second OH of the boronic acid. In addition, every crystal unit has two ABL kinase domains. Similar to **12**, a molecule of **14** bound to ABL KD non-covalently whereas another molecule of **14** binds to the second ABL kinase domain both non-covalently and covalently via the K271 residue.

Table S3. X-Ray data collection and refinement statistics for ABL KD-14 complex

	ABL-14
Wavelength	0.9537
Resolution range	49.08 - 2.3 (2.382 - 2.3)
Space group	P 21 21 2
Unit cell	105.692 132.302 56.344 90 90 90
Total reflections	71740 (7031)
Unique reflections	35911 (3519)
Multiplicity	2.0 (2.0)
Completeness (%)	99.92 (99.94)
Mean I/sigma(I)	8.74 (1.50)
Wilson B-factor	36.35
R-merge	0.049 (0.362)
R-meas	0.069 (0.513)
R-pim	0.049 (0.362)
CC1/2	0.998 (0.76)
CC*	0.999 (0.929)
Reflections used in refinement	35900 (3518)
Reflections used for R-free	2000 (196)
R-work	0.205 (0.277)
R-free	0.237 (0.338)
CC(work)	0.953 (0.829)
CC(free)	0.944 (0.721)
Number of non-hydrogen atoms	4458
macromolecules	4294
solvent	164
Protein residues	532
RMS(bonds)	0.003
RMS(angles)	0.54
Ramachandran favored (%)	96.53
Ramachandran allowed (%)	3.47
Ramachandran outliers (%)	0.00
Rotamer outliers (%)	0.00
Clashscore	2.16
Average B-factor	44.14
macromolecules	44.21
solvent	42.39

*Statistics for the highest-resolution shell are shown in parentheses. ^a $R_{merge} = \frac{\sum_h \sum_i |I_{hi} - \langle I_h \rangle|}{\sum_h I_{hi}}$, where I_{hi} is the i th observation of the reflection h , while $\langle I_h \rangle$ is its mean intensity. ^bR-factor = $\frac{\sum ||F_{obs}| - |F_{calc}||}{\sum |F_{obs}|}$. ^cR-free was calculated with 5% of reflections excluded from the whole refinement procedure.

Table S4. Selectivity Scores for PPY-A (7) and compound 14

Compound Name	Selectivity Score Type	Number of Hits	Number of Non-Mutant Kinases	Screening Concentration (nM)	Selectivity Score
7	S(35)	14	90	1000	0.156
7	S(10)	3	90	1000	0.033
7	S(1)	2	90	1000	0.022
14	S(35)	14	90	1000	0.156
14	S(10)	9	90	1000	0.1
14	S(1)	2	90	1000	0.022

Table S5. Caco-2 test results for compounds 7, 13 and 14

Compound Name	Average Values					Classification
	Papp (10 ⁻⁶ cm/sec)		Efflux Ratio	A to B % Recovery	B to A % Recovery	
	Apical to Basal	Basal to Apical				
7	13.42	27.94	2.09	64.67	75.85	HIGH
13	0.00	0.00	NC	0.50	63.00	LOW
14	0.00	9.23	>9.23	68.50	83.68	LOW
Digoxin	1.26	17.00	13.46	79.43	87.69	LOW
Propranolol	25.41	22.06	0.87	116.23	87.09	HIGH
Atenolol	0.47	0.47	1.13	83.50	91.40	LOW

Table S6. Caco-2 test results for compound 14 in the presence and absence of PGP and BCRP inhibitors

Compound Name	Inhibitor	Average Values					Classification
		Papp (10 ⁻⁶ cm/sec)		Efflux Ratio	A to B % Recovery	B to A % Recovery	
		Apical to Basal	Basal to Apical				
14	-	0.00	11.84	>11.84	79.75	94.50	LOW
14	Elacridar	0.00	8.29	>8.29	69.50	85.88	LOW
14	KO143	0.00	7.34	>7.34	76.50	78.08	LOW
Digoxin	-	0.00	18.51	>18.51	81.20	87.92	LOW
Digoxin	Elacridar	3.16	4.59	1.46	78.43	88.21	MEDIUM
Estrone-3-sulfate	-	0.00	31.82	>31.82	69.70	89.33	LOW
Estrone-3-sulfate	KO143	2.05	5.35	2.63	66.52	85.50	MEDIUM
Propranolol		21.46	24.48	1.15	67.97	91.86	HIGH
Atenolol		0.00	0.57	NC	95.30	89.83	LOW

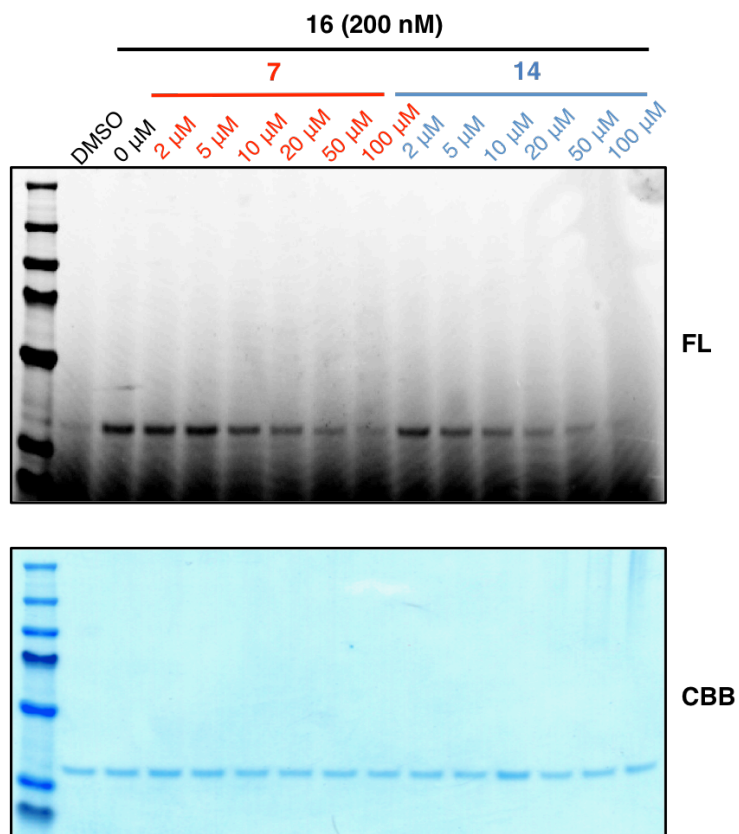


Figure S10. Competition study of compound **16** against PPY-A (**7**) and **14** using purified ABL kinase domain (35 kDa) in PBS at *pH* 7.5. Samples of pure ABL kinase domain were treated with **7** and **14** at different concentrations (0, 2, 5, 10, 20, 50 and 100 μ M) for 1 h, followed by alkynylated probe **16** at 200 nM for another 1 h. FL – In-gel fluorescence scanning; CBB – Coomassie brilliant blue staining.

In the above competition assay, the ABL kinase domain (35 kDa) was treated with PPY-A (**7**) and **14** at different concentrations, followed by addition of **16**. Results show that both PPY-A (**7**) and **14** successfully competed with **16** for binding to the active site of the ABL kinase domain with a dose-response relationship (**Figure S10**). Interestingly, **14** showed an observably stronger effect than **7**.

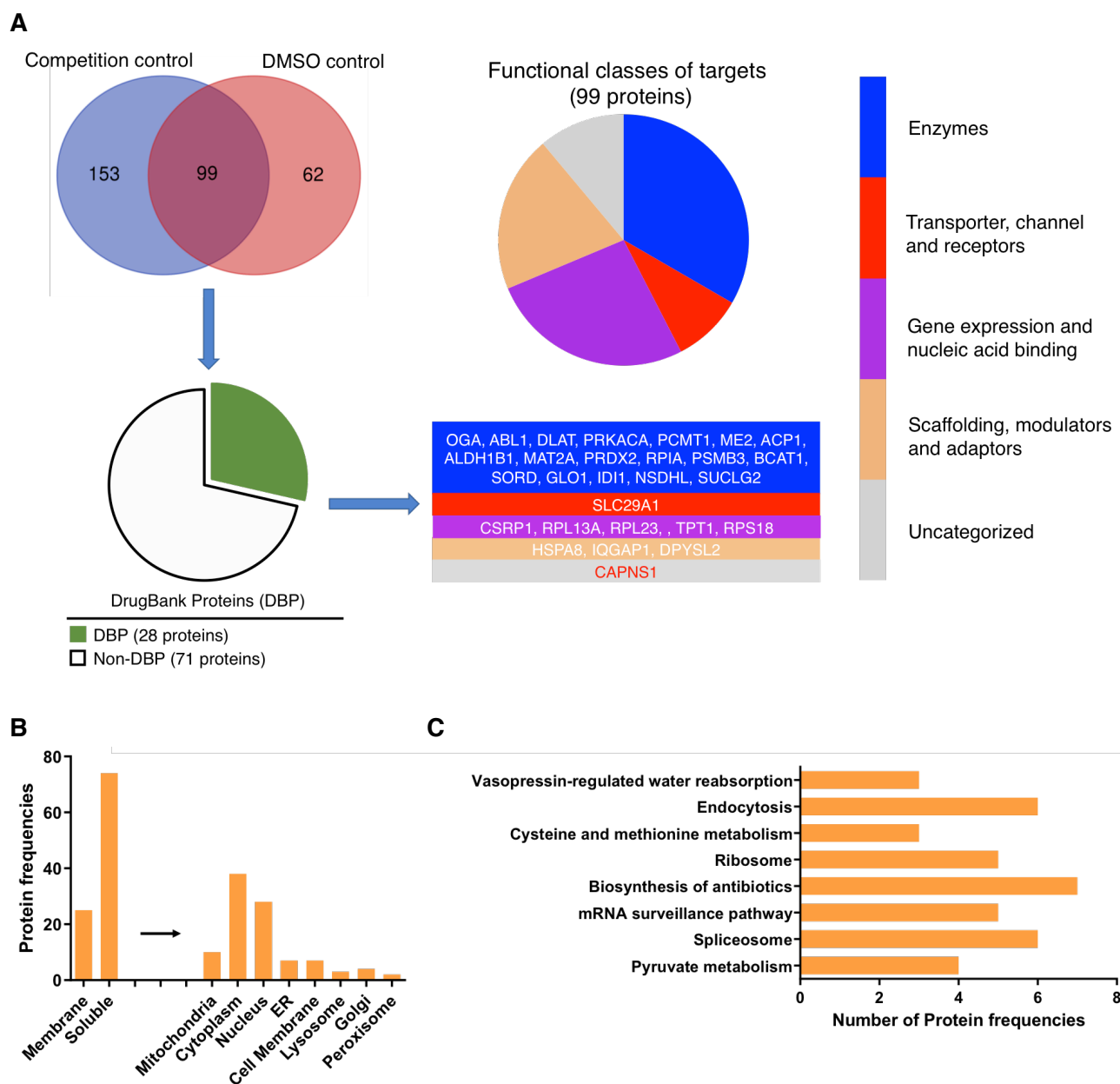


Figure S11. (A-C) Analysis of targets identified from chemoproteomics experiments of **16** in Ba/F3 cells. (A) left: Venn diagram showing the shared 99 targets (28 DrugBank proteins and 71 non-DrugBank proteins) identified under two different experimental conditions (competition and DMSO); right: functional classification of both shared 99 targets and identified DrugBank proteins. (B) Analysis of the shared 99 targets based on presence (membrane) or absence (soluble) of known/predicted transmembrane domains and known/predicted subcellular distribution. (C) Biological pathways in which the 99 targets are involved, as generated from KEGG database.

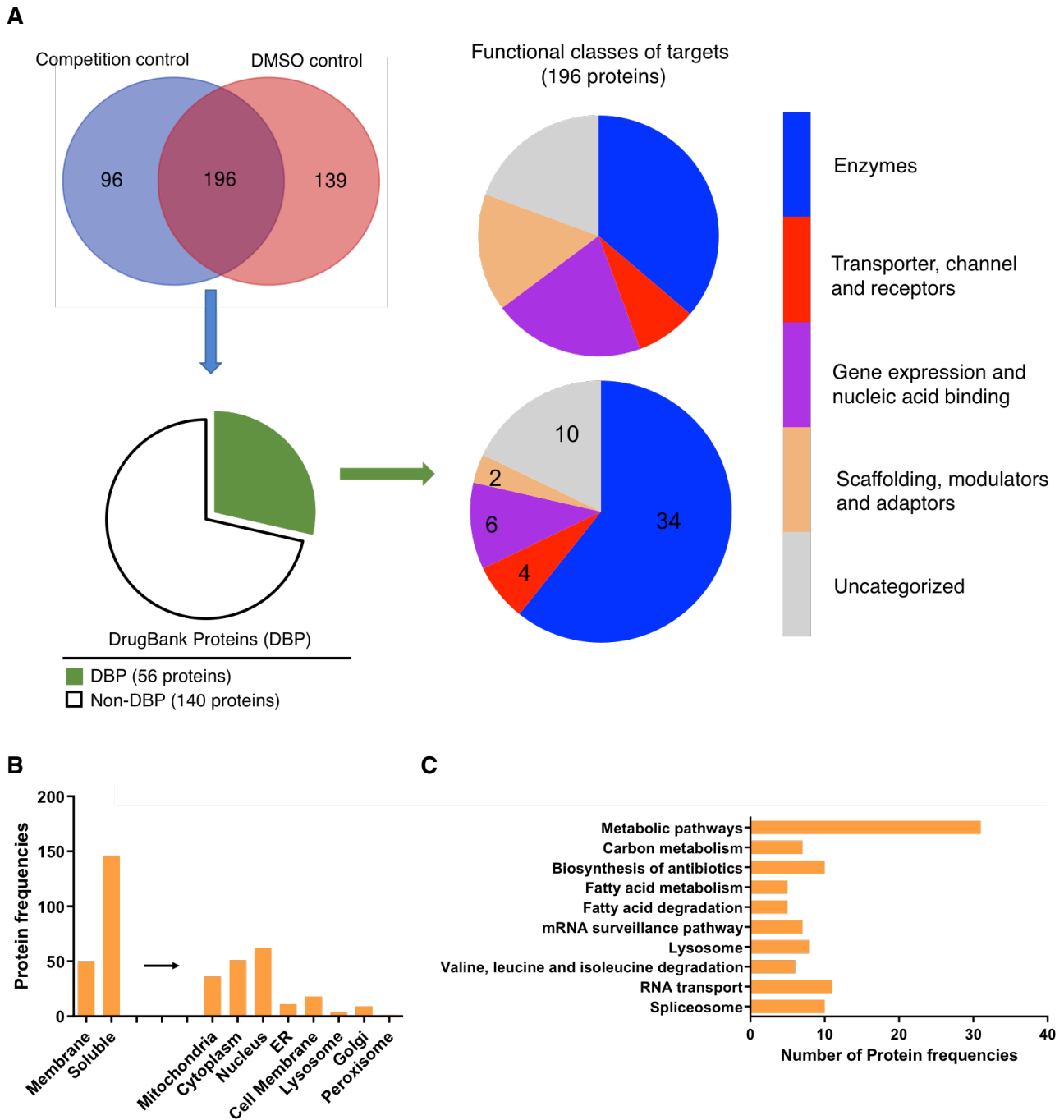


Figure S12. (A-C) Analysis of targets identified from chemoproteomics experiments of **16** in K562 cells. (A) left: Venn diagram summarizing the shared 196 targets (56 DrugBank proteins and 140 non-DrugBank proteins) identified from two experimental conditions (competition and DMSO); right: functional classification of both the shared 196 targets and identified DrugBank proteins. (B) Analysis of the shared 196 targets based on presence (membrane) or absence (soluble) of known/predicted transmembrane domains and known/predicted subcellular distribution. (C) Biological pathways in which the 196 targets are involved, as generated from KEGG database.

Table S7. List of shared 39 targets from both K562 and Ba/F3^{BCR-ABL} cells (See **Figure 3F**).

Gene	Protein Description	Prot_ID
HNRNPDL	Heterogeneous nuclear ribonucleoprotein D-like	O14979
PRPF40A	Pre-mRNA-processing factor 40 homolog A	O75400
EIF3J	Eukaryotic translation initiation factor 3 subunit J	O75822
ABL1	Tyrosine-protein kinase ABL1	P00519
CAPNS1	Calpain small subunit 1	P04632
SLC3A2	4F2 cell-surface antigen heavy chain	P08195
GNAI3	Guanine nucleotide-binding protein G(i) subunit alpha	P08754
TPT1	Translationally-controlled tumor protein	P13693
GLB1	Beta-galactosidase	P16278
PCMT1	Protein-L-isoaspartate(D-aspartate) O-methyltransferase	P22061
ME2	NAD-dependent malic enzyme, mitochondrial	P23368
ALDH1B1	Aldehyde dehydrogenase X, mitochondrial	P30837
RPIA	Ribose-5-phosphate isomerase	P49247
ACADVL	Very long-chain specific acyl-CoA dehydrogenase, mitochondrial	P49748
DNM2	Dynamin-2	P50570
FXR1	Fragile X mental retardation syndrome-related protein 1	P51114
RAB5C	Ras-related protein Rab-5C	P51148
SRP54	Signal recognition particle 54 kDa protein	P61011
UBE2N	Ubiquitin-conjugating enzyme E2 N	P61088
ARF3	ADP-ribosylation factor 3	P61204
SNRPD1	Small nuclear ribonucleoprotein Sm D1	P62314
TIMM50	Mitochondrial import inner membrane translocase subunit TIM50	Q3ZCQ8
LARP1	La-related protein 1	Q6PKG0
H2AW	Histone H2A type 3	Q7L7L0
MOB1B	MOB kinase activator 1B	Q7L9L4
PABPN1	Polyadenylate-binding protein 2	Q86U42
CELF1	CUGBP Elav-like family member 1	Q92879
MAGOHB	Protein mago nashi homolog 2	Q96A72
MMS19	MMS19 nucleotide excision repair protein homolog	Q96T76
SLC29A1	Equilibrative nucleoside transporter 1	Q99808
EHD1	EH domain-containing protein 1	Q9H4M9
TOMM22	Mitochondrial import receptor subunit TOM22 homolog	Q9NS69
BCCIP	BRCA2 and CDKN1A-interacting protein	Q9P287
CPSF3	Cleavage and polyadenylation specificity factor subunit 3	Q9UKF6
RAB21	Ras-related protein Rab-21	Q9UL25
CORO1C	Coronin-1C	Q9ULV4
DDX19B	ATP-dependent RNA helicase DDX19B	Q9UMR2
FIS1	Mitochondrial fission 1 protein	Q9Y3D6
RBM8A	RNA-binding protein 8A	Q9Y5S9

*It is interesting that the expected target, ABL-1, was the only kinase that was identified from above experiments at a high confidence level, indicating high specificity of our probe towards kinases.

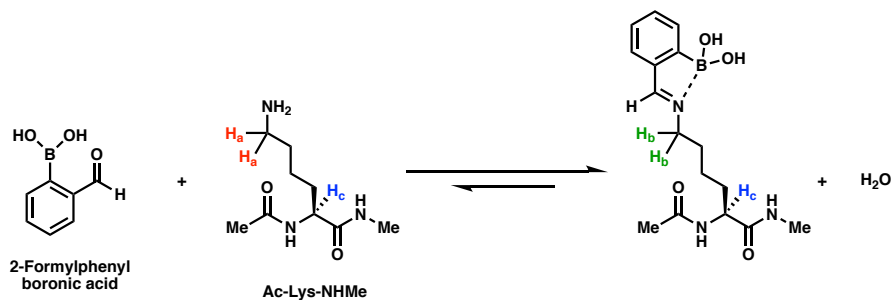
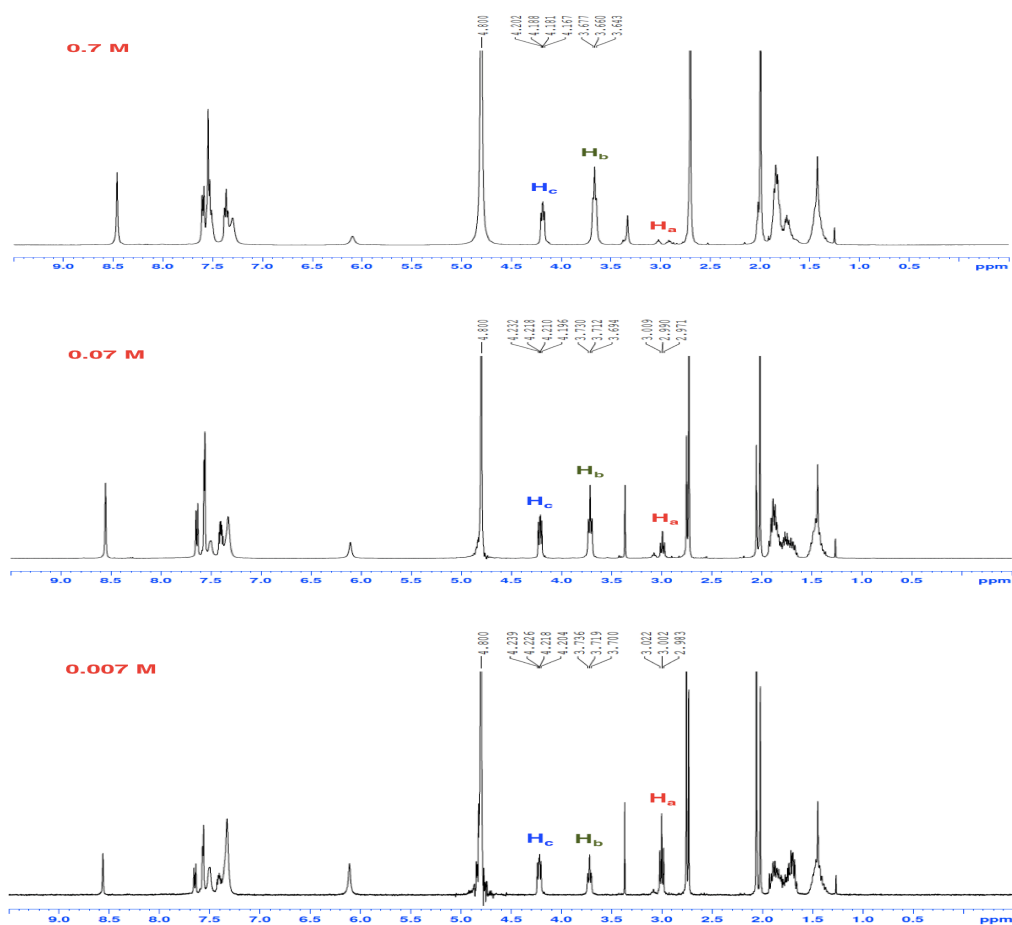
A**B**

Figure S13. (A) Reversible formation of the imine product formed between 2-formylphenyl boronic acid and Ac-Lys-NHMe. (B) ¹H NMR studies of the imine product formed between 2-formylphenyl boronic acid and Ac-Lys-NHMe. (A) At 0.7 M. (B) At 0.07 M. (C) At 0.007 M.

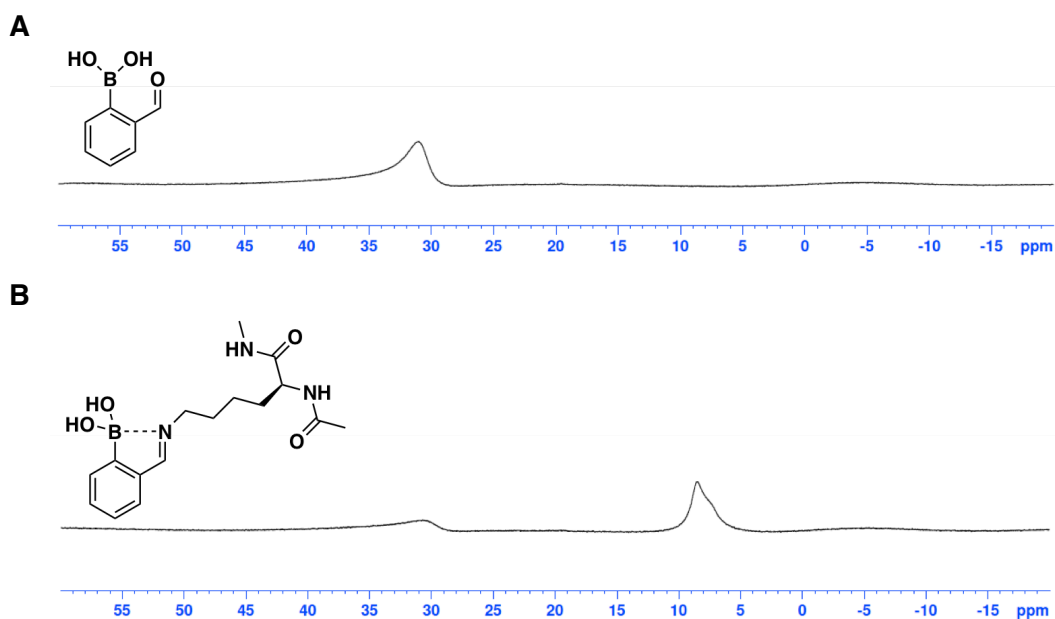


Figure S14. ^{11}B NMR studies of 2-formylphenylboronic acid and the iminoboronate product at 150 mM in D_2O . (A) 2-Formylphenylboronic acid. (B) Imine product.

In this experiment (**Figures S13 & S14**),^[15] 2-formylphenyl boronic acid and Ac-Lys-NHMe were mixed in D_2O at a concentration of 0.7 M (1:1 ratio) and the equilibrium was monitored using the relative intensity ratio of H_b/H_a (**Figure S13**). When the samples were diluted by 10 and 100 times using D_2O , the ^1H NMR spectra showed an increase of peak intensity for H_a , indicating that the equilibrium favored the backward reactions (**Figures 15B**). By Le Chatelier's principle, when more D_2O was added, the backward reaction was favored, pushing the equilibrium to the left.

In a ^{11}B NMR experiment,^[16] 2-formylphenylboronic acid alone displayed a peak at about 31.0 ppm (**Figure S14A**). Mixing 2-formylphenylboronic acid with Ac-Lys-NHMe in D_2O (1:1 ratio) resulted in a new peak at 8.6 ppm, which was characteristic of anionic boron, aka iminoboronate (**Figure S14B**).

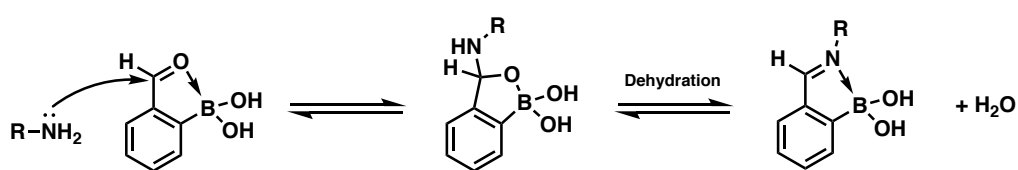


Figure S15. Proposed mechanism for the conjugation between an amine and 2-formylphenyl boronic acid.¹³

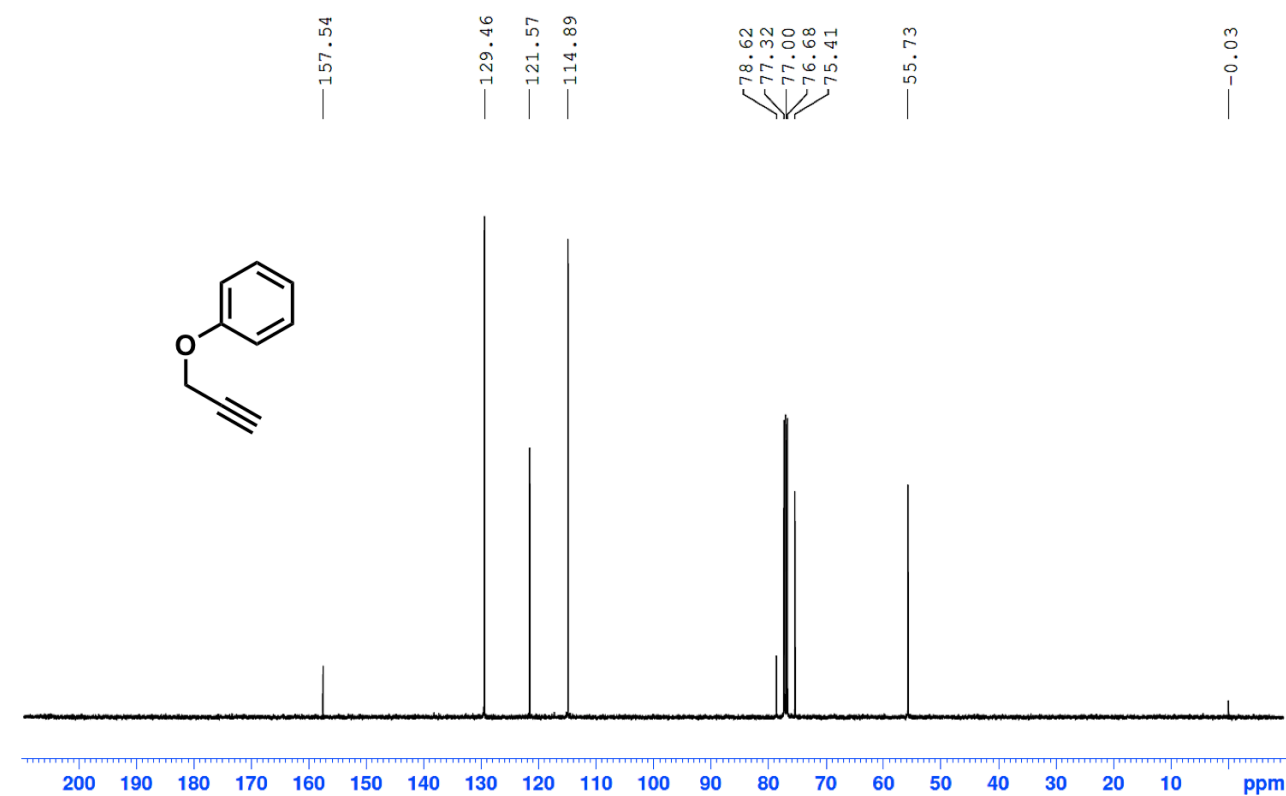
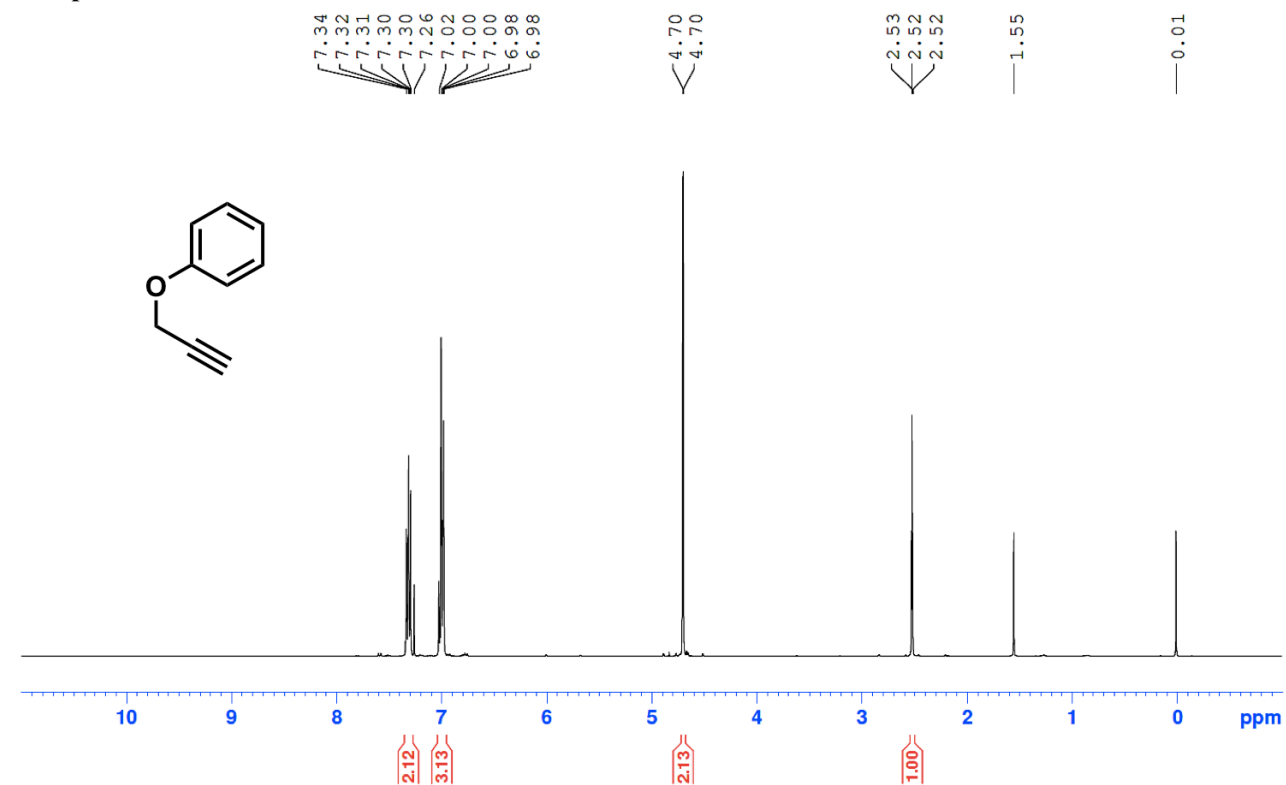
As shown in **Figure S15**, the formation of the imine is facilitated by the boronic acid which acts as a Lewis acid,¹² and this explains the difference seen between compound **10** and **12** in the biochemical assay and mass spectrometry. The crystal structure shows the structure of the final covalent adduct that has been observed in these experiments.

The model reactions and experiments including the ^{11}B NMR studies suggested that the iminoboronate is formed and the same happens when **12** reacts in the active site of ABL kinase. The crystal structures with the ABL kinase domain shows an intermediate in the formation of the iminoboronate which is only slowly formed as shown by our biochemical assay results.

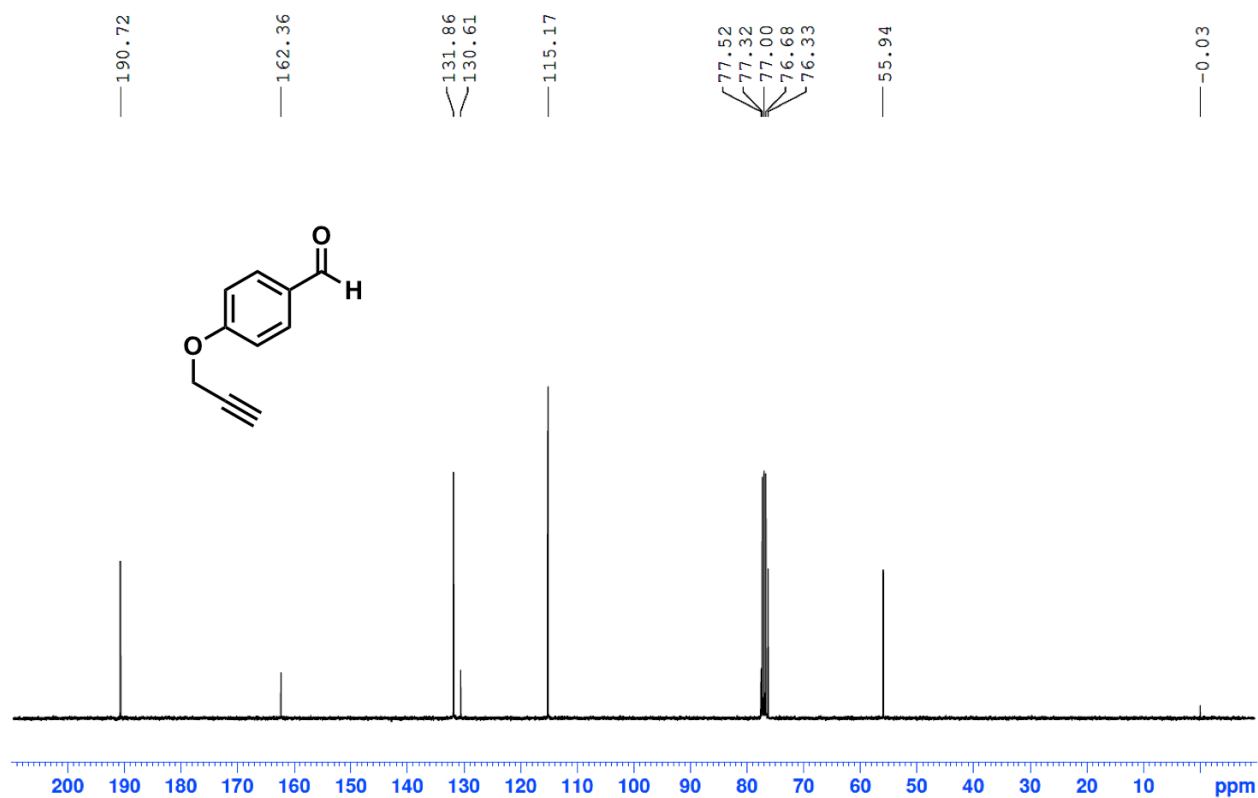
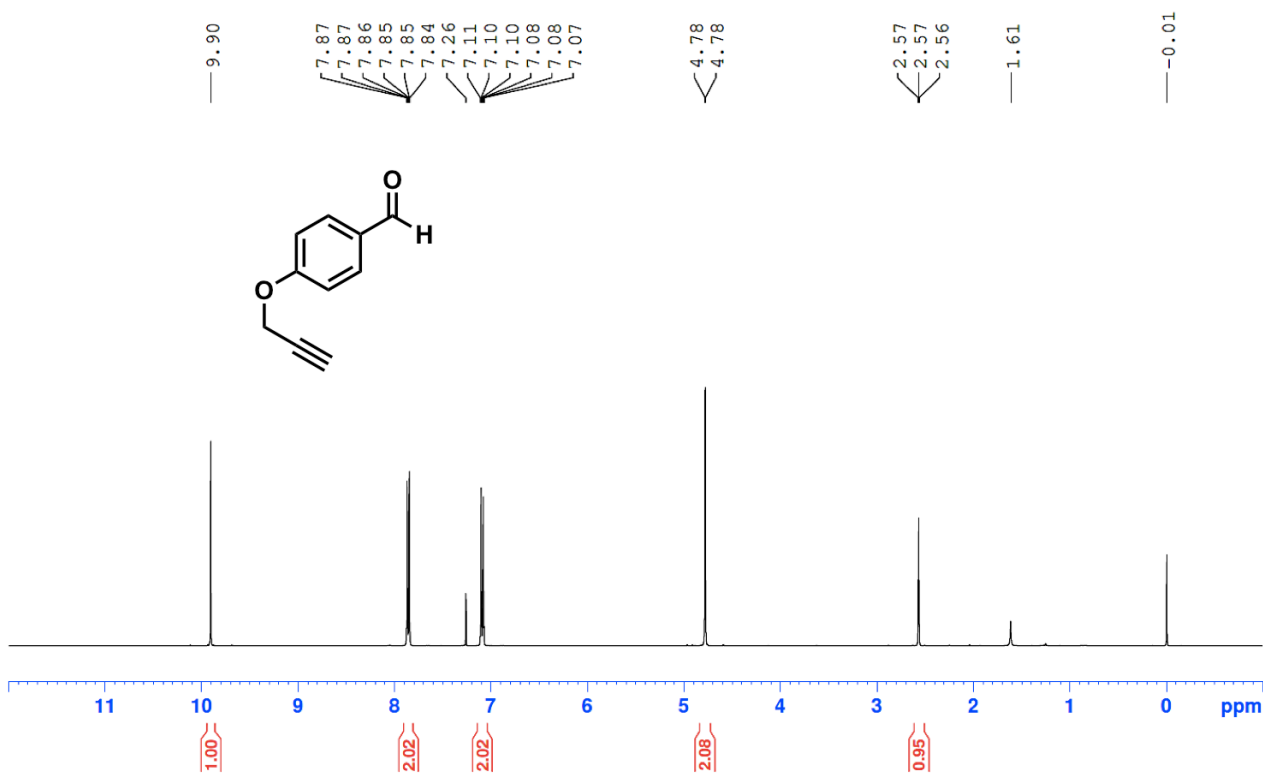
5. References

- [1] T. Zhou, L. Parillon, F. Li, Y. Wang, J. Keats, S. Lamore, Q. Xu, W. Shakespeare, D. Dalgarno, X. Zhu, *Chem. Biol. Drug Des.* **2007**, *70*, 171–181.
- [2] C. J. Stress, P. J. Schmidt, D. G. Gillingham, *Org. Biomol. Chem.* **2016**, *14*, 5529–5533.
- [3] J. S. Bajwa, G. P. Chen, K. Prasad, O. Repič, T. J. Blacklock, *Tetrahedron Lett.* **2006**, *47*, 6425–6427.
- [4] D. A. Shannon, R. Banerjee, E. R. Webster, D. W. Bak, C. Wang, E. Weerapana, *J. Am. Chem. Soc.* **2014**, *136*, 3330–3333.
- [5] M. A. Seeliger, M. Young, M. N. Henderson, P. Pellicena, D. S. King, A. M. Falick, J. Kuriyan, *Protein Sci.* **2005**, *14*, 3135–3139.
- [6] T. M. McPhillips, S. E. McPhillips, H. J. Chiu, A. E. Cohen, A. M. Deacon, P. J. Ellis, E. Garman, A. Gonzalez, N. K. Sauter, R. P. Phizackerley, S. M. Soltis, P. Kuhn, *J. Synchrotron Radiat.* **2002**, *9*, 401–406.
- [7] W. Kabsch, *Acta Crystallogr. D.* **2010**, *66*, 125–132.
- [8] A. J. McCoy, R. W. Grosse-Kunstleve, P. D. Adams, M. D. Winn, L. C. Storoni, R. J. Read, *J. Appl. Crystallogr.* **2007**, *40*, 658–674.
- [9] P. Emsley, B. Lohkamp, W. G. Scott, K. Cowtan, *Acta Crystallogr. D.* **2010**, *66*, 486–501.
- [10] P. V. Afonine, R. W. Grosse-Kunstleve, N. Echols, J. J. Headd, N. W. Moriarty, M. Mustyakimov, T. C. Terwilliger, A. Urzhumtsev, P. H. Zwart, P. D. Adams, *Acta Crystallogr.* **2012**, *68*, 352–367.
- [11] Q. Zhao, X. Ouyang, X. Wan, K. S. Gajiwala, J. C. Kath, L. H. Jones, A. L. Burlingame, J. Taunton, *J. Am. Chem. Soc.* **2017**, *139*, 680–685.
- [12] B. R. Lanning, L. R. Whitby, M. M. Dix, J. Douhan, A. M. Gilbert, E. C. Hett, T. O. Johnson, C. Joslyn, J. C. Kath, S. Niessen, L. R. Roberts, M. E. Schnute, C. Wang, J. J. Hulce, B. Wei, L. O. Whiteley, M. M. Hayward, B. F. Cravatt, *Nat. Chem. Biol.* **2014**, *10*, 760–767.
- [13] S. Tyanova, T. Temu, P. Sinitcyn, A. Carlson, M. Y. Hein, T. Geiger, M. Mann, J. Cox, *Nat. Methods* **2016**, *13*, 731–740.
- [14] J. M. Bradshaw, J. M. McFarland, V. O. Paavilainen, A. Bisconte, D. Tam, V. T. Phan, S. Romanov, D. Finkle, J. Shu, V. Patel, T. Ton, X. Li, D. G. Loughhead, P. A. Nunn, D. E. Karr, M. E. Gerritsen, J. O. Funk, T. D. Owens, E. Verner, K. A. Brameld, R. J. Hill, D. M. Goldstein, J. Taunton, *Nat. Chem. Bio.* **2015**, *11*, 525–531.
- [15] G. Akçay, M. A. Belmonte, B. Aquila, C. Chuaqui, A. W. Hird, M. L. Lamb, P. B. Rawlins, N. Su, S. Tentarelli, N. P. Grimster, Q. Su, *Nat. Chem. Biol.* **2016**, *12*, 931–936.
- [16] A. Bandyopadhyay, J. Gao, *Chem. Eur. J.* **2015**, *21*, 14748–14752.

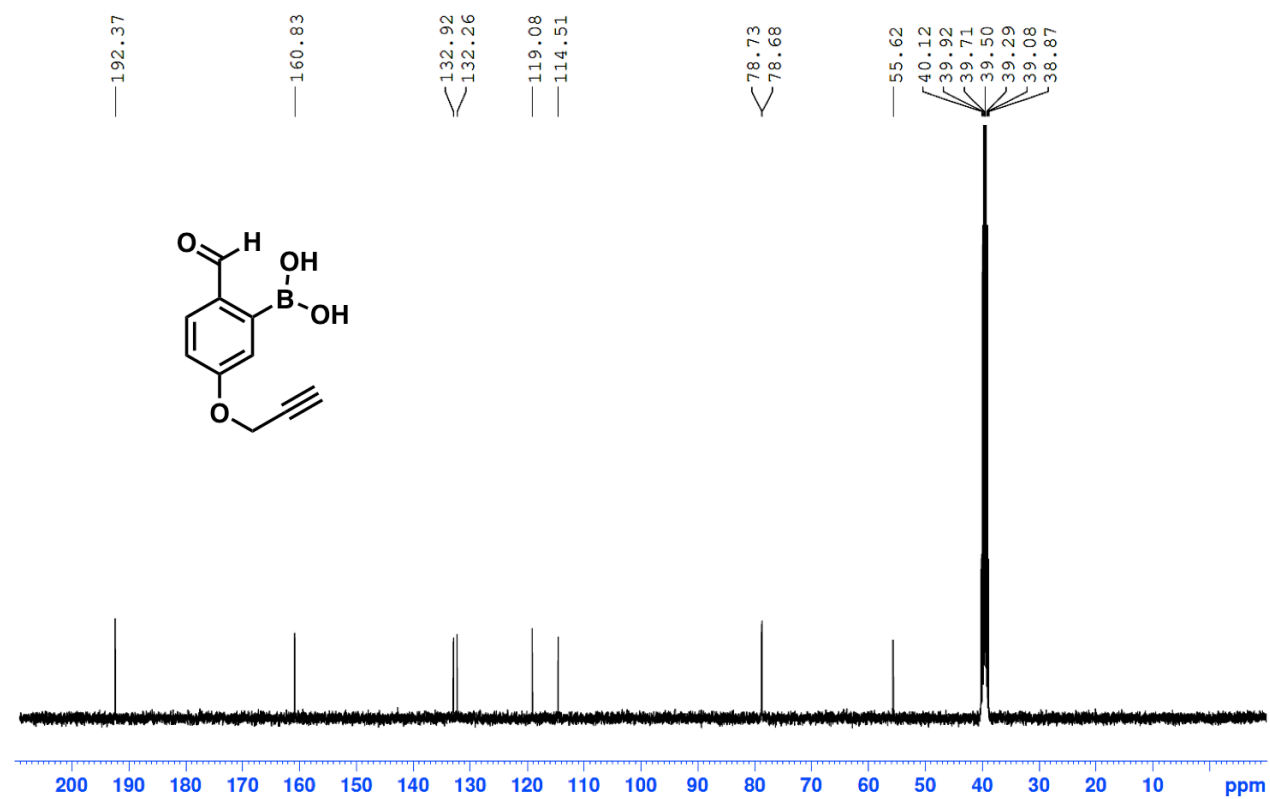
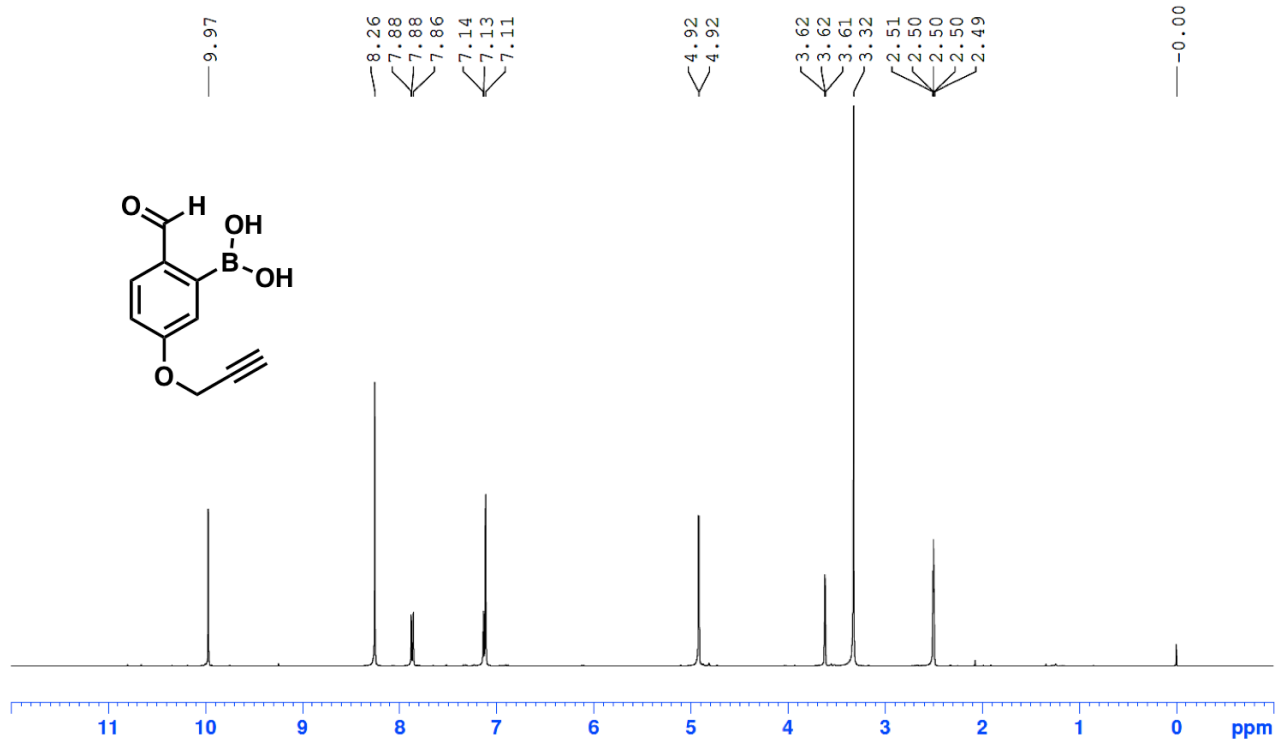
6. NMR Spectra Compound 1



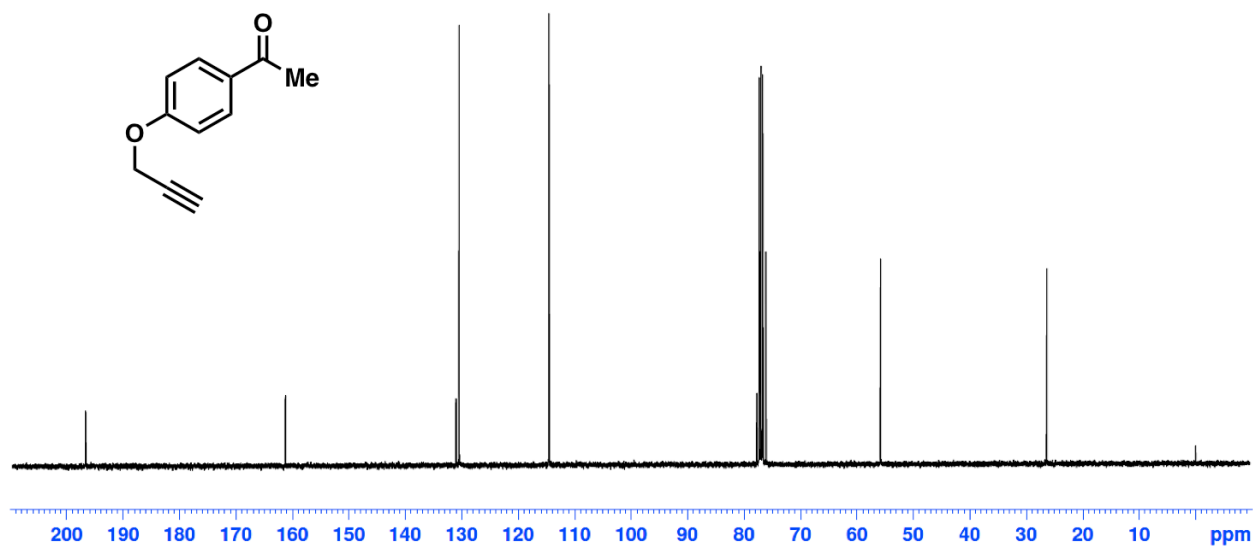
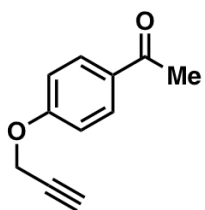
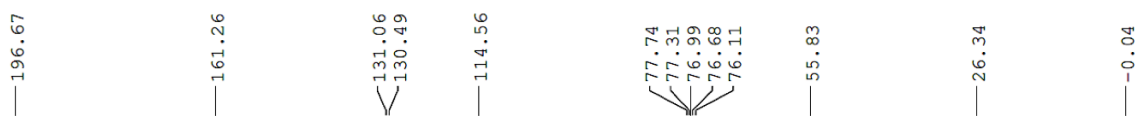
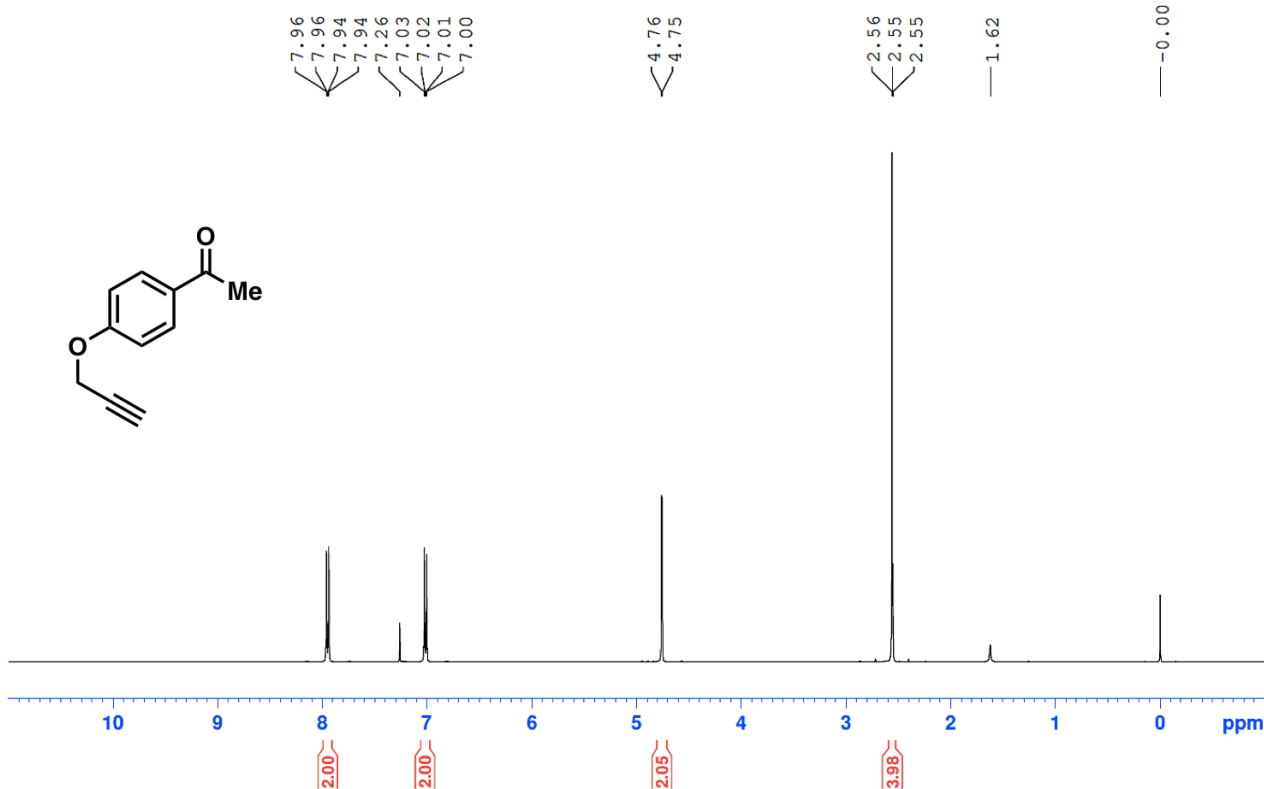
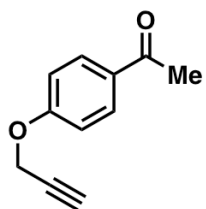
Compound 2



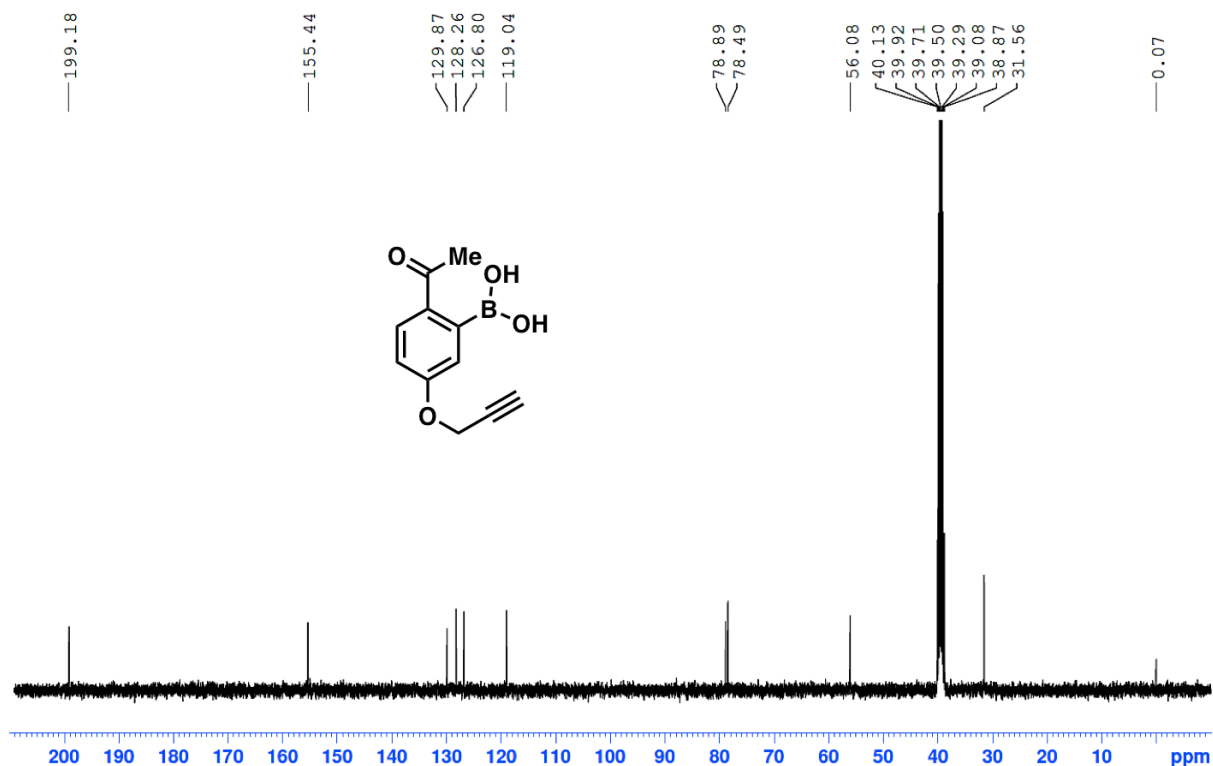
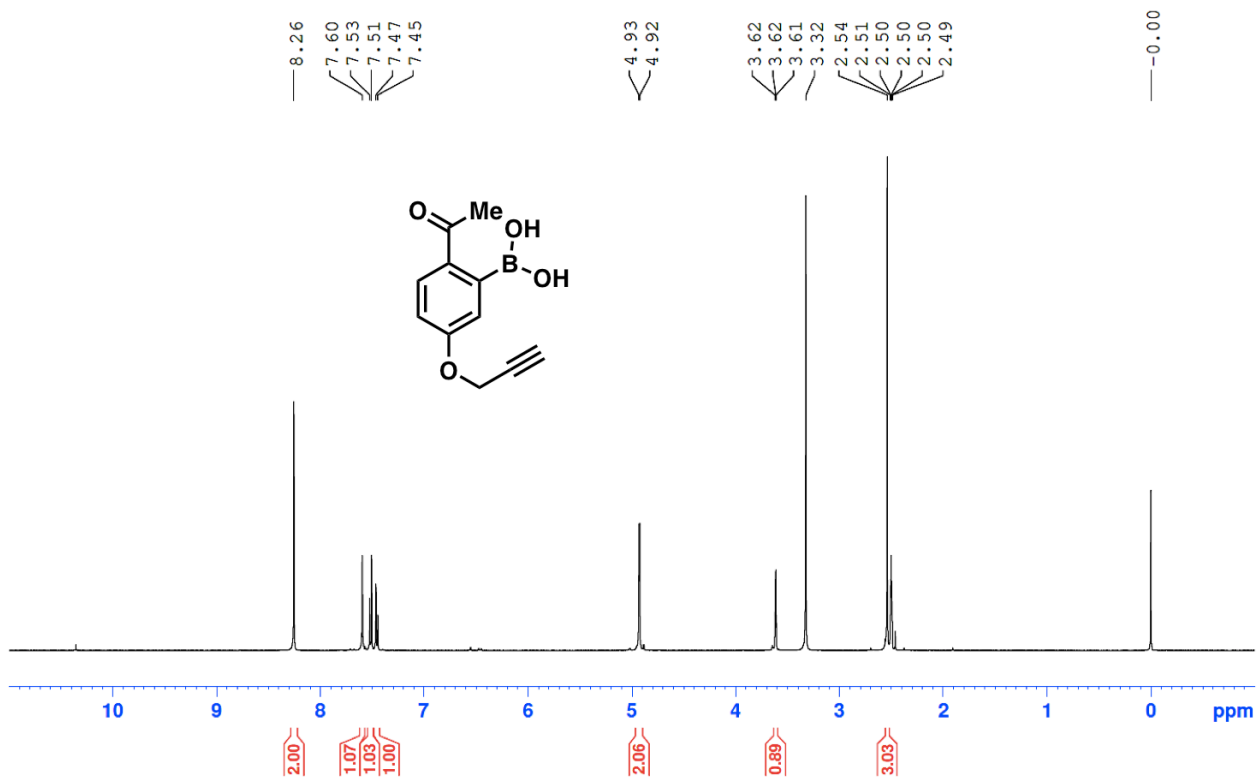
Compound 3



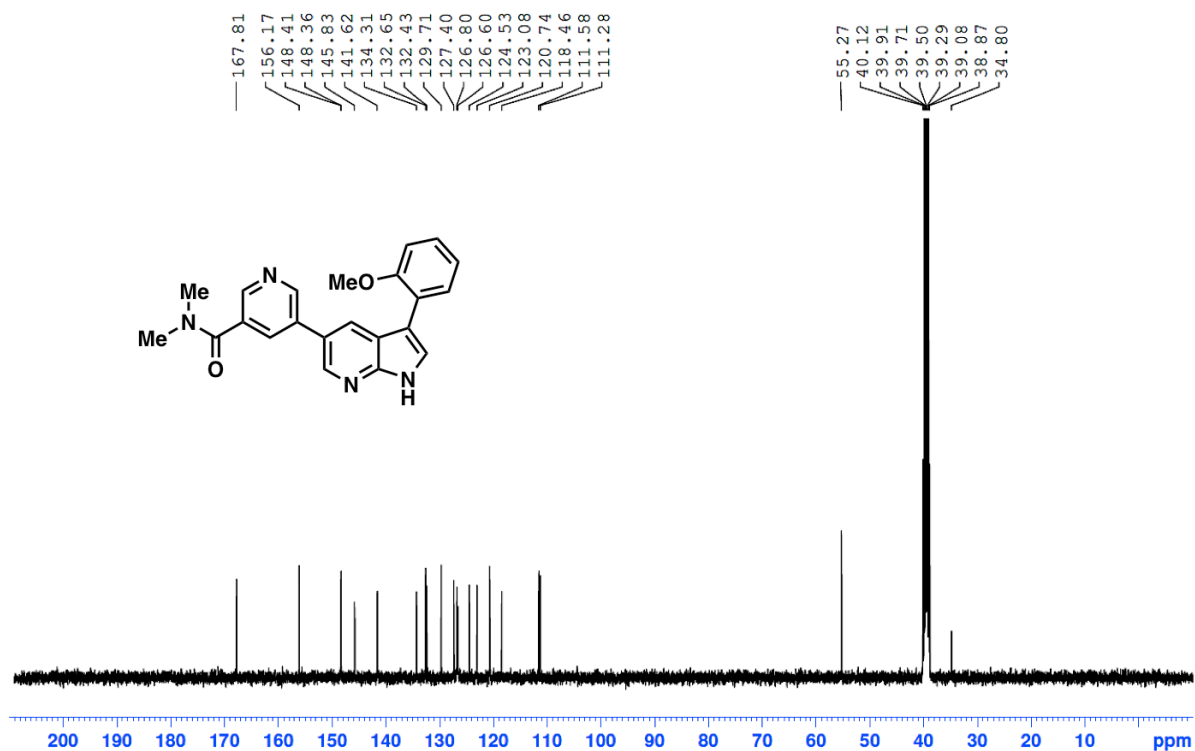
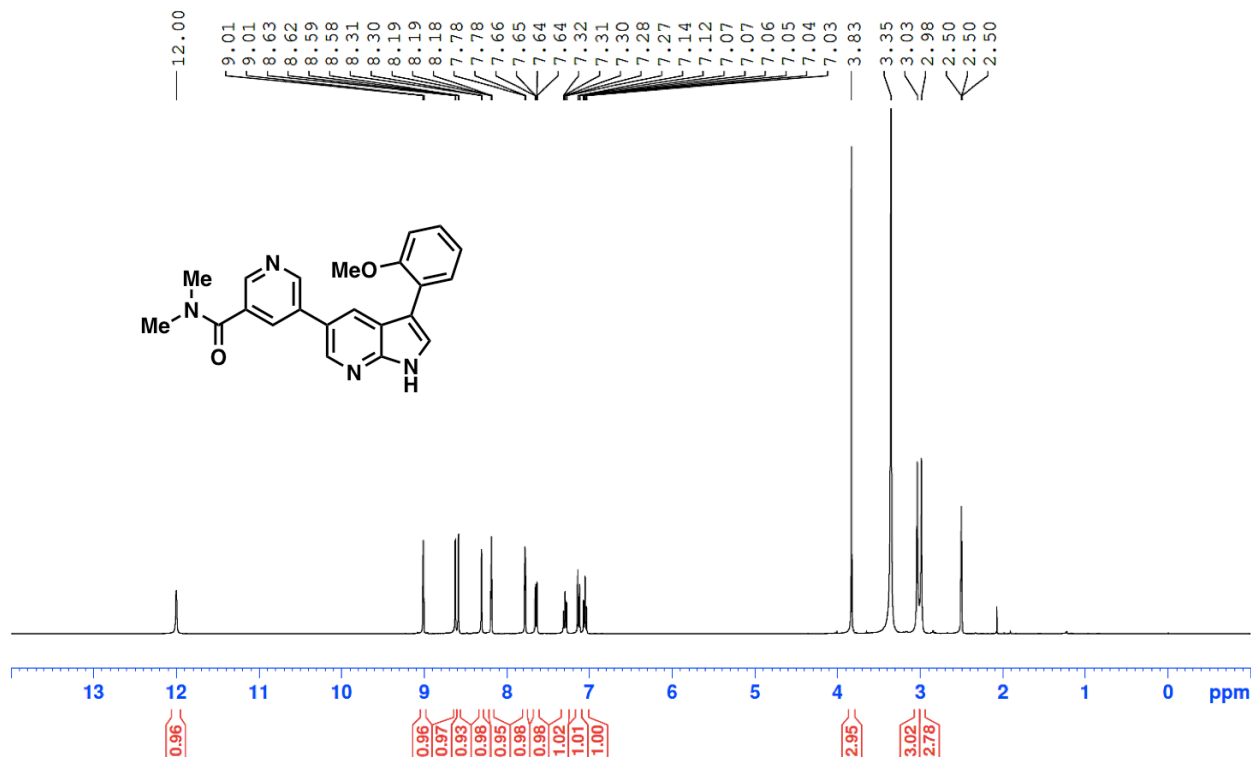
Compound 4



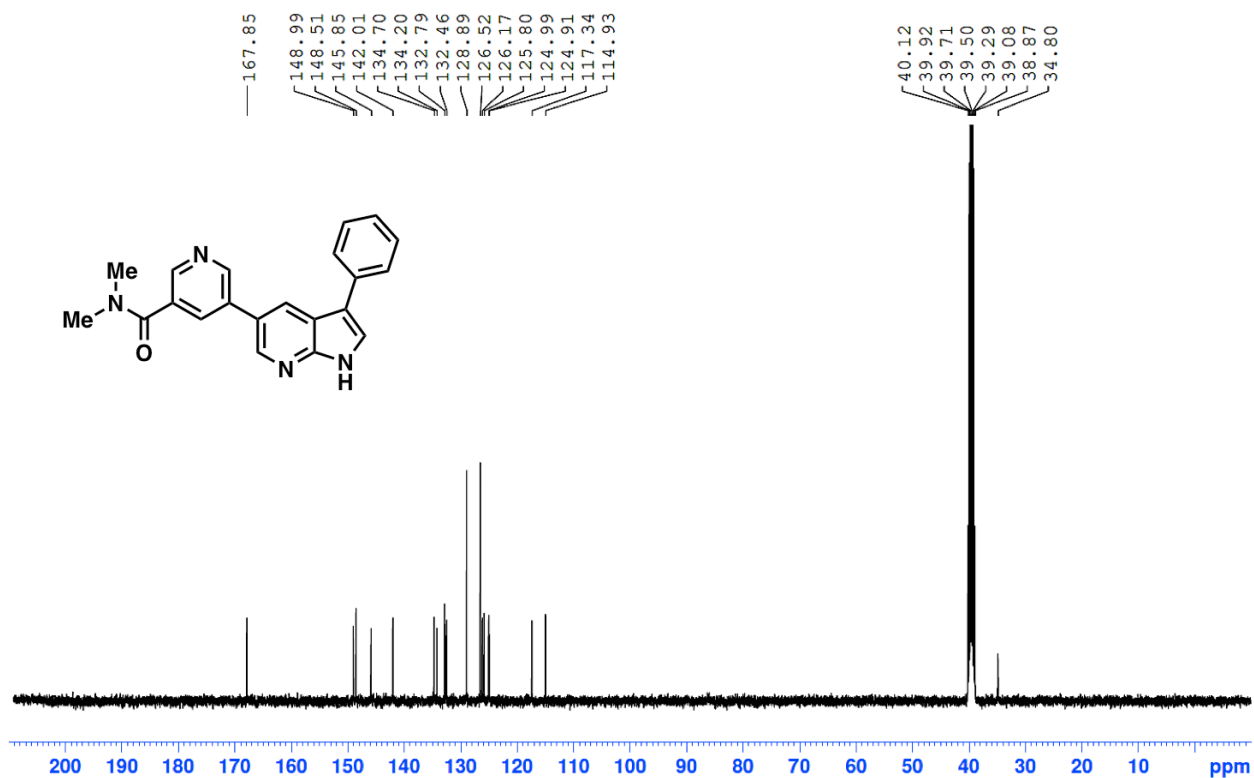
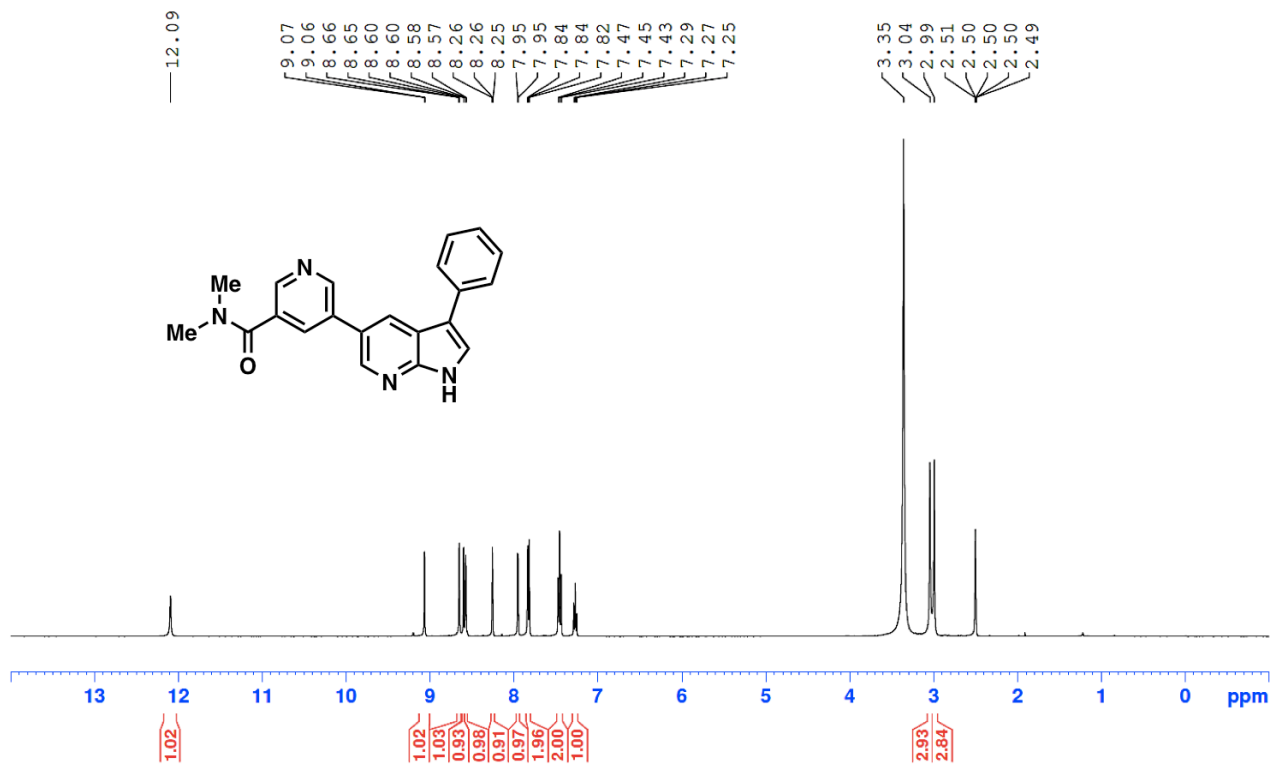
Compound 5



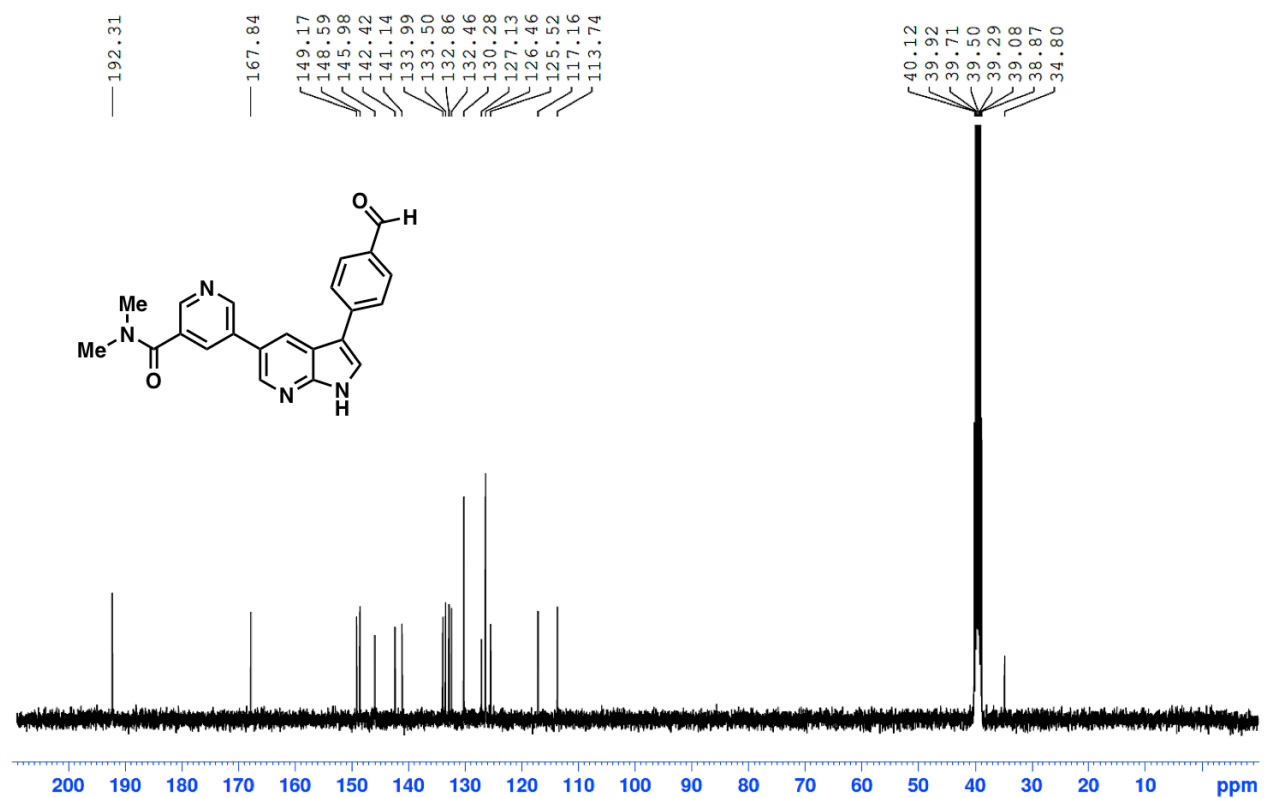
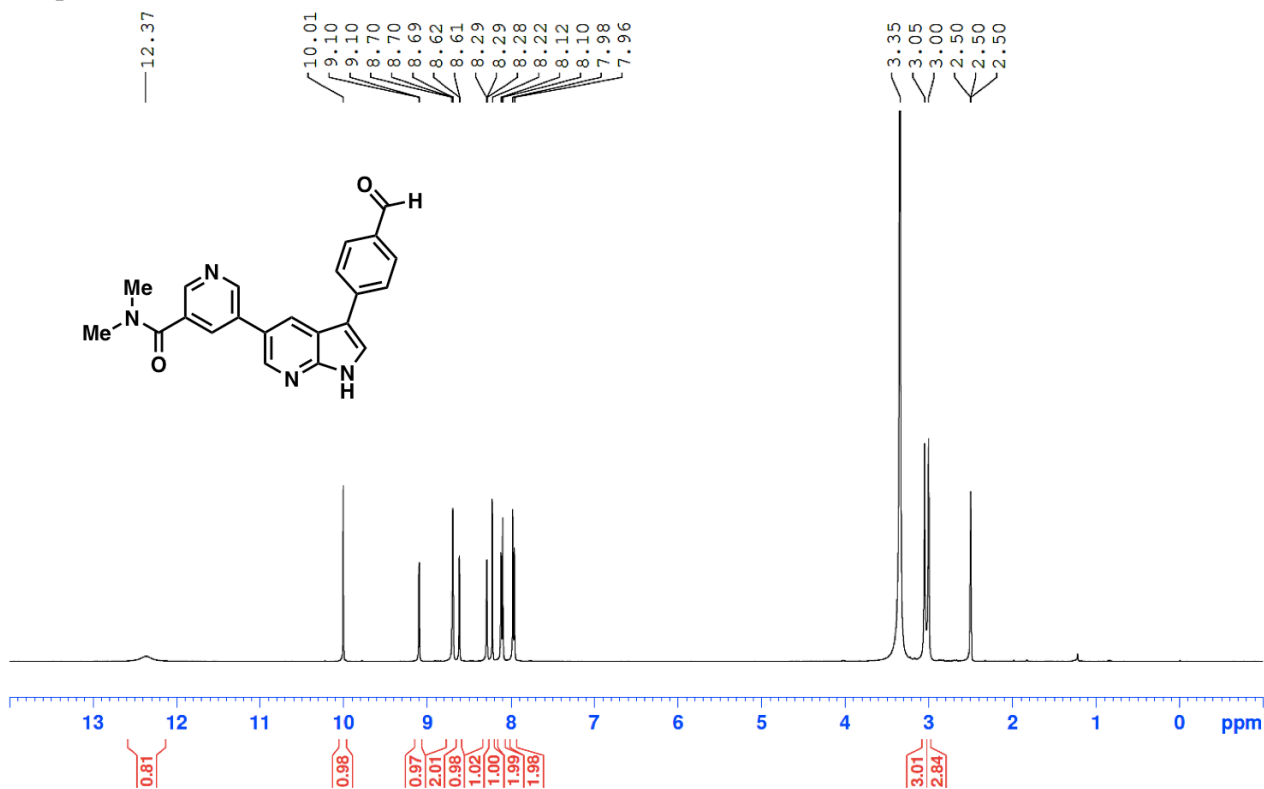
Compound 7



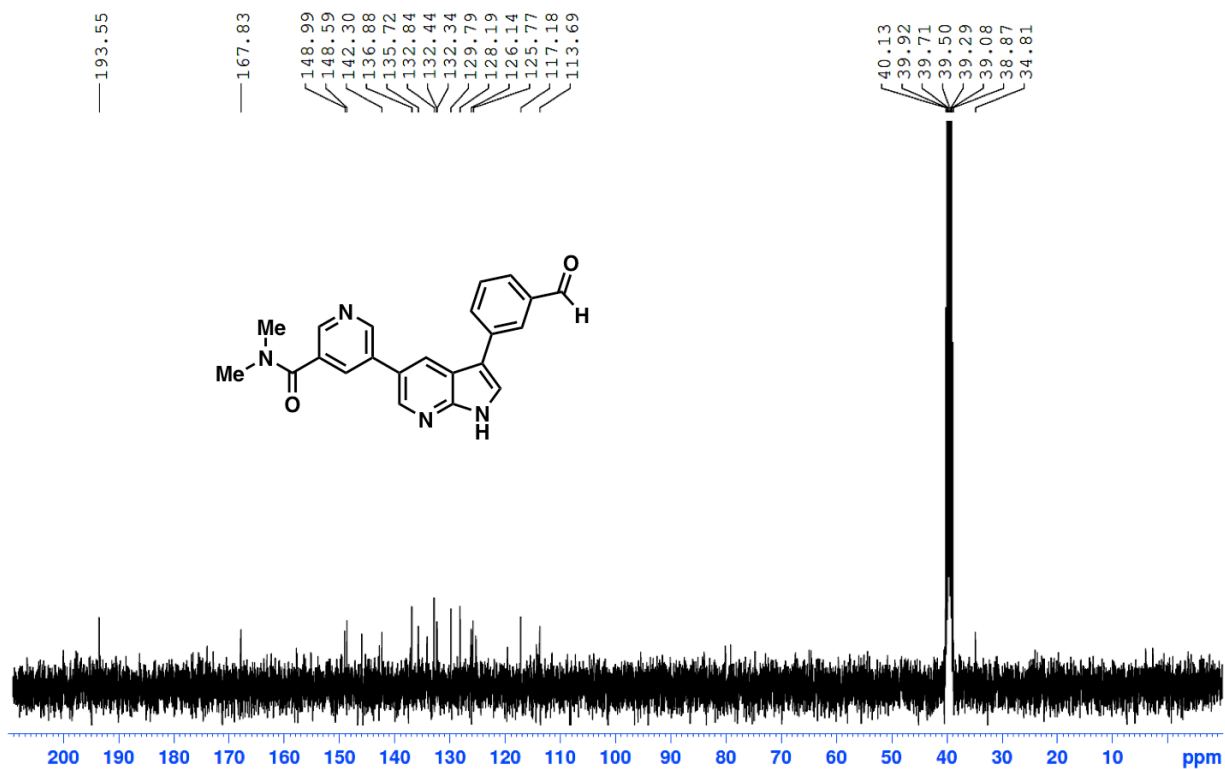
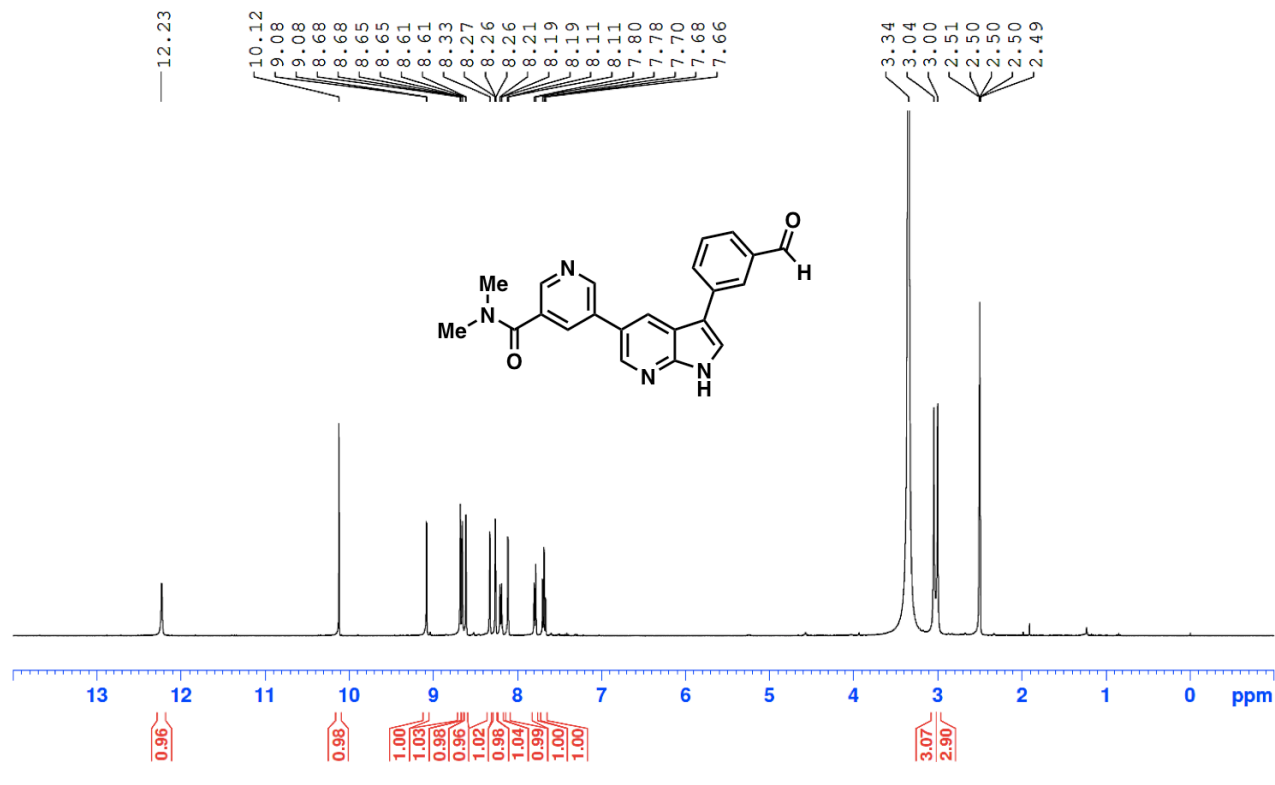
Compound 8



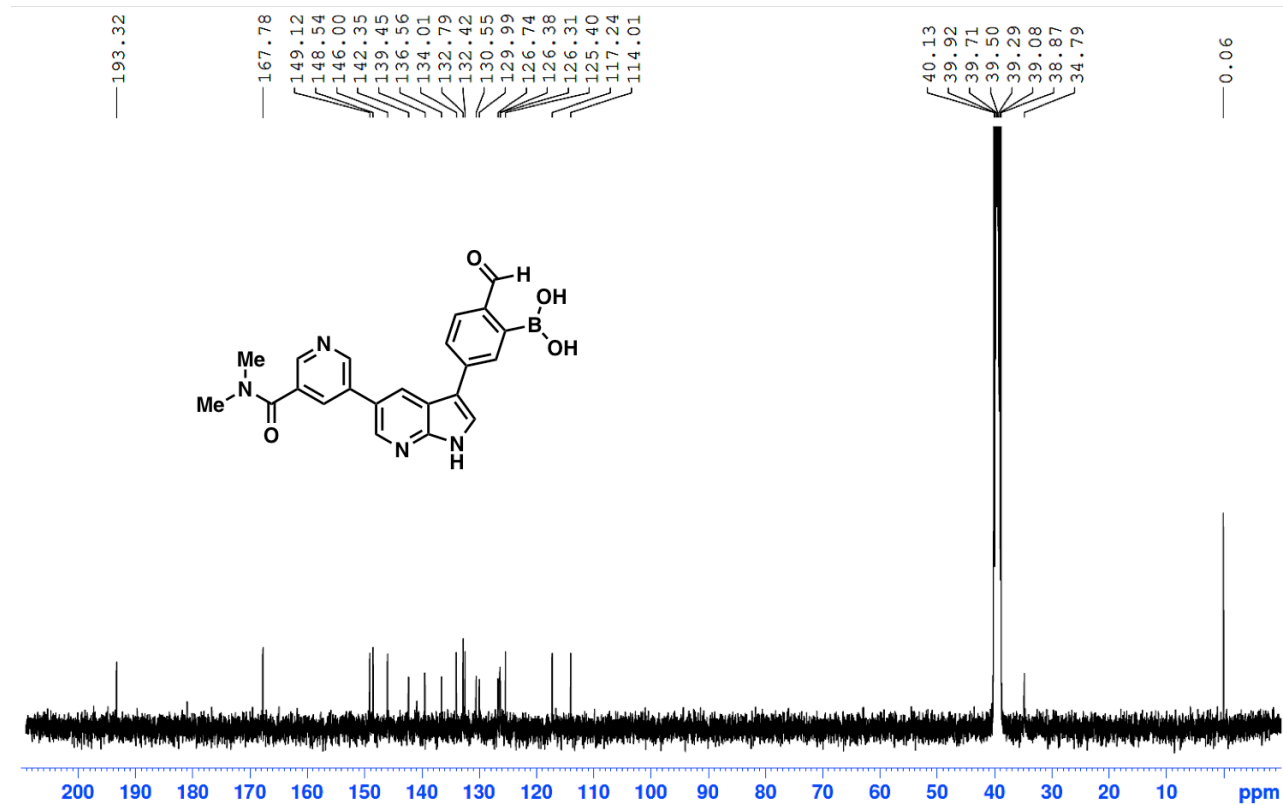
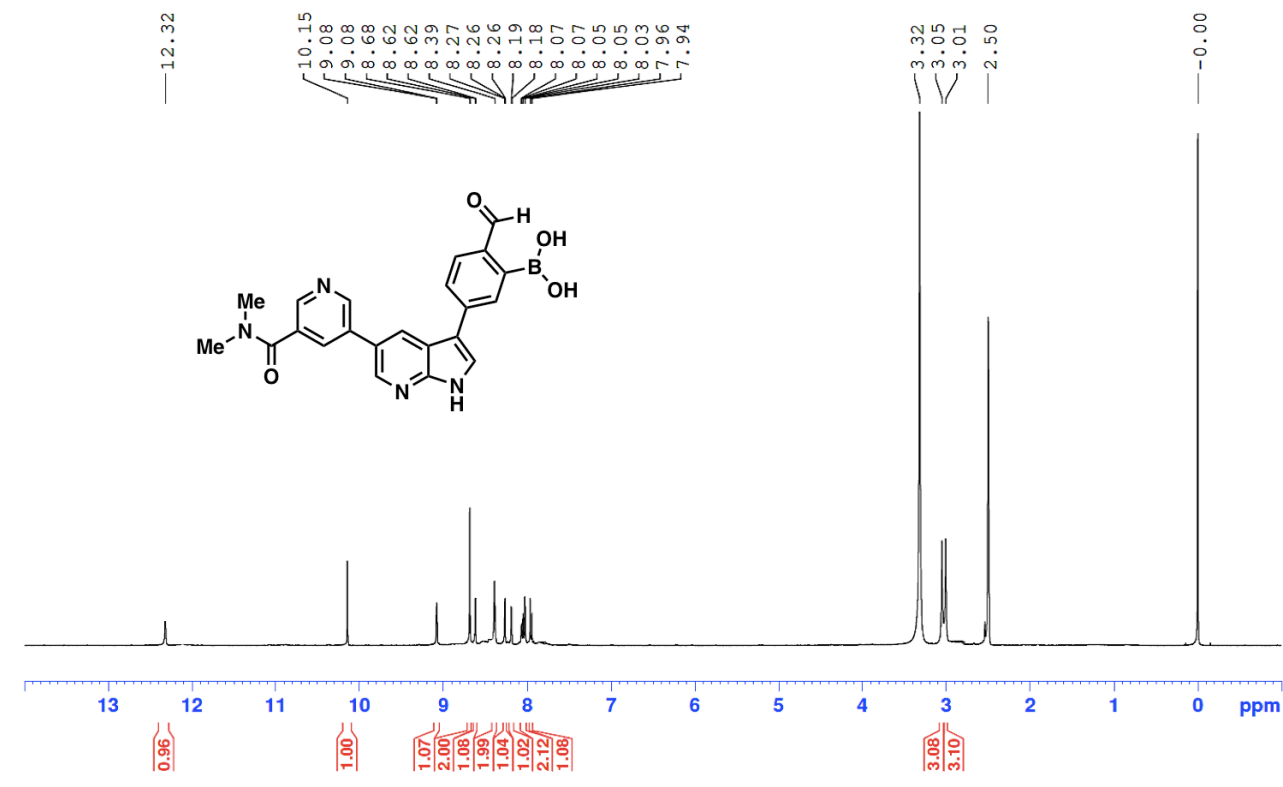
Compound 9



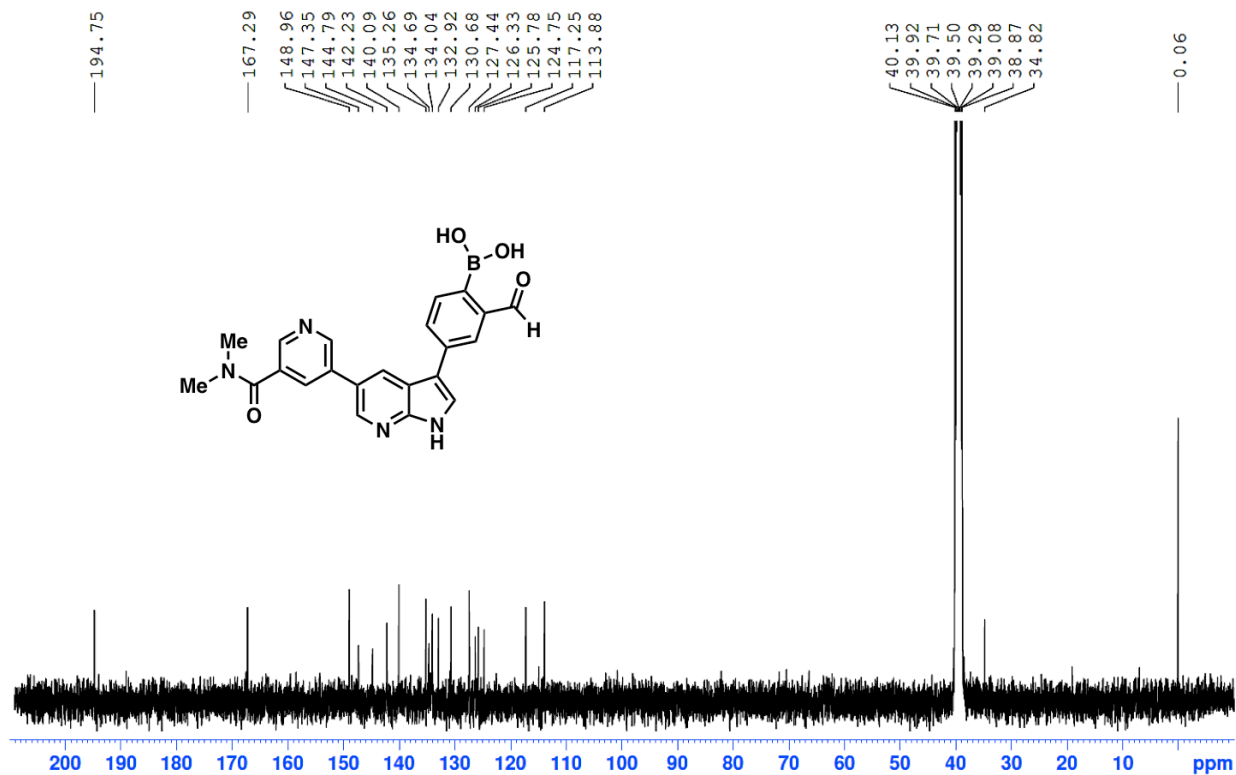
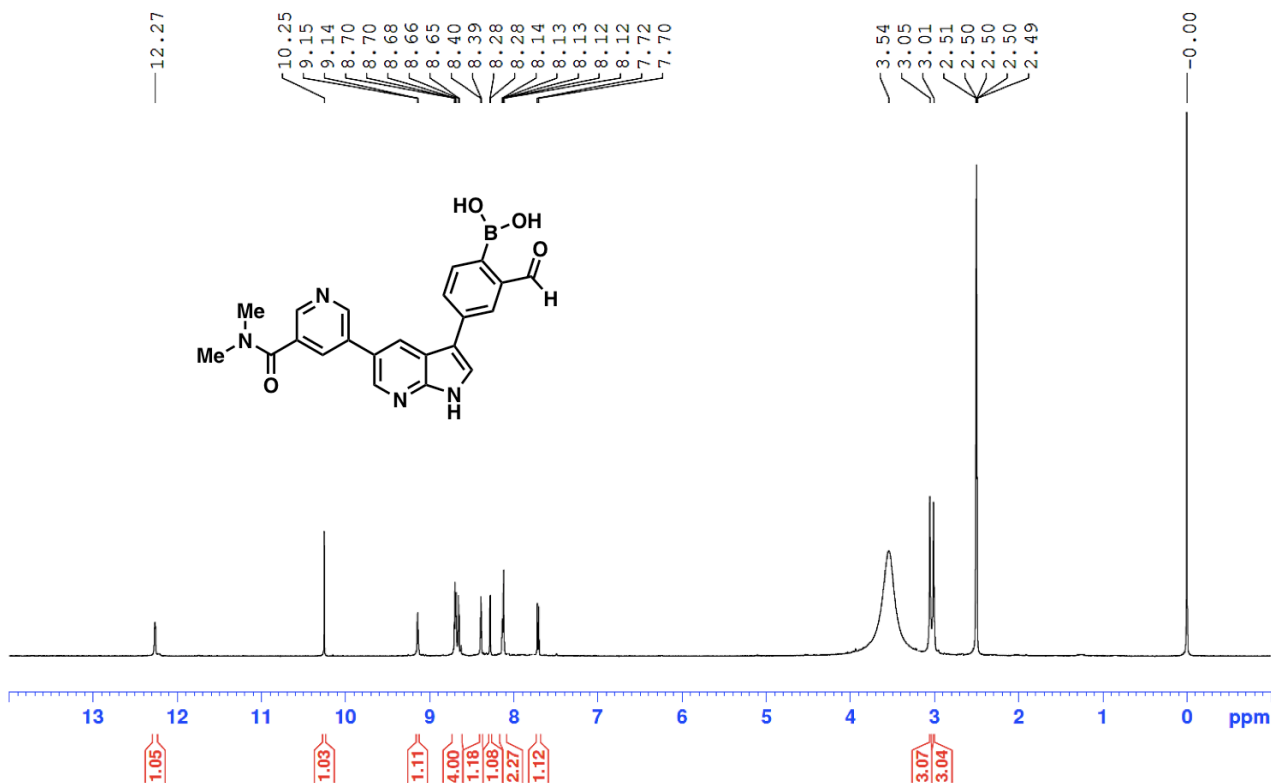
Compound 10



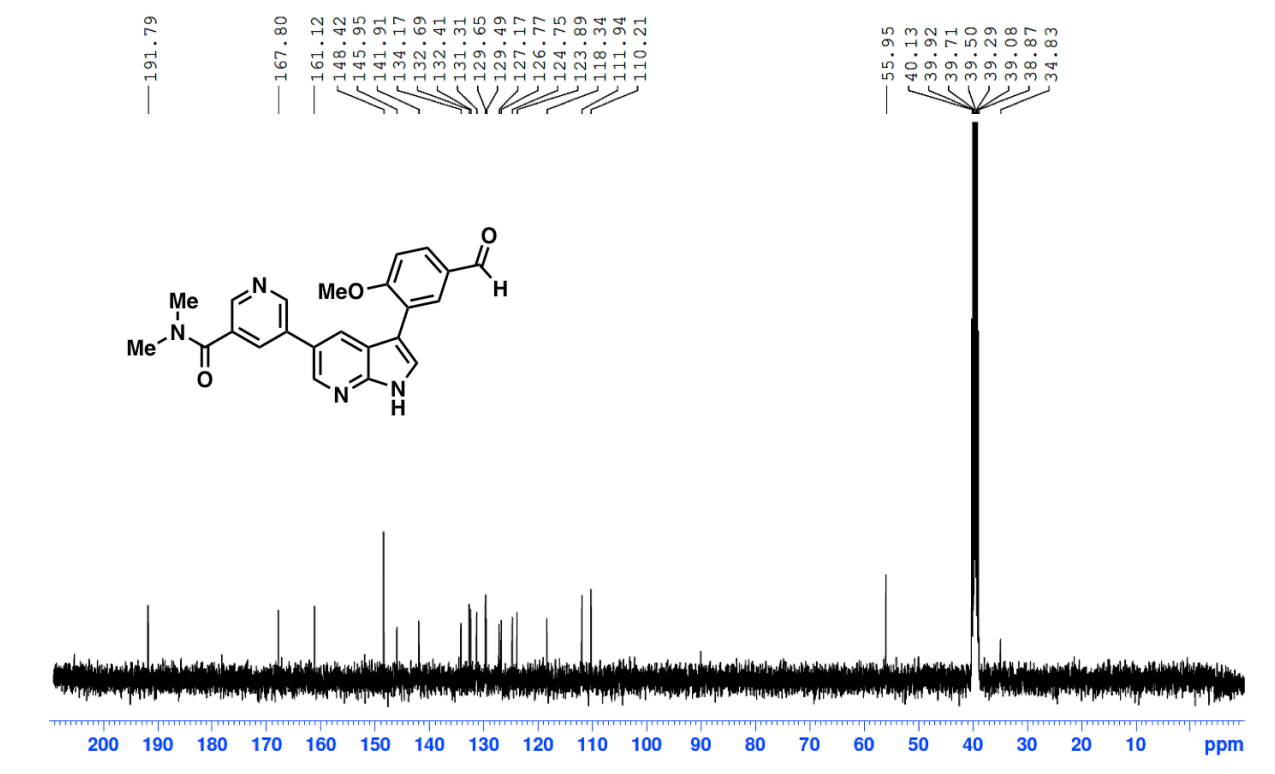
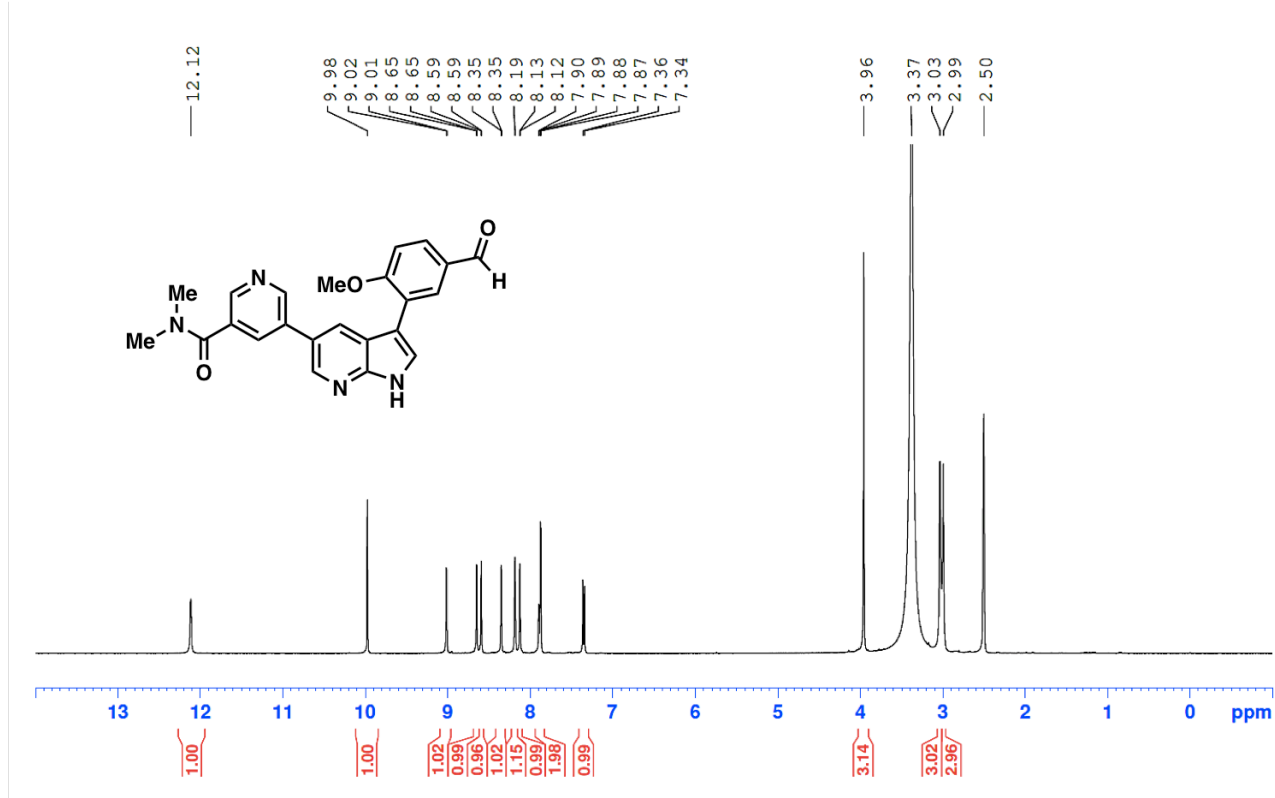
Compound 11



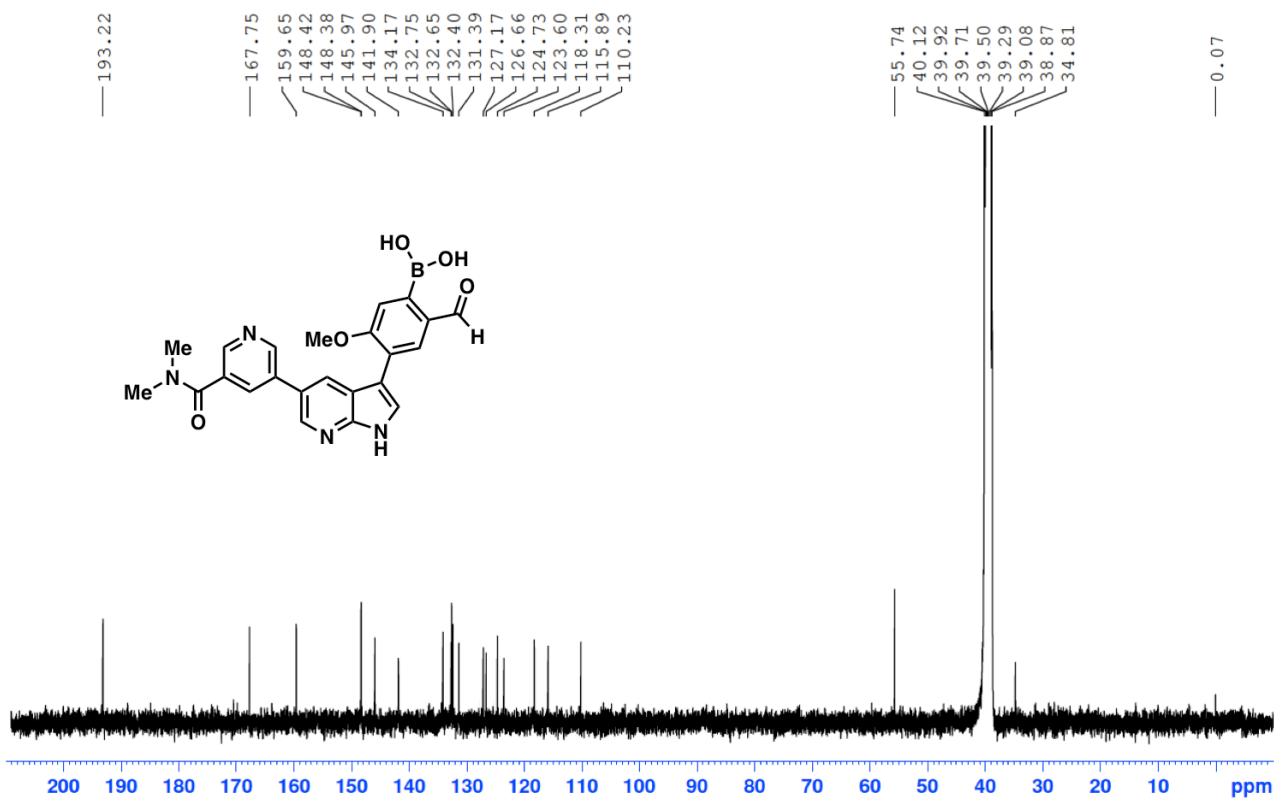
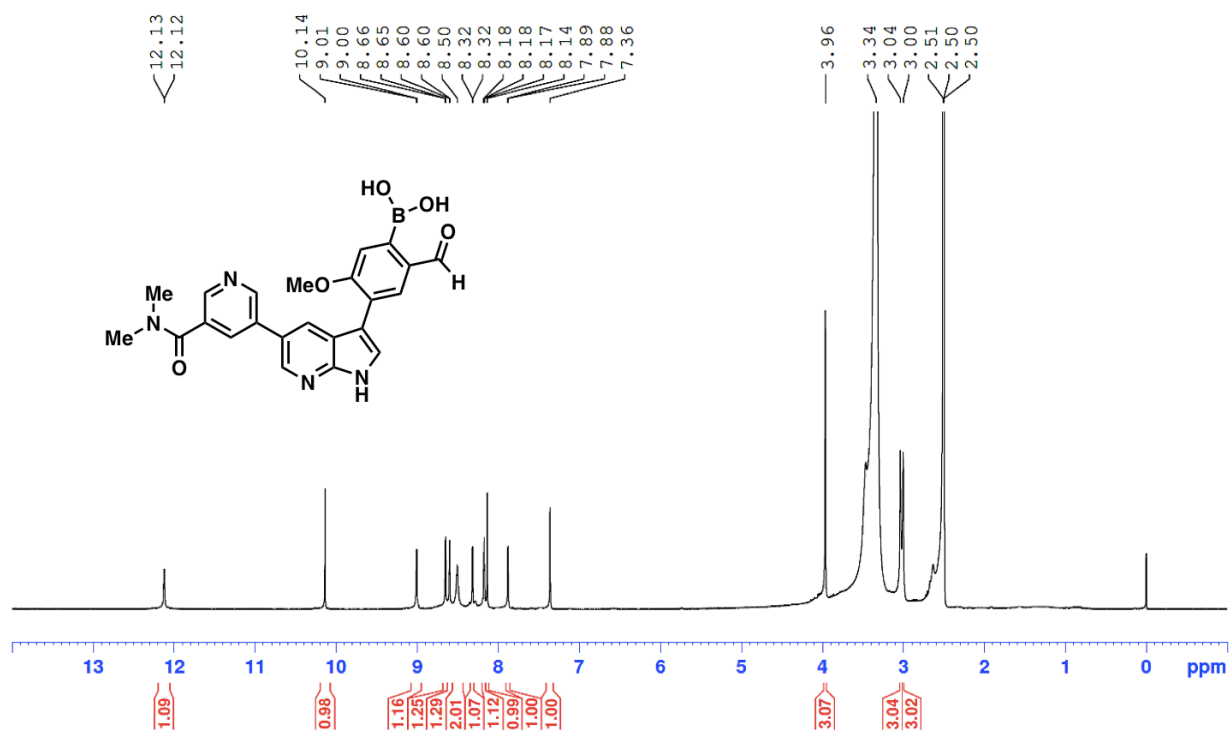
Compound 12



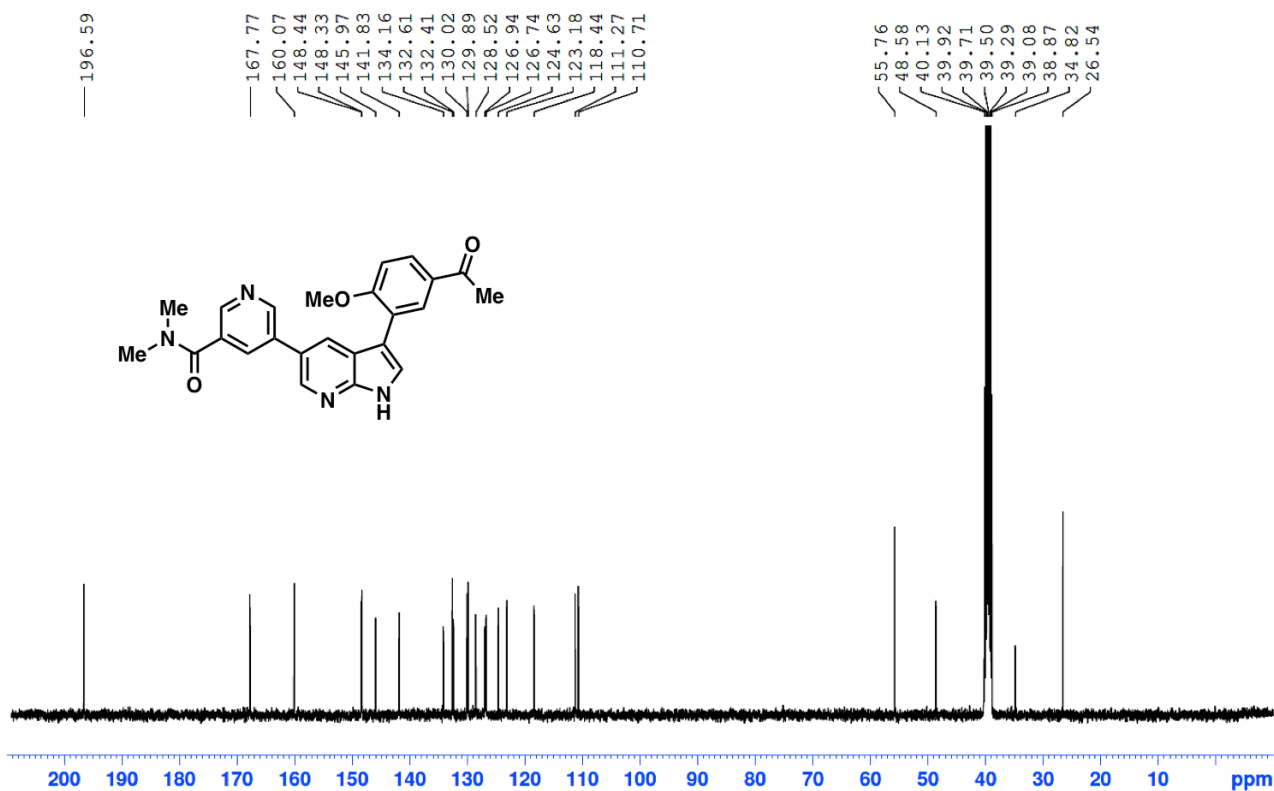
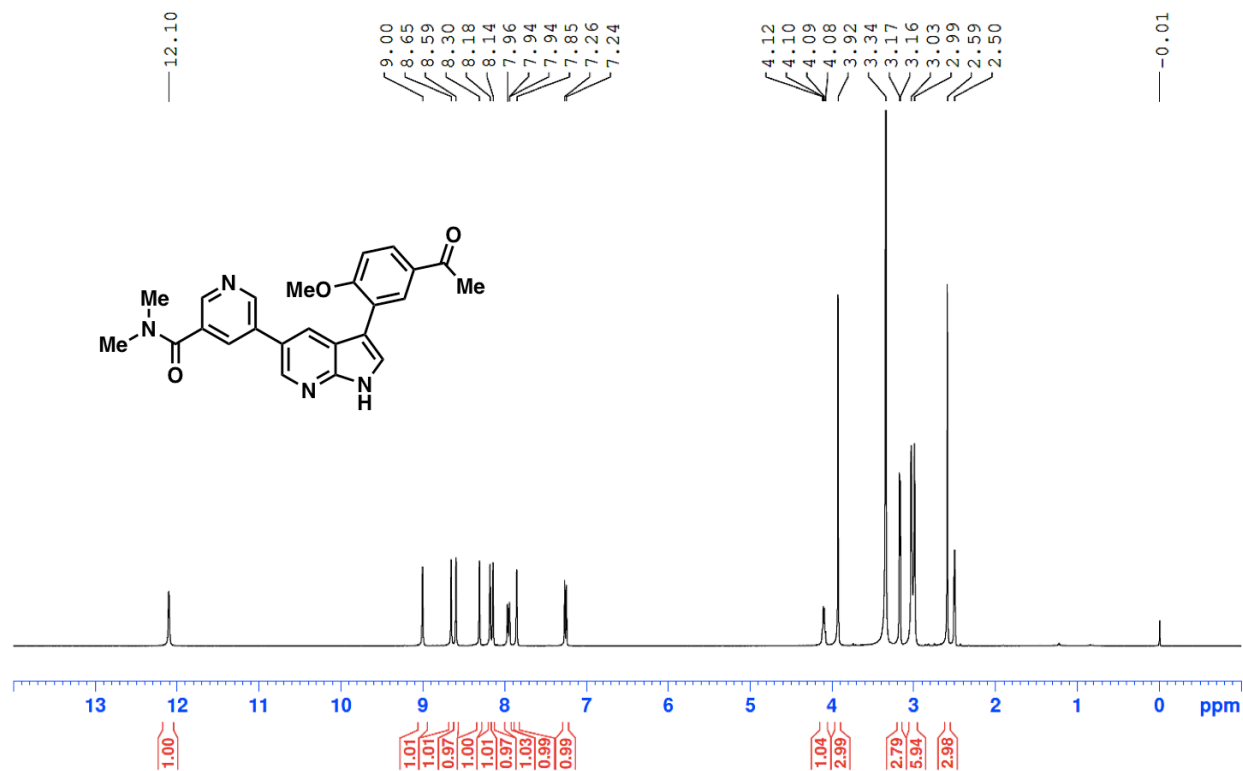
Compound 13



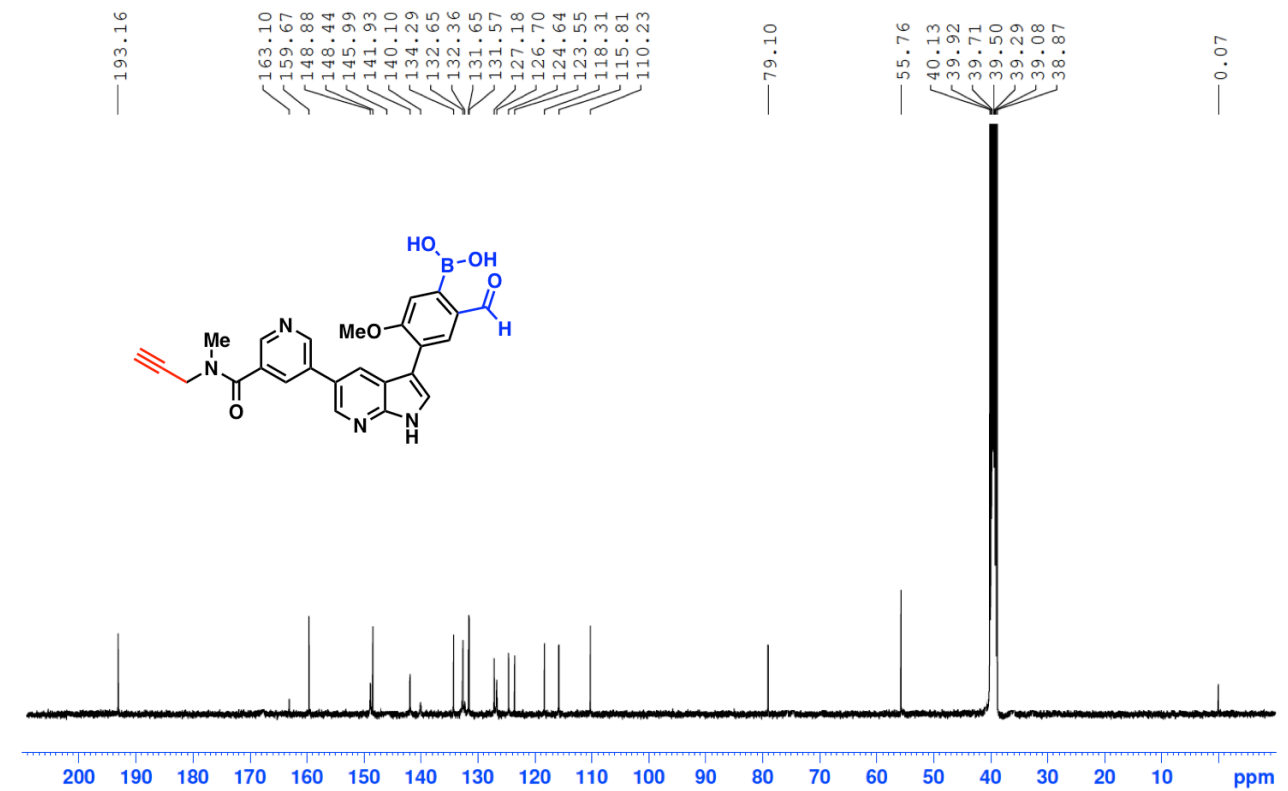
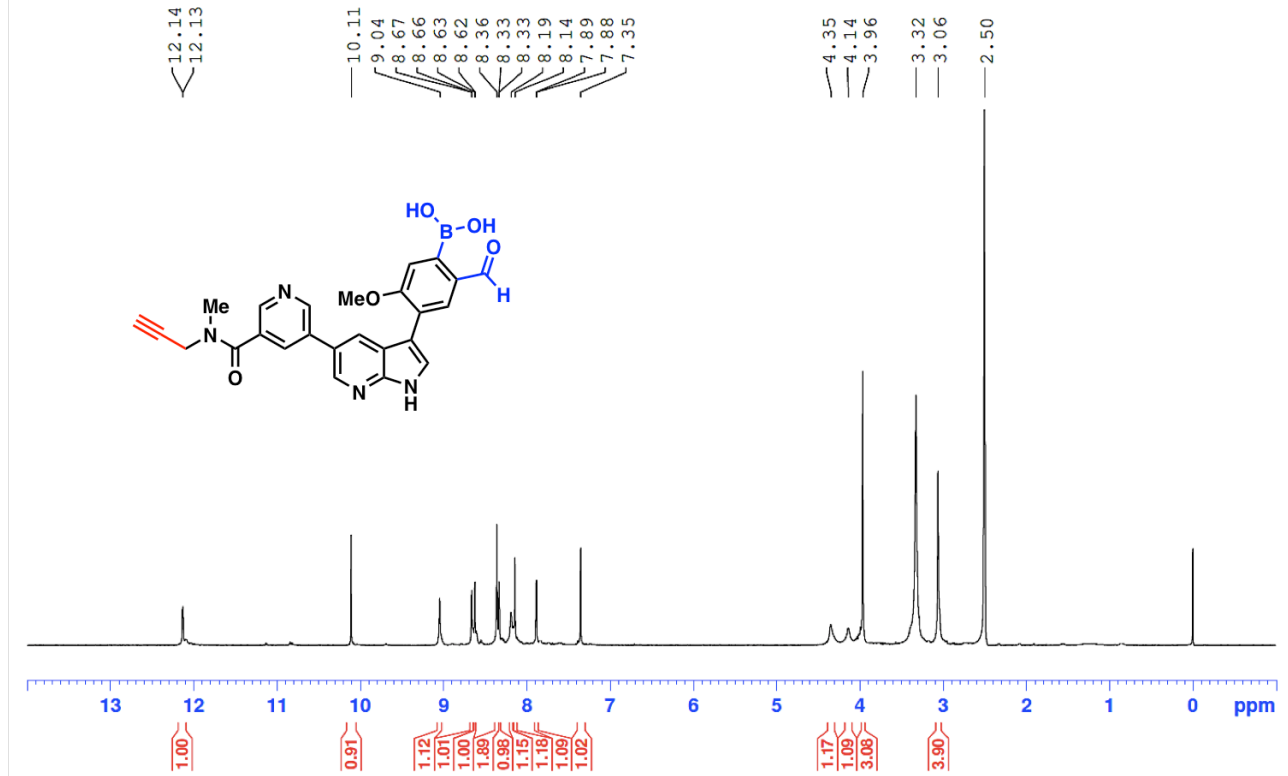
Compound 14



Compound 15



Compound 16



David_YSQ SI_ChemRxiv.pdf (18.35 MiB)

[view on ChemRxiv](#) • [download file](#)
